DESIGN AND CONSTRUCTION OF REDUCED SIZE PLANAR SPIRAL ANTENNA IN THE 0.5-18 GHz FREQUENCY RANGE

A THESIS SUBMITTED TO
THE GRADUATE SCHOOL OF NATURAL AND APPLIED SCIENCES
OF
MIDDLE EAST TECHNICAL UNIVERSITY

BY

İNANÇ YILDIZ

IN PARTIAL FULFILLMENT OF THE REQUIREMENTS FOR THE
DEGREE OF MASTER OF SCIENCE
IN
ELECTRICAL AND ELECTRONICS ENGINEERING

OCTOBER 2004

Approval of the Graduate School of Natural and Applied Sciences

Prof. Dr. Canan ÖZGEN
Director

I certify that this thesis satisfies all the requirements as a thesis for the degree of Master of Science.

Prof. Dr. İsmet ERKMEN
Head of Department

This is to certify that we have read this thesis and that in our opinion it is fully adequate, in scope and quality, as a thesis for the degree of Master of Science.

Prof. Dr. Altunkan HIZAL
Supervisor

Examining Committee Members

Assoc. Prof. Dr. Sencer KOÇ (METU, EE) _____

Prof. Dr. Altunkan HIZAL (METU, EE) _____

Prof. Dr. Nilgün GÜNALP (METU, EE) _____

Assoc. Prof. Dr. Gülbin DURAL (METU, EE) _____

Ufuk KAZAK M.S.E.E (ASELSAN) _____

I hereby declare that all information in this document has been obtained and presented in accordance with academic rules and ethical conduct. I also declare that, as required by these rules and conduct, I have fully cited and referenced all material and results that are not original to this work.

Name, Last name: İnanç YILDIZ

Signature :

ABSTRACT

DESIGN AND CONSTRUCTION OF REDUCED SIZE PLANAR SPIRAL ANTENNA IN THE 0.5-18 GHz FREQUENCY RANGE

YILDIZ, İnanç

M.S., Department of Electrical and Electronics Engineering
Supervisor: Prof. Dr. Altunkan HIZAL

October 2004, 106 pages

In this thesis, theoretical and practical evaluation of usual spiral antenna is revised. Working principles of both types of planar spiral antennas as Equiangular and Archimedean are introduced. A predesigned microstrip tapered balun used for feeding section of a spiral antenna is simulated on Ansoft® HFSS™ software. Successful simulation results are obtained and measurements of implemented balun structure are made by using an HP® 8722 D vector network analyzer.

Antenna measurement techniques used in this study are introduced. Measurement set-ups are defined and some preliminary knowledge is given on these.

As the main matter of thesis, reduced size planar spiral antennas are designed and implemented. Return loss, gain; radiation and polarization patterns of antennas are measured. Datasets of measurements are compared with each other and with reference spiral antenna. Quite promising results are obtained and size reduction of spiral antenna is achieved in many aspects.

Key words: Microstrip Tapered Balun, Reduced Size Planar Spiral Antenna.

ÖZ

0.5-18 GHz FREKANS BANTLI
KÜÇÜLTÜLMÜŞ DÜZLEMSEL SPİRAL ANTENLERİN
TASARIMI VE YAPIMI

YILDIZ, İnanç

Yüksek Lisans, Elektrik ve Elektronik Mühendisliği Bölümü
Tez Yöneticisi: Prof. Dr. Altunkan HIZAL

Ekim 2004, 106 sayfa

Bu tezde, bilinen spiral antenin teorik ve pratik değerlendirilmesi gözden geçirilmiştir. Düzlemsel spiral antenlerin Equiangular ve Archimedean olarak iki çeşidi ve çalışma prensipleri tanıtılmıştır. Bir spiral antenin besleme kısmında kullanılan önceden tasarlanmış mikroşerit incelen balun Ansoft® HFSS™ yazılımda simüle edilmiştir. Başarılı simülasyon sonuçları elde edilmiş ve gerçekleştirilen balunun ölçümleri HP® 8722 D vektör devre analizörü kullanılarak yapılmıştır.

Bu çalışmada kullanılan anten ölçüm teknikleri tanıtılmıştır. Ölçüm düzenekleri tanımlanmış ve bunlar hakkında bir kısım önbilgi verilmiştir.

Tezin esas çalışma konusu olarak, küçültülmüş düzlemsel spiral antenler tasarlanmış ve yapılmıştır. Antenlerin geriye dönme kaybı, kazancı; ışınım ve polarizasyon örüntüleri ölçülmüştür. Ölçüm verileri birbirleriyle ve referans spiral antenle karşılaştırılmıştır. Oldukça ümit verici sonuçlar elde edilmiş ve spiral antenin boyutunun küçültülmesi birçok yönüyle başarılı olmuştur.

Anahtar Kelimeler: Mikroşerit İncelen Balun, Küçültülmüş Düzlemsel Spiral Anten

To my family

ACKNOWLEDGEMENTS

I wish to express my sincere gratitude to Prof. Dr. Altunkan Hızal for his supervision, valuable guidance and helpful suggestions.

I would like to express my sincere appreciation to all of the RF Design Group members for their valuable friendship, help and support. I am also grateful to ASELSAN® Inc. for facilities provided for the completion of this thesis.

I would like to extend my special appreciation and gratitude to my family and my friends for their encouragement, endless love and understanding of my spending lots of time on this work.

TABLE OF CONTENTS

PLAGIARISM……iii
ABSTRACT……iv
ÖZ…..…….….vi
DEDICATION……..……viii
ACKNOWLEDGEMENTS……..…….ix
TABLE OF CONTENTS……x

CHAPTER

1 INTRODUCTION 1

2 STUDY OF MICROSTRIP TAPERED BALUNS 3

2.1 Introduction 3

2.2 Microstriplines 3

2.3 Geometry of Linearly Tapered Microstrip Balun 5

2.4 Linearly Tapered Microstrip Baluns Designed for Planar Spiral antennas and EM Simulations using Ansoft® HFSS™ 7

2.5 Balun's Balance and Matching Performance Measurements 8

3 PLANAR SPIRAL ANTENNAS 10

3.1 Introduction 10

3.2 Planar Equiangular Spiral Antennas 10

3.3 Planar Archimedean Spiral Antennas 13

3.4 Radiation Patterns and Polarization 14

3.5 Backing Cavity Design 14

3.6 Feed Circuit 15

4 ANTENNA MEASUREMENT TECHNIQUES 17

4.1 Input Return Loss and VSWR Measurements of Spiral Antennas 17

4.2 Anechoic Chamber 18

4.3 Gain Measurement Techniques 18

4.4 Polarization Measurements 22

4.4.1 Polarization Pattern Method 24

5 IMPLEMENTATIONS AND MEASUREMENTS OF SPIRAL ANTENNAS WITH DIFFERENT DESIGN PARAMETERS 26

5.1 Introduction 26

5.2 AutoCAD® Drawing Tool 27

5.3 Manufacturing Techniques of Spiral Antennas 28

5.4 Designed Spiral Antennas 28

5.5 Measurements of Spiral Antennas 32

5.5.1 Input Return Loss Measurements of Spiral Antennas 32

5.5.2 Primitive Gain Comparison and Radiation Pattern Measurements of Spiral Antennas 36

5.5.3 Polarization Pattern Measurements of Spiral Antennas 68

6 CONCLUSION..... 73

REFERENCES..... 76

APPENDICES

A. "User Friendly AutoLISP® Program for Planar Spiral Antenna Drawing" by Ekrem ORAN……...79

B. Effective Dielectric Constant and Characteristic Impedance of Microstrip Lines……90

C. Characteristic Impedance of Parallel Strips Separated by a Dielectric Sheet…….……...92

D. RF Ohmic Resistance and Current Distribution of a Spiral Antenna……93

CHAPTER 1

INTRODUCTION

For military systems; it is very crucial that all components should have a very wide band frequency characteristic. RF sensing devices of these systems as spiral antennas, meet this requirement with their inherent frequency independent structure. In that manner, use of the spiral antennas in military and civil systems has a large spectrum including ESM suites, direction finding applications and etc [1,2,3,12].

Considering the further needs of military systems, the equipment used in these systems should have narrow size. As the technology advances, operating frequency of these systems is getting wider and the material size is getting narrower, so the previously designed spiral antenna has to be modified to meet the size limitations and operating frequency specifications.

In conclusion, the aim of this thesis can be stated as follows; reducing the size of previously designed spiral antennas by preserving the frequency independent characteristic and acceptable radiation pattern properties of the antenna.

Commonly, spiral antennas are composed of a PCB spiral card, a balun transformer, and an absorber loaded backing cavity.

In this thesis Chapter 2 examines the microstrip-tapered balun theory and gives an evaluation about previously designed baluns and their feeding characteristics of spiral antennas. Ansoft® HFSS™ program is used for realizing simulations of microstrip-tapered baluns.

In Chapter 3, the two types of spiral antennas named Equiangular and Archimedean are discussed. Physical and electromagnetic properties of these two types are presented. Basic design parameters with their effects to antenna performance including pattern and polarization characteristics and impedance matching properties of the antennas detailed with graphs and equations are given. This chapter also includes previous studies on spiral antennas and an investigation of earlier designs.

Antenna measurement techniques are discussed in Chapter 4 and use of antenna measurement techniques for this thesis is considered. SWR, return loss, gain, radiation and polarization pattern measurement set-ups are defined in this section.

Chapter 5 gives a detailed description of implementations of spiral antennas theoretically and practically. Different design parameters are introduced and their effects on antenna performance are discussed. Three spiral antennas with different design parameters are implemented and their performances are compared with each other and also with reference spiral antenna whose size should be reduced.

In Chapter 6, results of the study in this thesis are evaluated and a detailed conclusion is given. Also, later work is defined and use of this study for later work is discussed.

CHAPTER 2

STUDY OF MICROSTRIP TAPERED BALUNS

2.1 Introduction

Transmission lines like the coaxial cables are unbalanced structures but a spiral antenna is a balanced structure, so an electromagnetic transition between two media is needed in order to feed the spiral antenna properly. Also an impedance matching section having a wide frequency bandwidth is needed to implement matching between two media having different characteristic impedances [1,3].

Earlier version of the microstrip-tapered balun design already used in feeding sections of spiral antennas is examined and different simulations of the structure is realized using Ansoft® HFSS™ program, and also reflection loss and insertion loss measurements of the structure are implemented using a vector network analyzer.

2.2 Microstriplines

Microstripline is a quasi TEM mode transmission structure and implementing circuits with microstriplines can be economical. Basic applications of microstriplines can be extended to many low-to-medium power radars associated with electronic countermeasure systems, some segments of point-to-point radio links, and certain parts of satellite communication links. Microstrip transmission lines are widely used in microwave (hybrid) integrated circuits (MIC)

for these systems. Most of the structures are also suitable for various high-speed digital applications [3,4].

Electromagnetic fields related to microstriplines are actually complex although microstriplines have a simple geometric structure (see Figure 2.1). Accurate and thorough analysis requires quite elaborate mathematical treatment. However simple approaches to quasi-TEM mode calculations combined with frequency-dependent expressions yield quite acceptable design accuracy. Accuracies within 1 percent are generally achievable [3,4].

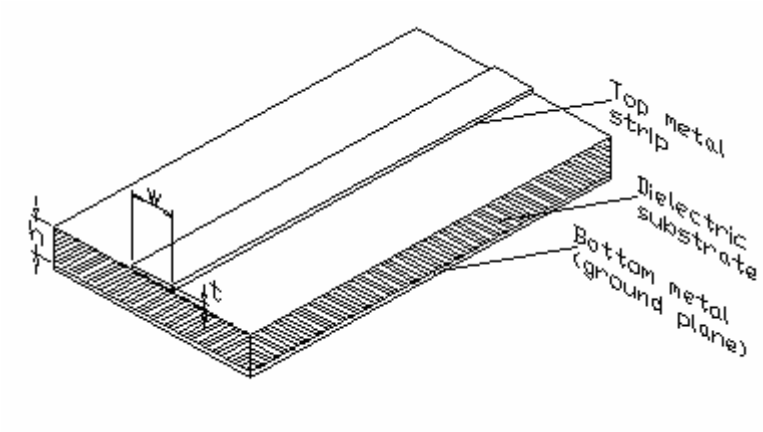

Figure 2.1 Geometric Structure of Microstripline [3]

MICs using microstrip can be designed for frequencies ranging from a few gigahertz, or even lower, up to many tens of gigahertz. At higher frequencies, particularly into millimeter wavelength ranges, losses (including radiation losses) increase greatly, higher-order modes become a considerable problem and fabrication tolerances become exceedingly difficult to meet. It is thought that the frequency limit for the extensive use of microstrip is roughly around 60 GHz [3,4].

2.3 Geometry of Linearly Tapered Microstrip Balun

Linearly tapered microstrip balun is used as an impedance transformer network in feeding sections of spiral antennas. The conversion from unbalanced to balanced line relies on a gradual change of cross section of the line. Geometry of a simple microstrip tapered balun is given in Figure 2.2 [3].

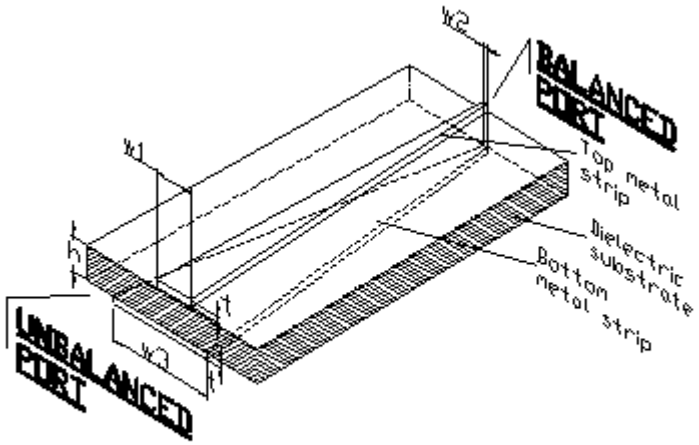

Figure 2.2 Linearly Tapered Microstrip Balun [3]

At the input, the cross section of the line resembles microstrip, while at the output the strips are of equal width, constituting a balanced line. Ideally the balanced line should support only odd modes [3].

In order to design a tapered microstrip balun we need the characteristic impedances of this line at the input and the output ports. Ansoft® HFSS™ program guided us to find these values by using the dimensions of the line [1].

Simulations are based on two 3D model of linearly tapered microstrip balun structure. First one is the simulation of the balun alone with the port impedances are normalized according to the characteristic impedances of the balanced and unbalanced ports derived by HFSS™ program from the dimensions of the microstrip line (see Figure 2.3). Second one is the simulation of two identical baluns connected to each other at their balanced ports (see Figure 2.4).

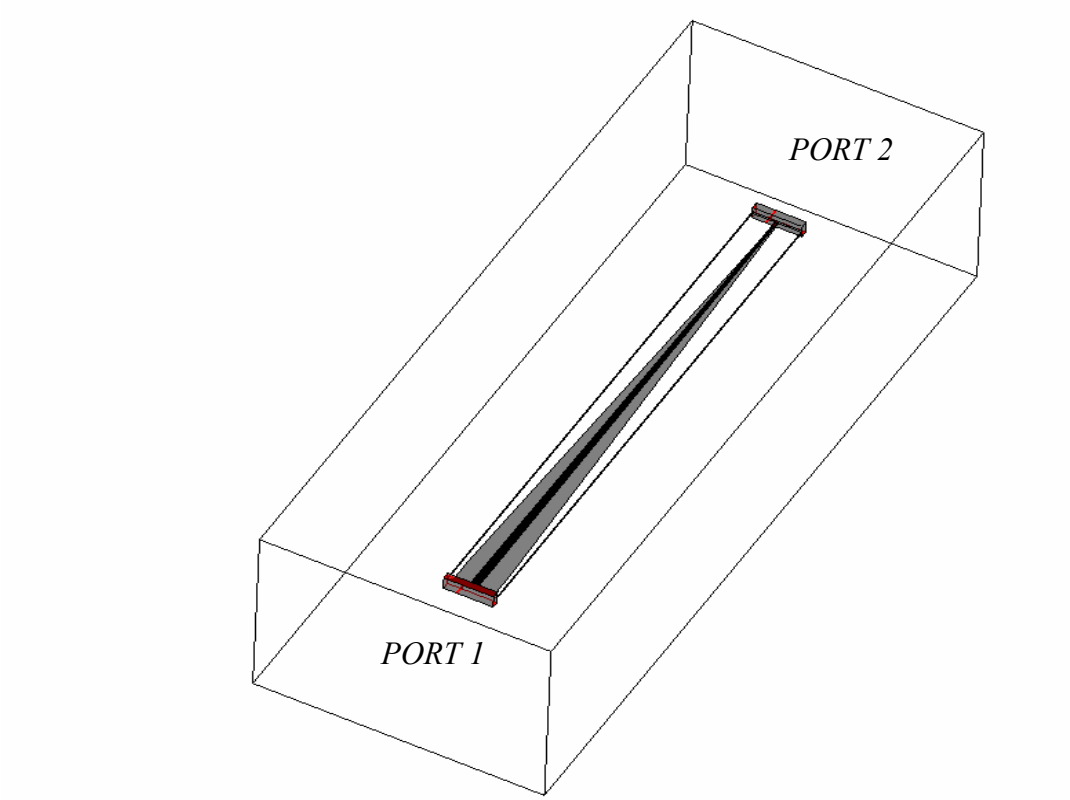

Figure 2.3 HFSS Model of one balun

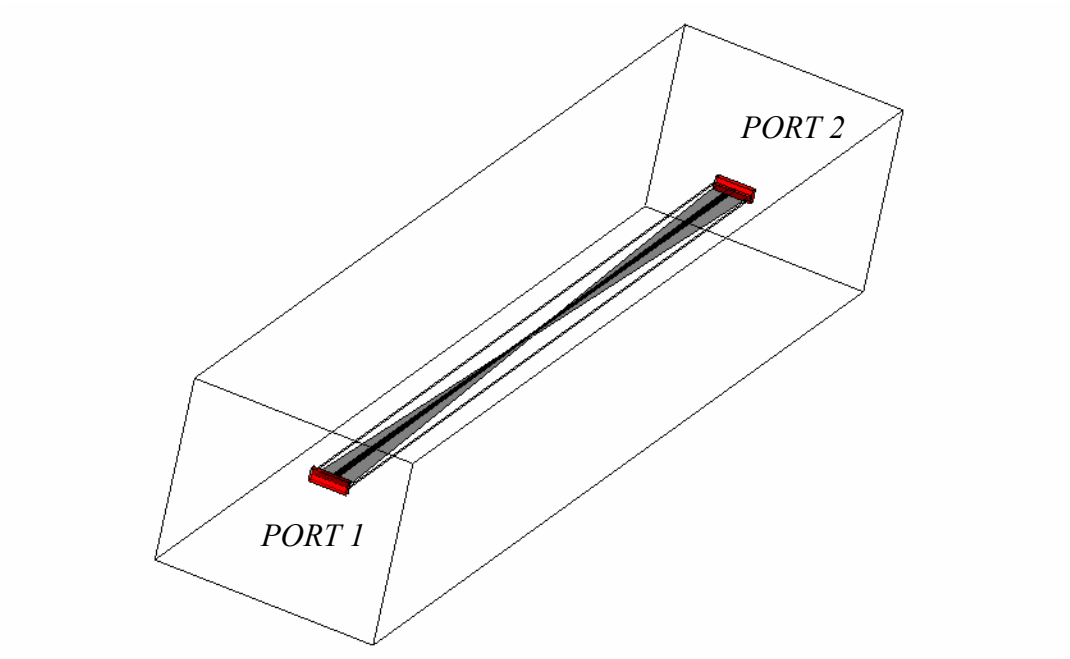

Figure 2.4 HFSS Model of two baluns

2.4 Linearly Tapered Microstrip Baluns Designed for Planar Spiral antennas and EM Simulations using Ansoft® HFSS™

Previously designed Linearly Tapered Microstrip Baluns were examined using Ansoft® HFSS™ program and return loss and insertion loss characteristics are obtained along the wide frequency band of spiral antenna. In this structure, double side copper coated Roger's® Duroid 5880, whose dielectric constant is ε_r**=2.2,** dielectric thickness is **h=0.381 mm**, and copper metallization thickness is **t=17.5 microns** has been used as the base material of the balun.

At the balanced port we need approximately 130 ohms as the input impedance of the spiral antenna and since it has already been known that coaxial cable impedance is 50 ohms at the unbalanced port. With the help of formulas given in the Appendix B and C theoretical values of impedances at the two ports of balun are calculated, 50 Ohms input impedance at unbalanced port can be achieved by choosing **1.15 mm** for **w1** and 120 Ohms input impedance at unbalanced port can be achieved by choosing **0.35 mm** for **w2**. Simulations showed that the values **1.15 mm** for **w1** and **0.35 mm** for **w2** and for **5.76** for **w3** as seen in Figure 2.2 are appropriate for an acceptable return loss and insertion loss characteristics. Simulation results for return loss and insertion loss characteristics of one balun and two baluns connected at their balanced ports are shown below Tables 2.1 and 2.2.

Table 2-1 S parameters (in dB) and impedance values of one balun with respect to frequency.

Frequency (GHz)	S11	S12	S21	S22	Z(port1)	Z(port2)
0,5	-5,41	-1,49	-1,49	-5,38	33,08	130
1	-13,2	-0,254	-0,254	-12,9	32,602	130
2	-15,5	-0,204	-0,204	-14,8	32,781	130
4	-16	-0,16	-0,16	-16	32,554	130
8	-23,7	-0,117	-0,117	-21,5	33,099	130
12	-29,5	-0,0231	-0,0231	-29,5	33,223	130
15	-20,8	-0,0696	-0,0696	-20,6	34,142	130
18	-26,5	-0,0305	-0,0305	-26,4	36,118	130

Table 2-2 S parameters (in dB) and impedance values of two back-to-back connected baluns with respect to frequency.

Frequency (GHz)	S11	S12	S21	S22	Z(port1)	Z(port2)
0,5	-7,17	-0,944	-0,944	-7,17	32,795	32,768
1	-12,1	-0,341	-0,341	-12,1	33,311	33,402
2	-11,2	-0,409	-0,409	-11,2	31,733	32,622
4	-17,6	-0,189	-0,189	-17,7	32,563	31,682
8	-21,3	-0,218	-0,218	-22,3	32,557	32,933
12	-20,8	-0,0683	-0,0683	-20,7	33,517	34,164
15	-41,1	-0,0477	-0,0477	-38,7	34,498	34,713
18	-32,6	-0,0652	-0,0652	-31,6	34,872	35,286

2.5 Balun's Balance and Matching Performance Measurements

Using a HP® 8722 D vector network analyzer, return loss and insertion loss measurements have been made like the simulation of the two baluns connected to each other at their balanced ports. Return loss characteristics and Insertion loss characteristics of the baluns are shown in Figure 2.5 and Figure 2.6 respectively [1].

Figure 2.5 shows that the balun's impedance matching performance from 50 Ω to 130 Ω is acceptable since the return loss values are generally less than –10 dB. This corresponds to a SWR value smaller than 2. Also Figure 2.6 shows that insertion loss characteristics of the two back-to-back connected baluns are well enough. Besides these return loss and insertion loss values are better than the results of simulations. This is due to the loading effects of spiral arms and substrate of spiral PCB. So the input impedance of the antenna is closer to 120 Ohms (theoretical impedance value of parallel strip line calculated with the help of formulas in Appendix C) than the theoretical value of antenna input impedance 130 Ohms.

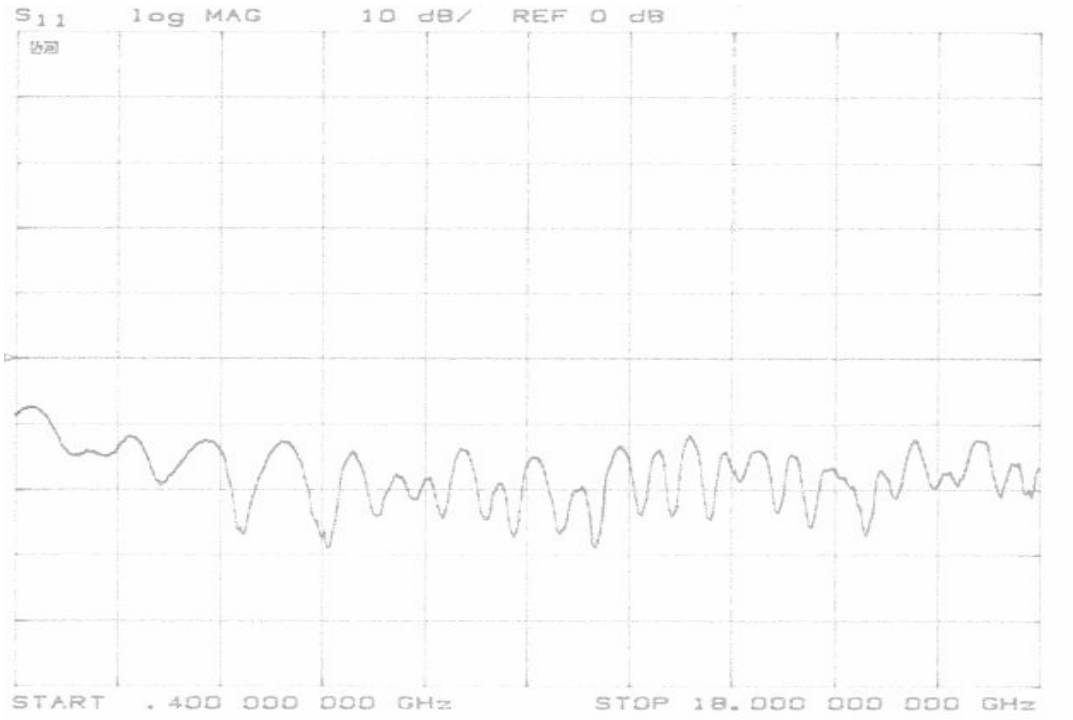

Figure 2.5 Input return loss measurement of Balun

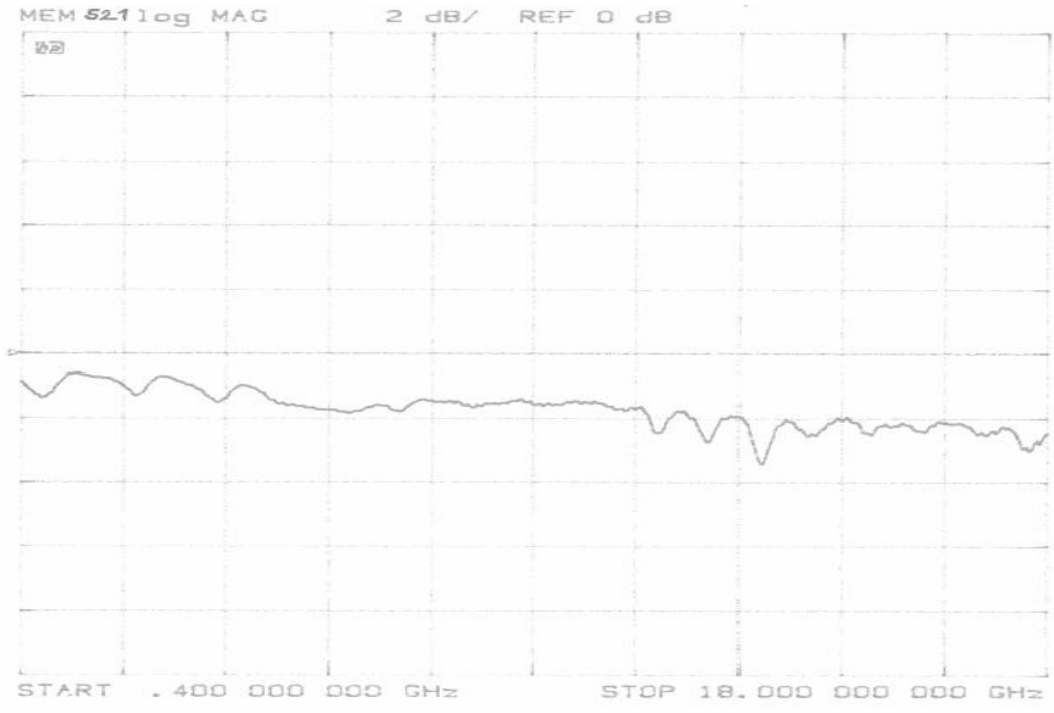

Figure 2.6 Insertion loss measurement of the Balun

CHAPTER 3

PLANAR SPIRAL ANTENNAS

3.1 Introduction

Fundamental properties of antennas like radiation pattern or polarization are based on its shape and dimensions expressed in wavelengths. Since wavelength is inversely proportional to frequency, antennas present frequency dependent characteristics commonly. On the other hand, very wide-band spiral antennas operate on the principle of frequency-independent antennas established first by Rumsey in 1957. His theory is based on the "angle concept" meaning that a structure, whose shape is defined by angles alone, with no wavelength expressions, should have frequency-independent characteristics [1,5].

3.2 Planar Equiangular Spiral Antennas

At the beginning, we can consider the equiangular spiral curve, which is shown in Figure 3.1 representing the polar coordinates of a point from the origin [1].

$$r(\phi)=r_0\tau(\phi) \tag{3.1}$$

where $\tau(\phi)=\exp(a\phi)$ and a is the flare rate of the spiral. The equiangular spiral curve can be used to achieve the angular structure of equiangular spiral antenna [1,2]. For any q there is a Ψ such that $qr(\phi)=r(\phi+\Psi)$. It is seen that $q=\tau(\Psi)$. Thus, if a region of the spiral corresponding to a frequency f_1 radiates for the condition

$k_1 r(\phi)=1$ where $k_1=2\pi/\lambda_1=2\pi\ f_1/c$, when the frequency is reduced to f_2, there is an exactly similar region on the spiral for which $k_2 r=1$. Also $k_1 r(\phi)=k_2 r(\phi+\Psi)=1$ gives $k_1/k_2=\tau(\Psi)$ or $\Psi=(1/a)\ln(k_1/k_2)$ in other words the similar region at f_2 is reached by rotating Ψ degrees from ϕ on the spiral. It is also evident that the radiated field has also rotated by Ψ. Far field expression for an antenna can be given by,

$$E(\theta,\phi,r)= e^{-jkr}/r\ [a_\theta F_\theta(\theta,\phi)+a_\phi F_\phi(\theta,\phi)] \tag{3.2}$$

where a_θ and a_ϕ are the unit vectors, $F_\theta(\theta,\phi)$ and $F_\phi(\theta,\phi)$ are the patterns. When the frequency is decreased by a factor of $\gamma= k_1/k_2$, the pattern rotates according to,

$$F_{\theta,\phi}\ (\theta,\phi+1/a\ \ln\gamma,\ f/\gamma)= F_{\theta,\phi}(\theta,\phi,f) \tag{3.3}$$

If the field is almost uniform with ϕ then the pattern rotation cannot be observed. The radiation field is circularly polarized which may be explained using the traveling wave nature of the current distribution and that the radiation region of the spiral corresponds to $kr(\phi)=1$ i.e $2\pi r(\phi)=\lambda$; two space orthogonal regions are separated by $\lambda/4$ and radiating elements are 90° out of phase results in circular polarization. The radiation mechanism of the spiral antenna can be explained on the basis of the traveling wave current model [6]. Figure 3.2 (b) shows the two arms of a spiral antenna. The points M and Q are diametrically opposite with respect to the center 0. For antiphase feeding at A and B, the phase of the traveling wave currents at M and Q are also opposite. The phases of the currents at Q and P are out of phase by $\Delta\phi=\beta(L_{PA}-L_{QB})+\pi$, where $\beta=k$ for TEM traveling wave currents. The phase difference becomes 2π at some point on the spiral and the currents in the vicinity of this point radiate constructively. The radius r where $\Delta\phi=2\pi$ can be found from $\Delta\phi=kL+\pi=2\pi$ [2].

$$L=(1+a^{-2})^{1/2}(r_P-r_Q) \tag{3.4}$$

where

$$r_P= r_0e^{a\phi},\ r_Q= r_0e^{a(\phi-\pi)} = r_Pe^{-a\pi} \tag{3.5}$$

$$k(1+a^{-2})^{1/2}\ r_P(1-e^{-a\pi})=\pi \tag{3.6}$$

$$kr_P=\pi/[(1+a^{-2})^{1/2}(1-e^{-a\pi})] \tag{3.7}$$

A usual expansion rate may be a=0.01 rad^{-1} for which kr_P=1.016. It is seen that for this value of "a" $2\pi r_P$=1.016λ, i.e. the diameter of the active region $2r_P=\lambda/\pi$. The radiation mechanism of a planar spiral antenna hence becomes apparent from Figure 3.2 (c). In-phase currents I_y<0° radiate constructively towards the boresight direction as a broadside array. The space orthogonal currents I_y<90° radiate also into the boresight direction, but with a 90° phase difference. 90° phase difference comes from the traveling wave nature of the current and the fact that the circumference is one wavelength. The resultant boresight field is thus circularly polarized. The sense of polarization depends on the direction of spiraling. In Figure 3.2 (a), the spiraling is in +ϕ direction and for a wave radiated into +z direction the wave is right hand circularly polarized wave. The radiated field rotates with the frequency by $\Psi=(1/a)\ln(f_1/f_2)$ where if $f_1>f_2$, rotation is Ψ degrees towards the center and vice versa occurs if $f_1<f_2$. The current distribution is decaying slowly up to active region (kr=1) and there is a small amount of radiation. After the active region the currents magnitude rapidly attenuates as a result of the radiation. The radiation pattern is bi-directional and almost rotationally symmetrical for a<0.2 rad^{-1}. For larger "a" pattern shows asymmetry and its rotation with frequency can be observed. The beamwidth is about 76° for a<0.2 rad^{-1} [2].

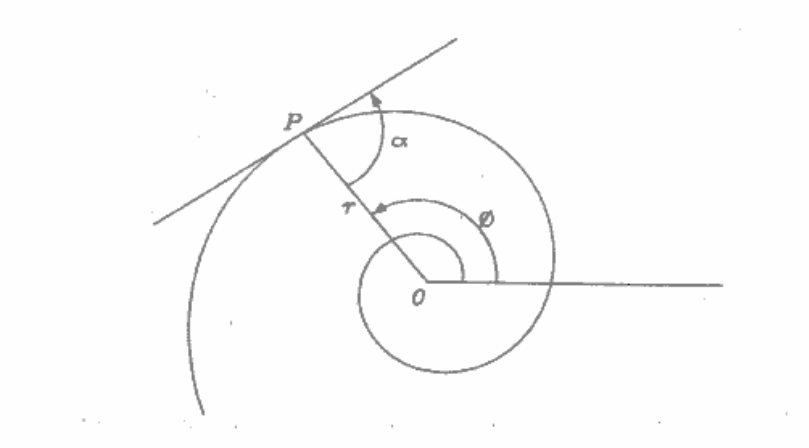

Figure 3.1 Basic Spiral Curve [1]

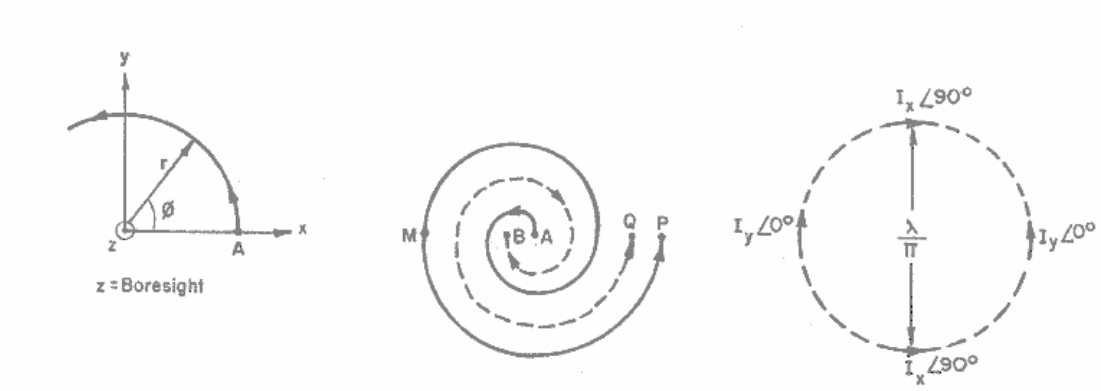

(a) (b) (c)

Figure 3.2 Explaining the radiation mechanism by the radiating ring current [2]

3.3 Planar Archimedean Spiral Antennas

This type of spiral antenna is characterized by the polar equation $r=r_0(1+a\phi)$ which is the first two terms of the Taylor's expansion of the equiangular spiral $r=r_0\exp(a\phi)$ for small values of "a". The Archimedean spiral also exhibits all the main characteristics of the equiangular spiral. The operation of this spiral has been explained by Kaiser [2,6] using the radiating band concept. For small $a<0.1$ Archimedean and Equiangular spiral antennas are almost equivalent as far as the principle of operation is concerned and they both radiate from a diameter of about λ/π [2,6]. For a given diameter of the antenna greater bandwidth is obtained with more tightly wounded spirals (i.e. for small "a" values). So

Archimedean spiral has a wider bandwidth with a given antenna diameter. However, the feed region of Archimedean spiral is more tight and for this reason, equiangular spirals are better for higher frequencies especially for f>18 GHz. The circular polarization characteristics of Archimedean spirals at the low frequency end are better compared to that of Equiangular spirals. The azimuthal symmetry and axial ratio of the Archimedean spiral is also better than that of equiangular spiral. Further improvement of the axial ratio can be obtained by resistive loading of spiral arms at the exterior terms. Making the last half turn of the spiral resistive or by absorptive painting aquadag between the two wires of last turn can either do this. The loading will reduce the end-reflected currents that radiate opposite sense of polarization. A disadvantage of the Archimedean spiral is that due to the large number of turns, the ohmic RF loss-resistance is large and this reduces the gain of the antenna [2].

3.4 Radiation Patterns and Polarization

Spiral antennas radiate Right Hand Circular Polarization to one side and Left Hand Circular Polarization to the other side. The radiating currents along the arms are traveling wave currents and their paths are clock-wise when considered from one side and counter clock-wise when considered from the other side. The radiated field from these traveling currents will also rotate in the direction same as the exciting currents. Therefore, the fields will be LHC polarized for clock-wise orientation of arms and RHC polarized for counter clock-wise orientation of arms [1,2].

3.5 Backing Cavity Design

It was stated that the spiral antenna has a bi-directional radiation pattern theoretically but in practical applications a unidirectional radiation is required. This can be achieved by mounting the spiral element onto the aperture of a cylindrical metallic cavity. The diameter of the cavity d_c is slightly larger than the

diameter of the spiral antenna at the lowest operating frequency. At $f=f_{low}$ $d_c=q\lambda/\pi$ where q is a factor ranging from $1<q<2$. The gain of the antenna considering the end loading of spiral arms approaches +4 dBli (relative to linear isotropic source) and the boresight axial ratio approaches to 1.5 dB at the same time, as the cavity diameter approaches to half wavelength ($d_c=0.5\lambda$). For $d_c=\lambda/\pi=0.318\lambda$ gain of the antenna G=-4 dBli and the axial ratio is 5 dB [20]. This implies an active radiating region of 0.18λ wide. The depth of the cavity should be ideally $\lambda/4$ so that the wave reflected from the bottom of the cavity are in phase with the wave in the desired direction. Note that during the reflection an extra π radians phase shift is acquired in addition to $\pi/2+\pi/2=\pi$ radians path-length phase shift with the conclusion of the image principle. The cavity depth is a characteristic dimension dependent upon the wavelength so the frequency independent characteristics of the antenna are destroyed. Consequently, empty cavities are appropriate only for narrow band spirals. For wide band applications (40:1 for instance), cavity should be loaded with a microwave absorber. Disadvantage of this method is the reduction of the gain approximately 3 dB since the half of the radiated power is fully absorbed [1,2].

3.6 Feed Circuit

A feature of complementary structures concerning their input impedance is as follows [1,7]. Consider a metal antenna with input impedance Z_{metal}. A complementary structure can be formed which is an antenna with air replacing the metal and metal replacing air and its input impedance will be Z_{air}. Using Babinet's principle that the impedance of complementary antennas are related as follows

$Z_{air}Z_{metal}=\eta^2/4$ (η is the free space intrinsic impedance)

If an antenna and its complement are actually same, they are called self-complementary and their impedances are equal.

$Z_{air}=Z_{metal}=\eta/2=188.5\ \Omega$

This relationship is frequency independent, and also holds true for the impedance matrix of the n-arm spiral antenna. On the other hand, it turns out that many frequency independent antennas are not ideally self-complementary and still have relatively constant impedance [1].

Since the spiral antenna with antiphase feeding presents a balanced load, the feeder should be a balanced transmission line with the characteristic impedance nearly about 60π=188.5 ohms ideally. But this value cannot be easily obtained practically. Due to the loading effect of dielectric substrate the impedance of the antenna reduces to $188.5/\sqrt{\varepsilon_r}$ =130 Ohms approximately for a dielectric constant of 2.2. It is different from the RF Ohmic resistance value given in Appendix D. In practice, we almost always need an unbalanced 50 ohms coaxial input connector to the antenna. Thus, a wide-band 130 ohms to 50 ohms balun becomes an essential component of the antenna. The most popular baluns are printed circuit version of Marchand's balun and the tapered coaxial balun [2,8]. Second one has the advantage that, it is simple to realize and transforms the impedance at the same time, disadvantage is that the length of the balun should be 0.5λ at the lowest operating frequency. Short baluns cause an unbalance at the feed point of the antenna, which has an adverse effect on axial ratio and produces beam squint (departure of electrical boresight from geometrical boresight). The beam squint is about 3° for good baluns and may increase to about 10° for poor baluns [2].

CHAPTER 4

ANTENNA MEASUREMENT TECHNIQUES

4.1 Input Return Loss and VSWR Measurements of Spiral Antennas

The input return loss and VSWR measurements of spiral antennas are made using HP® 8722 D Vector Network Analyzer. The measurement setup is shown in Figure 4.1. The network analyzer is calibrated by connecting open, short and load connectors to port-1, setting up the start and stop frequencies to 0.5 GHz and 18 GHz respectively [3].

It is important to keep the beam of the antenna clear from the objects that can cause reflections and affect the input return loss [3].

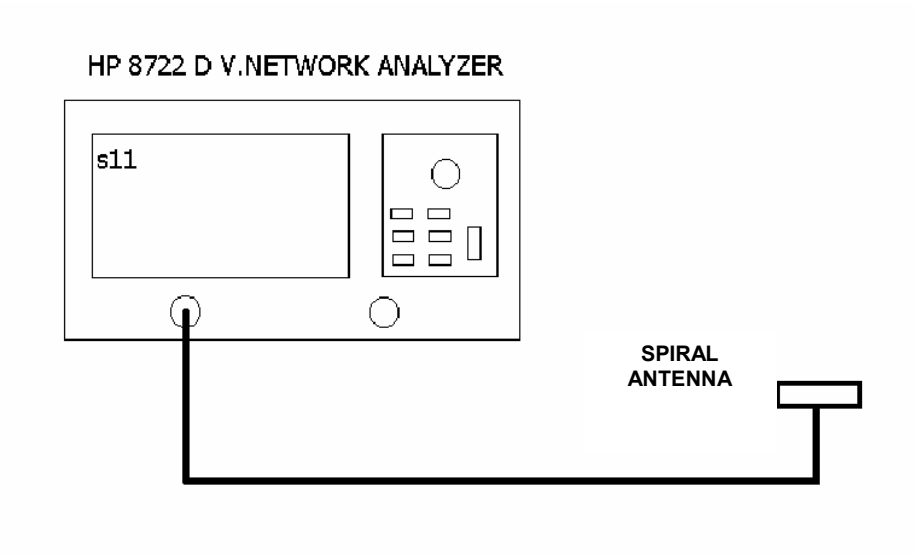

Figure 4.1 Input Return Loss Measurement Setup for Spiral Antennas [3]

4.2 Anechoic Chamber

Radiation pattern and polarization measurements of spiral antennas are made in an anechoic chamber shown in Figure 4.2. Anechoic chamber is a media that has very low-leveled reflection of electromagnetic waves from the walls of the room covered by the absorbers [1,3].

There are two types of anechoic chambers designed for antenna measurements: the rectangular and the tapered anechoic chamber. The top view of anechoic chamber in ASELSAN® Inc. and measurement setup is shown in Figure 4.2 and Figure 4.3 respectively [3,9].

The tapered anechoic chamber is designed in the shape of pyramidal horn that tapers from the small source end to a large rectangular test region, and with high quality absorbing material covering the side walls, floor and ceiling. The tapered anechoic chamber in the R&D department of ASELSAN® Inc. is used with an azimuth over elevation positioner holding up the antenna under test, a polarization positioner holding up the standard transmitter antenna, an HP® 8722 D model vector network analyzer, a Xerox® printer, and HP®PII series computers using programs written in HP®VEE program at ASELSAN® and which communicate with the above listed equipment through the aid of HP®-IB's [1,3,9].

4.3 Gain Measurement Techniques

The power gain of an antenna is 4π times the ratio of the power radiated per unit solid angle in the direction of maximum radiation to the net power accepted by the antenna from its generator. Two general categories of gain measurement methods exist. These are the "absolute-gain measurements" and the "gain transfer measurements" [3]. The first method is used when extremely high accuracies are necessary and is usually employed in laboratories that specialize in the calibration of standards. Here we use the second method in which the gain of the antenna under test is measured by comparing it to that of the standard gain antenna [3].

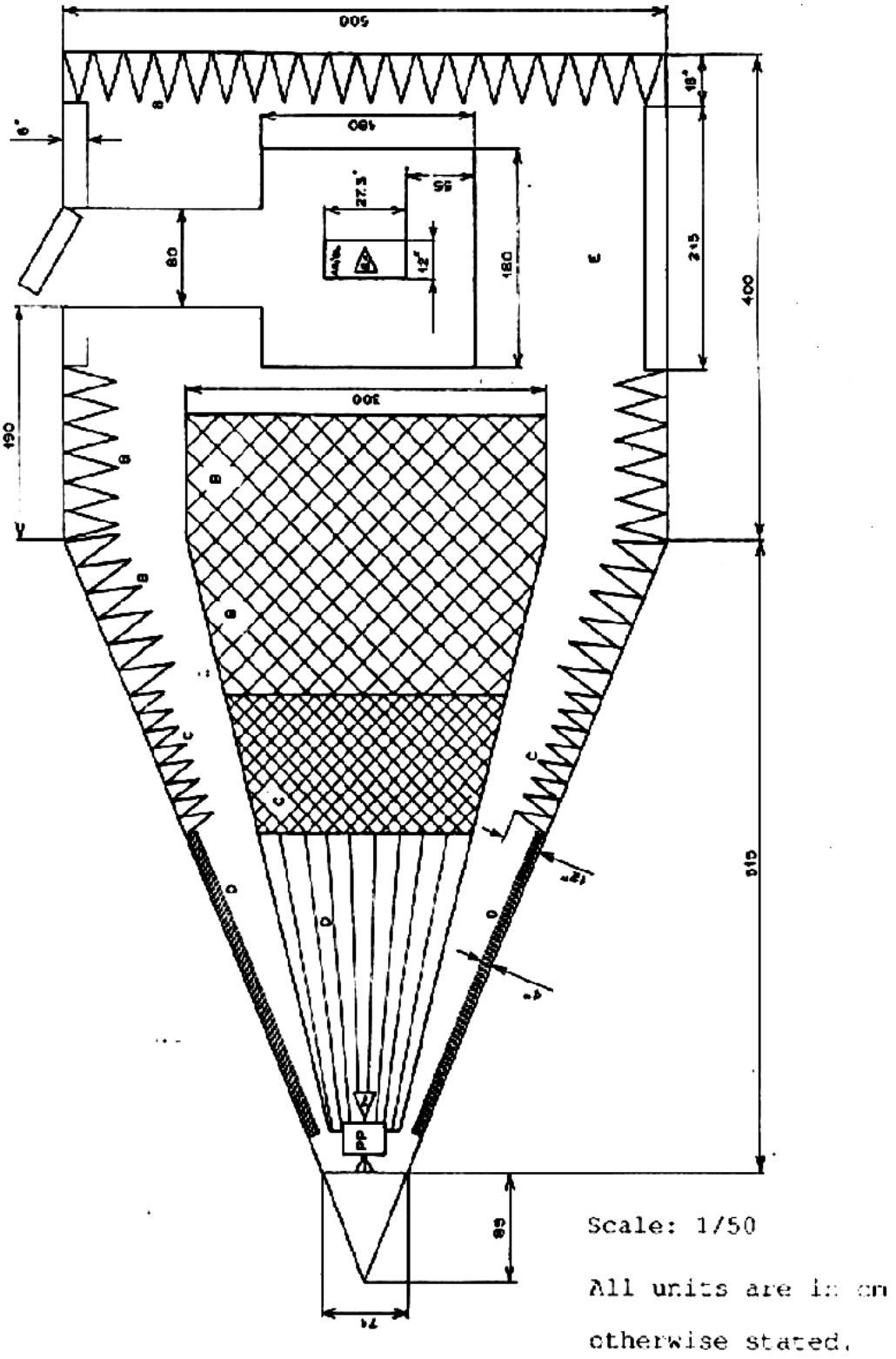

Figure 4.2 Top view of the Tapered Anechoic Chamber in ASELSAN® Inc [3,9].

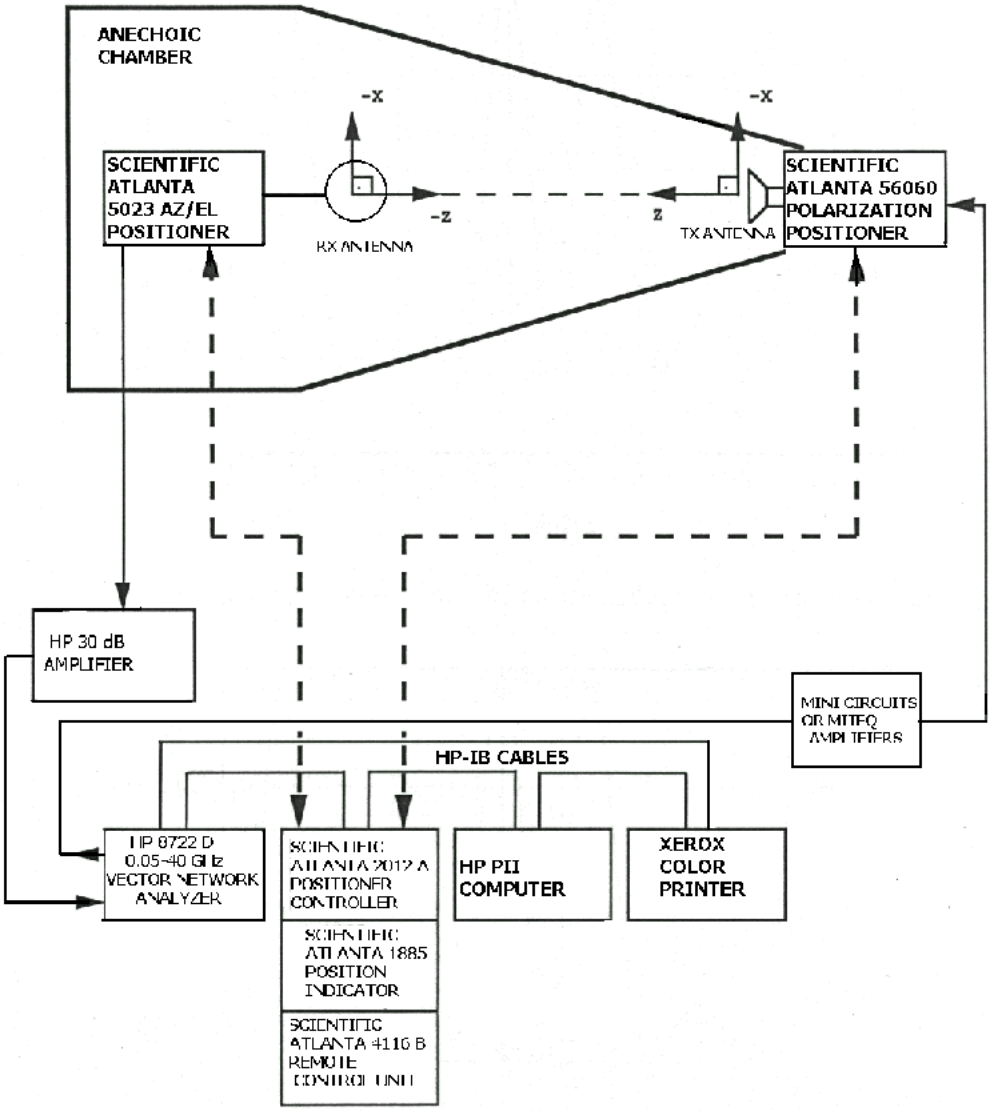

Figure 4.3 Antenna Measurement Setup in Anechoic Chamber [3,9]

The antennas to be used as gain standards must have the following properties:

- The gain of the antenna must be accurately known
- The antenna must have a high degree of dimensional stability
- The antenna must be linearly polarized.

From the Friis transmission formula it can be shown that the power gain $(G_T)_{dB}$ of the test antenna, in decibels, is given by

$$(G_T)_{dB} = (G_S)_{dB} + 10\log\left(\frac{P_T}{P_S}\right) \tag{4.1}$$

where $(G_S)_{dB}$ is the power gain of the gain standard antenna, P_T is the power received with the test antenna, and P_S is the power received with the gain standard antenna [3].

The power gains of circularly and elliptically polarized antennas are usually measured with the use of linearly polarized gain standards. In case of elliptically polarized antennas a difference of as much as the ellipticity ratio in decibels might occur. However, the circularly and elliptically polarized electric fields can be separated into two orthogonal linearly polarized components, and both can be measured separately. Thus, a single linearly polarized gain standard antenna can be employed and rotated $\pi/2$ radians to achieve two orthogonal measurements. From these partial power-gain measurements the total power gain $(G_T)_{dB}$ of the test antenna, in decibels, can be computed in the following manner:

$$G_T = \frac{G_S \cdot P_T}{P_S} \quad , \qquad P_T = P_{TV} + P_{TH} \tag{4.2}$$

hence

$$G_T = G_S \cdot \frac{(P_{TV} + P_{TH})}{P_S} \tag{4.3}$$

and

$$(G_T)_{dB} = 10\log(G_{TV} + G_{TH}) \tag{4.4}$$

Where G_{TV} and G_{TH} are the partial power gains with respect to vertical linear polarization and horizontal linear polarization, respectively [3,9,10].

In order to cover most of the 0.5-18 GHz frequency range a standard gain horn antenna (whose gain values with respect to frequency are given in Table 4.1) manufactured by Q-PAR Angus® were used:

Table 4-1 Gain values of horn antenna with respect to frequency

FREQUENCY (GHz)	GAIN (dBli)
1.5	7
2	11.6
3	14.3
4	16.5
5	17.7
6	18.7
7	20.1
8	20.4
9	21
10	20.8
11	20.9
12	21
13	22.4
14	23.2
15	23.9
16	23.2
17	22.7
18	24.2

4.4 Polarization Measurements

Polarization is a property of single-frequency electromagnetic radiation describing the shape and orientation of the locus of the extremity of the field vectors as a function of time [3,18].

There are several sources of error that will reduce the polarization purity (increase axial ratio above 0 dB). These include phase and amplitude errors in the orthogonal linear components, components that are not exactly orthogonal, and components that are elliptically polarized rather than perfectly linear.

The linearly polarized dipole source antenna is excited by a transmitter and illuminates the test antenna. The test antenna is in the far field of the source. The dipole essentially produces an electric field parallel to the dipole wire and then projected onto the sphere. Any plane containing the dipole in the z axis also contains the electric field vector; this is the E plane. The magnetic field intensity vector, H, must be perpendicular to the electric field and the Poynting vector which points radially away from sphere. This means the H plane (xy plane) magnetic field is parallel to the xy plane and tangent to the sphere [3,11].

There are several methods like polarization pattern or rotating source, but the method used in this thesis is polarization pattern method so detailed information is given only for this method.

4.4.1 Polarization Pattern Method

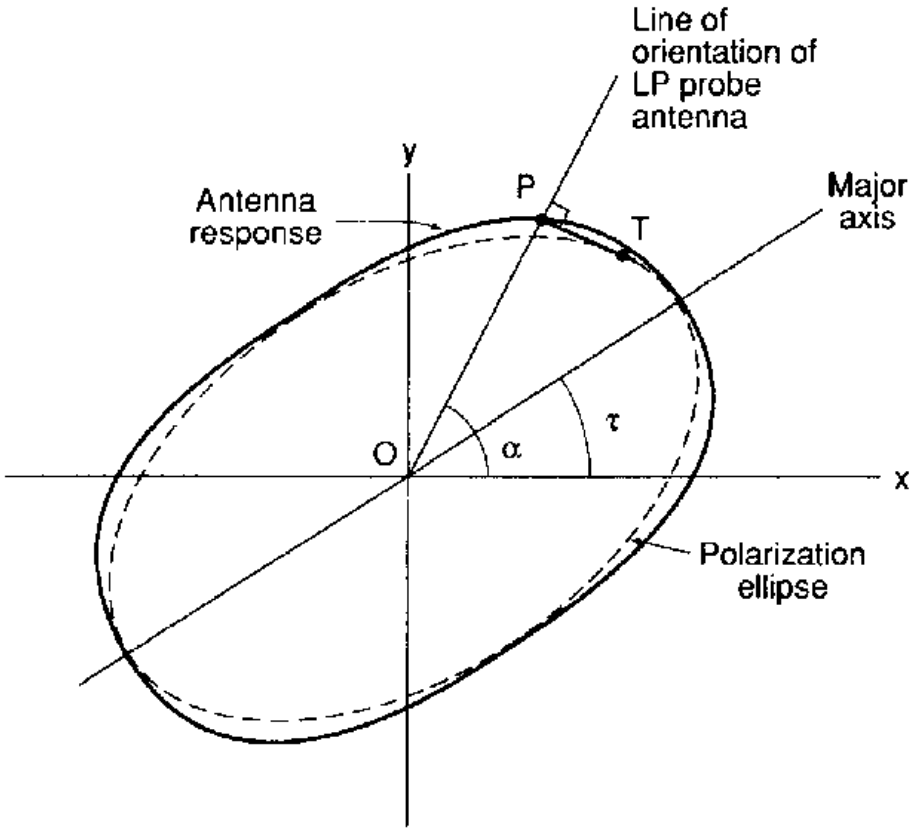

Figure 4.4 Polarization pattern (solid curve) of an elliptically polarized test antenna. It is the response to an incoming LP wave with orientation angle α. Polarization ellipse for the test antenna is also shown (dashed curve) [3].

Polarization pattern of an antenna is the amplitude response of an antenna as it is rotated about its axis when illuminated by a linearly polarized plane wave. The pattern is a polar plot of the response as a function of the relative angle between the illuminating LP wave orientation and a reference orientation of the antenna. Actually, it is easier to explain the polarization pattern with the test antenna operated as an elliptically polarized transmitting antenna and the receiving antenna as a linearly polarized probe. Reciprocity permits us to do this. The tip of the instantaneous electric field vector lies on the polarization ellipse and rotates at the frequency of the wave; that is, the electric vector completes ***f*** rotations around

the ellipse per second. The LP probe response (rms output voltage) is proportional to the projection of the peak of the electric field onto the LP orientation line at angle α. This is the distance OP in Figure 4.4 projected from the tangent point T on the ellipse. The locus of points P as the LP probe is rotated is fatter than the ellipse. Of course, for a CP antenna both curves are circular.

Note that the maximum and minimum of the polarization pattern are identical to the corresponding maximum and minimum of the polarization ellipse (when scaled to the same size). Although the measured polarization pattern does not give the polarization ellipse, it does produce the axial ratio magnitude of the antenna polarization, it is also obvious from Figure 4.4 that the tilt angle of the ellipse is determined as well. The polarization pattern produces the axial ratio magnitude,$\mathbf{R}$, and tilt angle,$\boldsymbol{\tau}$, of the polarization ellipse, but not the sense.

The sense can be determined by additional measurements. For example, two nominally CP antennas that are identical except for sense can be used as receiving antennas with the test antenna transmitting. The sense of the antenna with the greatest output is then the sense of the test antenna.

The polarization pattern method in many cases is a practical way to measure antenna polarization. If the test antenna is nearly circularly polarized, the axial ratio is near unity and measured results are insensitive to the purity of the LP probe. If the test antenna is exactly circular, tilt angle is irrelevant.

In the case of a test antenna that is nearly linearly polarized, axial ratio measurement accuracy depends on the quality of the LP probe, which must have an axial ratio much greater than that of the test antenna [3,11].

CHAPTER 5

IMPLEMENTATIONS AND MEASUREMENTS OF SPIRAL ANTENNAS WITH DIFFERENT DESIGN PARAMETERS

5.1 Introduction

In this thesis, it is very crucial that usual spiral antenna size should be reduced without losing its radiation pattern, polarization, gain and wide band characteristics.

At the beginning, a new design approach was thought as the matter of study and I planned to consider new spiral antenna designs. So, as the first step of design, simulations of spiral antenna structures in Ansoft® HFSS™ program are planned. Unfortunately, I could not achieve to my goal due to the complexity of spiral structure. Since, the spiral antenna was drawn using AutoCAD® program; the size of the imported "AutoCAD .dxf" file is too large to compute with Ansoft® HFSS™. Although I have reduced the detailed drawing of spiral antenna, simulation cannot be succeeded even if the simulation frequency values are chosen as small as possible. For every case, the resulted geometry was always too complex to be meshed. Consequently, I considered theoretical aspects and previous designs of spiral antennas and used them as a design guide for my study.

Three spiral antennas, whose critical design parameters are different, have been designed. But, in all of the designs there are some constant design parameters. These are "innermost arm width" and the "Archimedean arm width". Innermost arm width is limited to 0.1 mm since this size is the smallest considerable line thickness used in printed circuit boards (PCB). Archimedean arm

width is taken as 0.25 mm that is a reliable line thickness used in printed circuit boards. Equiangular arm is enlarging until it reaches the Archimedean arm width. At the same time, these parameters are same as with the spiral antenna whose size should be reduced [13].

Materials used as the PCB of the spiral antennas are Roger's® Duroid 5880 and Taconics'® duroid whose properties are given below:

- Roger's® Duroid 5880 with dielectric constant 2.2, copper metalization on one side with thickness 17.5 microns and insulation dielectric thickness of 381 microns.

- Taconics'® Duroid with dielectric constant 2.2, copper metalization on two sides with thickness 17.5 microns and insulation dielectric thickness of 381 microns.

Also Roger's® Duroid 5880 is chosen as the base material for reference spiral antenna and baluns of the spiral antennas. Since all of the dielectric constants are same for all materials, electromagnetic discontinuities between antenna and balun media are minimized.

5.2 AutoCAD® Drawing Tool

AutoCAD® is a mechanical drawing tool whose programming language AutoLISP® is used to draw PCB outlines of spiral antennas. Since AutoLISP® is powerful programming language, mathematical equations of spiral antennas are easily converged to artwork [3]. Using the AutoLISP® code that is written by Ekrem ORAN was used as the basis of spiral antenna designs in this study (see Appendix A for program details). It almost covers all details of a spiral antenna design including a sine modulation applied to spiral arms. This sine modulation is called "wiggle" and its amplitude is proportional to the ratio of simultaneous and outer most radii and user input "magnitude of wiggle". Also simple modifications

are applied to this program like width of feed detail; magnitude and number of wiggles. In addition, using this program the transition between Equiangular and Archimedean sections of spiral antenna is achieved; meaning innermost arm width is taken as 0.1 mm that is the limiting parameter of the design since it is the narrowest considerable thickness of lines in PCB technology. It enlarges until it reaches a reliable line thickness of 0.25 mm, which is the Archimedean arm width [13].

5.3 Manufacturing Techniques of Spiral Antennas

PCBs of spiral antennas are first drawn using AutoCAD® tool and their AutoCAD.dxf files are formed. After that these drawings are converted to GERBER® files that are the recognized file type by photo plotters. Using these photo plotters negatives of PCB drawings are obtained. Third step of the process is to expose the material of PCBs to ultraviolet light in order to make the material acid resistive using these negative films of drawings. Then by removing the film material is sunk into copper removing acid and PCBs' substrate areas are etched. Finally, circuit is gold or nickel plated in order to prevent oxidation of metallic parts [1,3].

After forming PCB of spiral antennas electromechanical mounting of antenna is realized. First, PCB of the balun is soldered to SMA connector and then to PCB of the antenna with the help of gold ribbons mounted on the soldering paths of two PCBs. Secondly, Eccosorb® AN 77 absorber and Rohacell® HF 71 foam is cut in desired dimensions with a hole centering each material. Spiral, balun and connector assembly is put into case of the antenna upon the assembly of absorber placed between two foam layers.

5.4 Designed Spiral Antennas

As it was stated before there are 3 spirals with different design parameters especially affecting the low frequency characteristics of the antennas. Variable

design parameters for these antennas are “outer radius, number of wiggles and distance between the arms of antenna at the feed point”. The design parameters of the antennas are given in Table 5.1. First one of the spiral antennas was implemented in ASELSAN® Inc. on PCB of Taconics’®. Second and third ones were implemented in LINTEK® Pty. Limited on PCB of Roger’s® Duroid 5880.

Spiral 1 has an outermost radius of 80 mm with peripheral length of P=473.4 mm (calculated by measuring the wiggle size in AutoCAD®) that corresponds to an electrical length of λ=473.4 mm and f=0.634 GHz.

Spiral 2 has an outermost radius of 85 mm with peripheral length of P=906 mm (calculated by measuring the wiggle size in AutoCAD®) that corresponds to an electrical length of λ=906 mm and f=0.336 GHz.

Spiral 3 has an outermost radius of 75 mm with peripheral length of P=870 mm (calculated by measuring the wiggle size in AutoCAD®) that corresponds to an electrical length of λ=870 mm and f=0.345 GHz.

Reference spiral antenna has an outermost radius of 108 mm with peripheral length of P=678.6mm that corresponds to an electrical length of λ=678.6 mm and f=0.442 GHz.

Table 5-1 Design parameters of spiral antennas.

NAME	MATERIAL	Feed Distance (mm)	Number of Wiggles	Mag. of Wiggle	Outer Radius (mm)
Spiral 1	Taconics’®	0.61	18	8	80
Spiral 2	Roger’s Duroid 5880®	0.4	100	8	85
Spiral 3	Roger’s Duroid 5880®	0.53	100	8	75
Ref. Spiral	Roger’s Duroid 5880®	0.79	-	-	108

Figure 5.1 Spiral antennas designed for this study and reference spiral

Figure 5.2 PCB of Spiral 1

Figure 5.3 PCB of Spiral 2

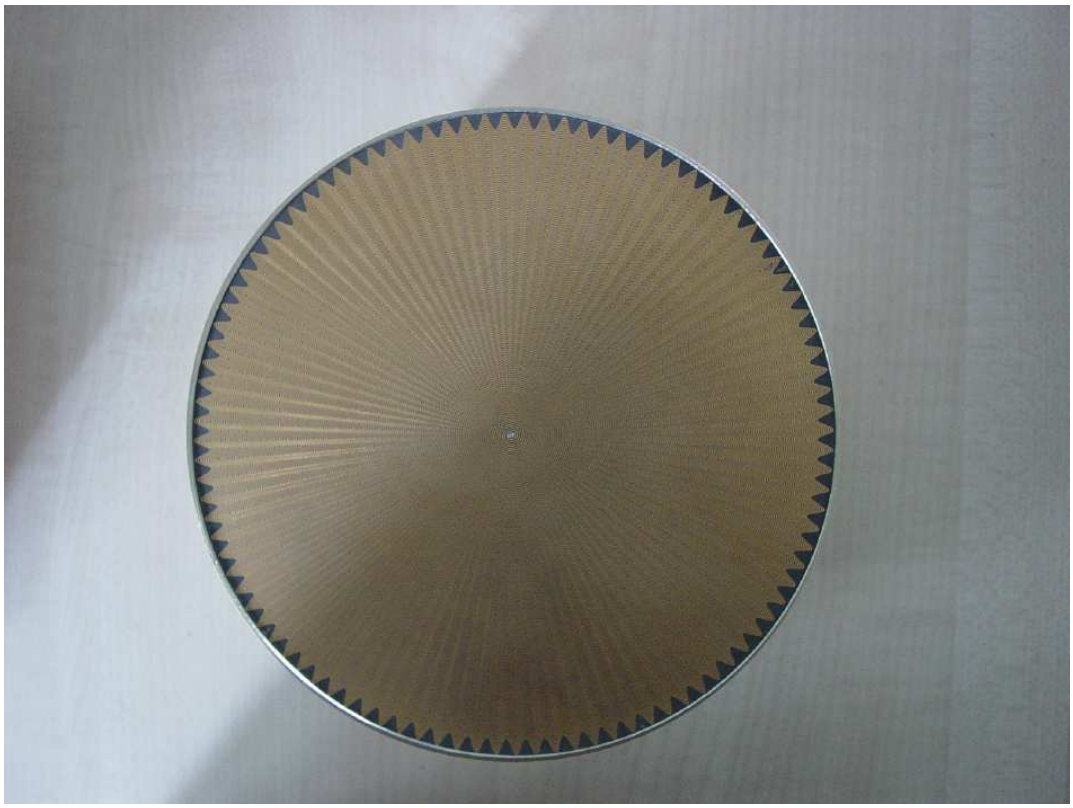

Figure 5.4 PCB of Spiral 3

5.5 Measurements of Spiral Antennas

5.5.1 Input Return Loss Measurements of Spiral Antennas

Input return loss and VSWR measurements of spiral antennas were performed using the simple method described in Section 4.1 and plotted to graphs below. (See Figure 5.5 and Figure 5.6)

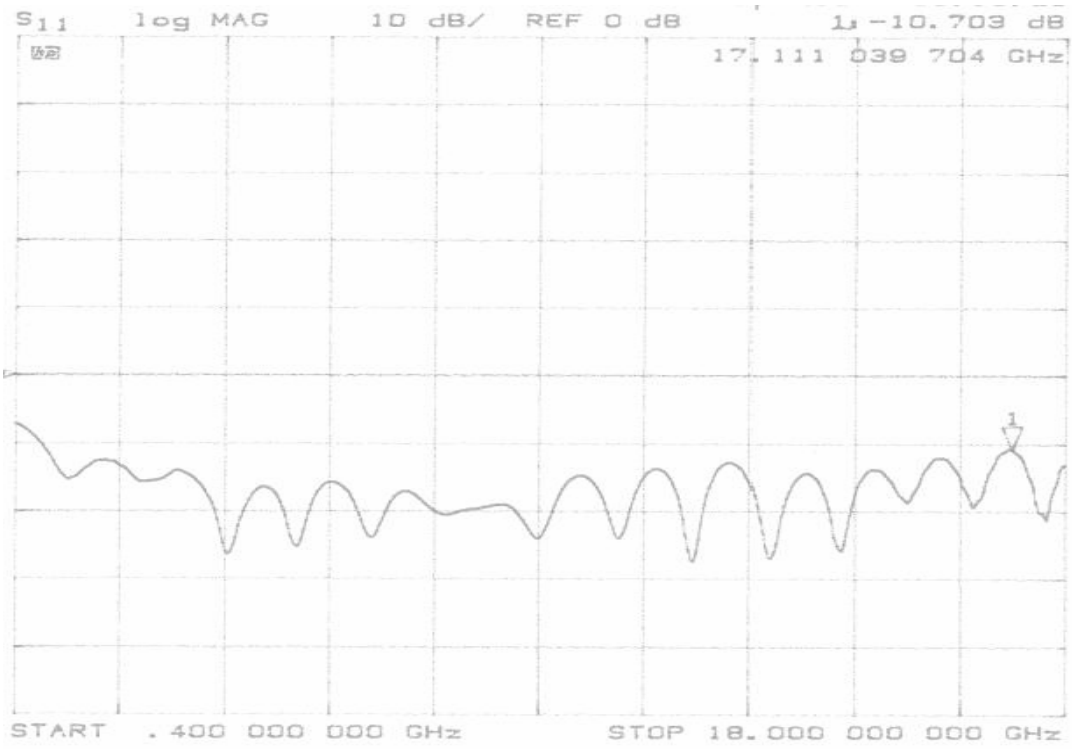
S11 log MAG 10 dB/ REF 0 dB
1: -10.703 dB
17.111 039 704 GHz
START .400 000 000 GHz
STOP 18.000 000 000 GHz

(a)

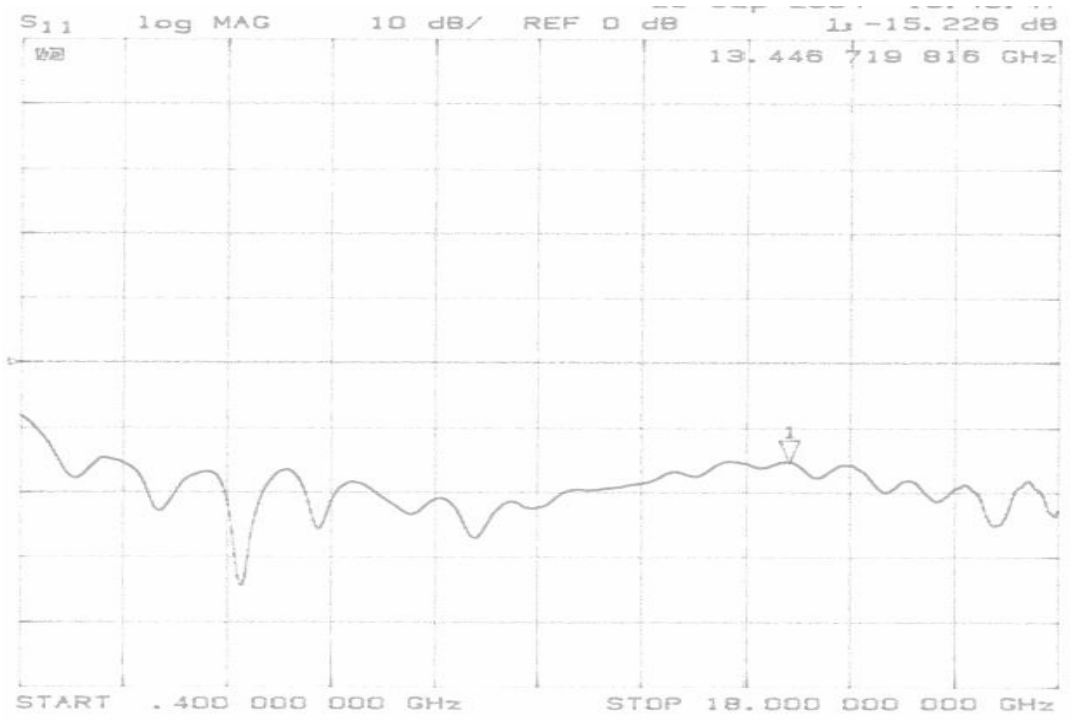
S11 log MAG 10 dB/ REF 0 dB
1: -15.226 dB
13.446 719 816 GHz
START .400 000 000 GHz
STOP 18.000 000 000 GHz

(b)

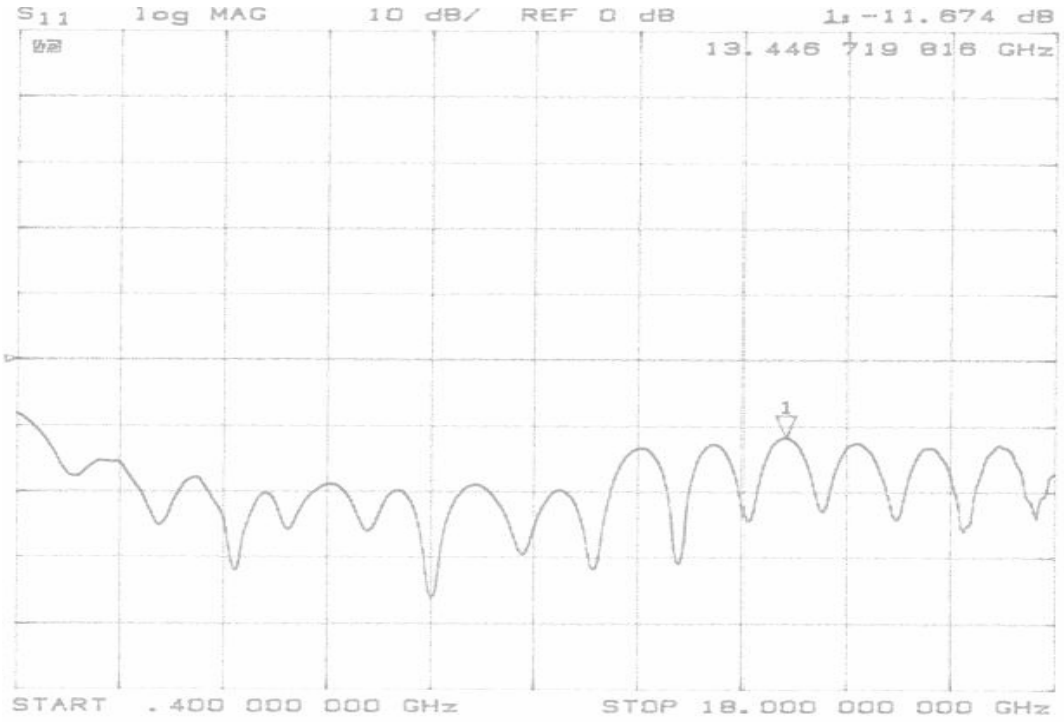

(c)

Figure 5.5 S11 versus frequency of Spiral 1 (a), Spiral 2 (b), Spiral 3 (c)

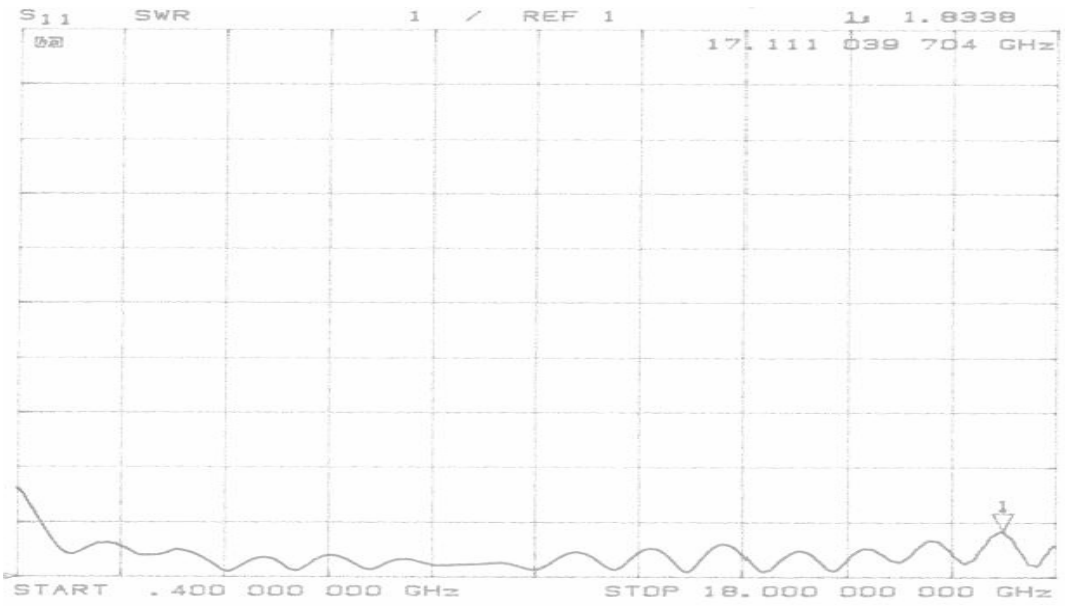

(a)

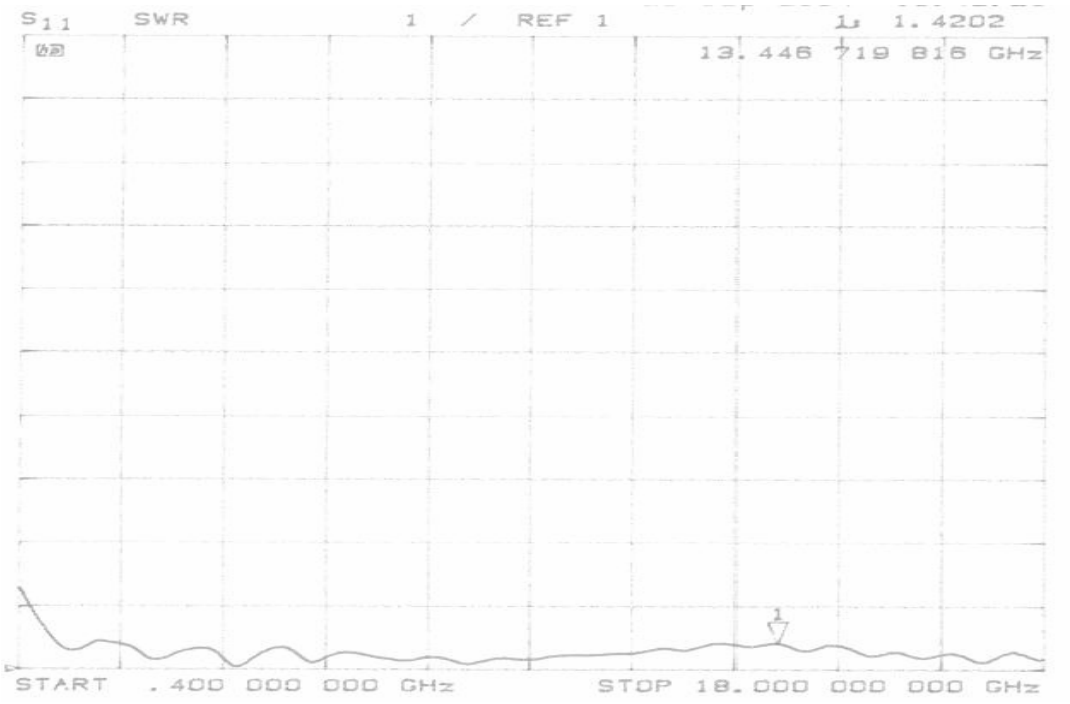

(b)

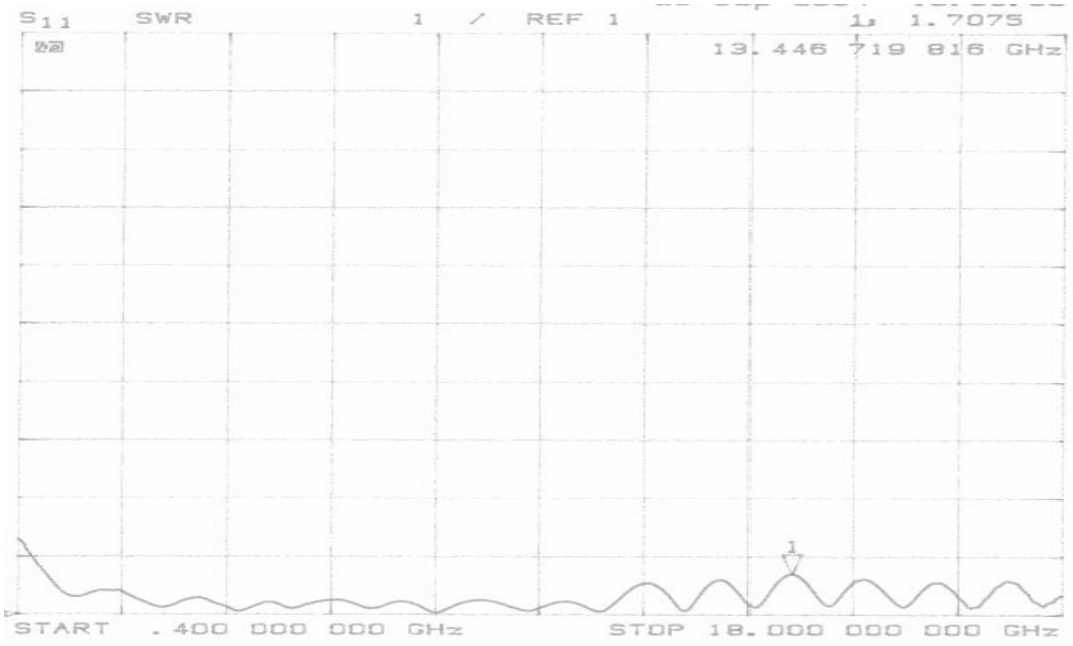

(c)

Figure 5.6 VSWR versus frequency of Spiral 1 (a), Spiral 2 (b), and Spiral 3 (c)

These measurements showed that the VSWR and return loss performance of the three spirals are nearly same. Small differences between the characteristics are arisen from the sensitivity of the soldering at the feed point of the antenna. Balun structure almost showed its performance as it was given in Chapter 2. Consequently, impedance matching of the antennas is well enough to radiate power efficiently. For all of the antennas VSWR value is smaller than 2, meaning nearly 90% of the incident power is transmitted into the feed of the spiral antenna.

5.5.2 Primitive Gain Comparison and Radiation Pattern Measurements of Spiral Antennas

Throughout these measurements, different configurations are considered regarding the position of the honeycomb; absorber and foam of the spiral antenna. Also different case sizes of spiral antennas are considered during the measurements. Gains of the spiral antennas are specified relative to the reference spiral especially for lower frequencies since the critical parameter for the size reduction was the lower cut off frequency.

Configuration 1 is given below Figure 5.7.

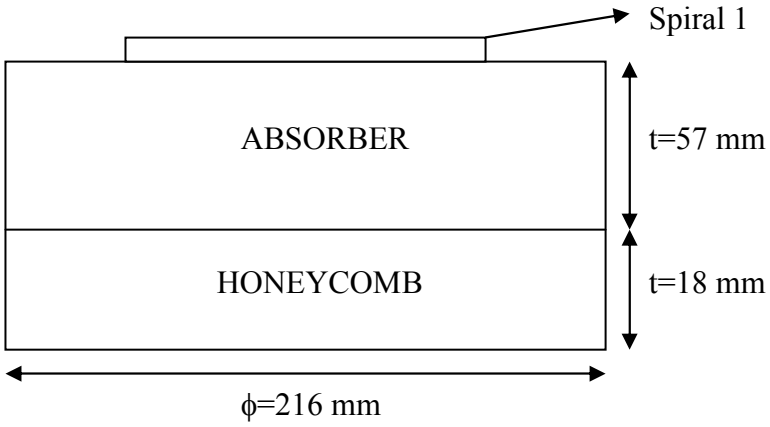

Figure 5.7 First assembly of Spiral 1

For this configuration radiation pattern measurements at some frequencies are given below Figure 5.8. As it can be seen from the graphs, axial ratio of spiral antenna is very low, the pattern symmetry is not corrupted and also pattern shape is almost smooth. But the gain of the spiral antenna compared to the reference spiral antenna, has been reduced, especially near the lower cut-off frequency as it was shown in Figure 5.9. This gain reduction is due to the absorption loss of the Eccosorb® AN–77 given in Figure 5.10. At lower frequencies (for f<1.8 GHz), absorption of the material is very low and so most of field is reflected. Consequently, this has a destructive effect on main field of the spiral antenna according to the image theory. This problem cannot be observed at higher frequencies (for f>4 GHz) as it was shown in Figure 5.11.

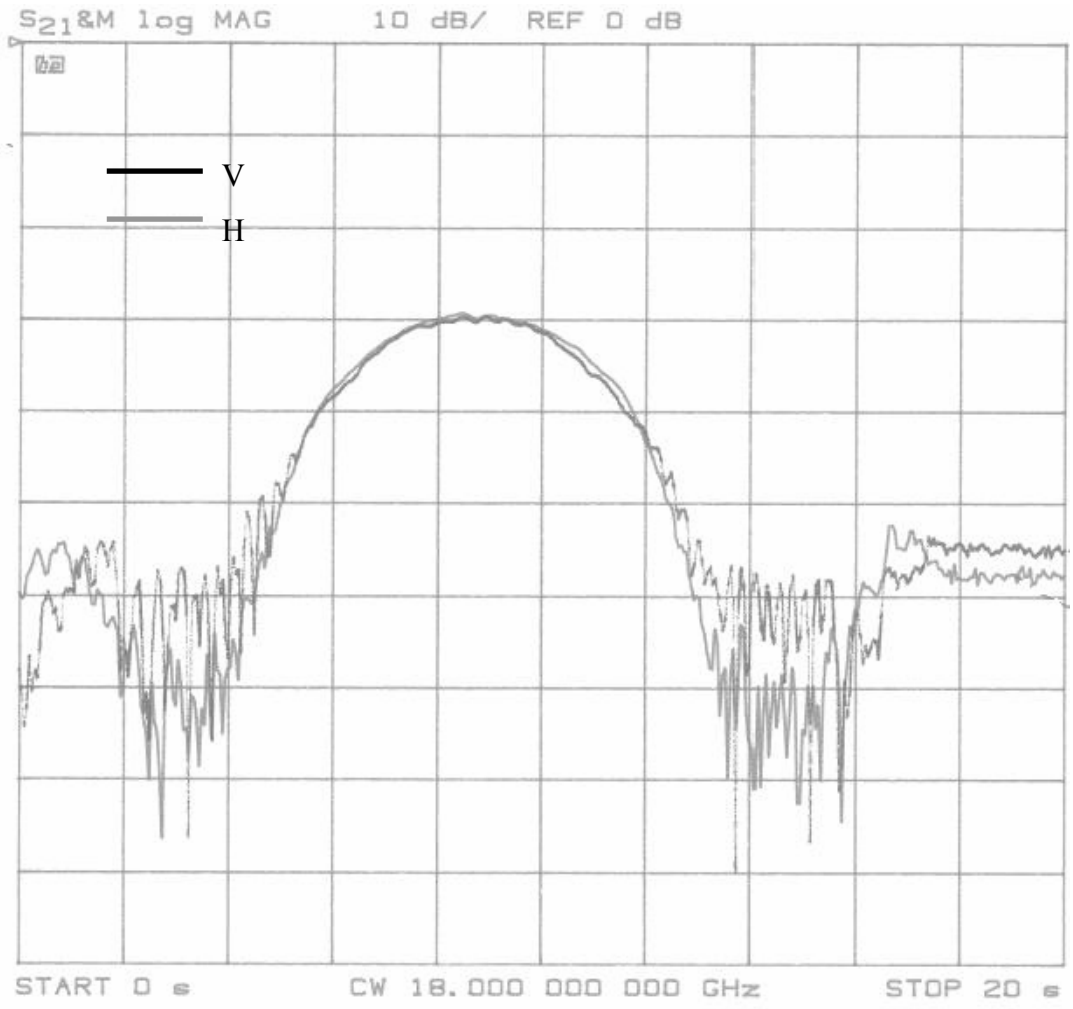

(a)

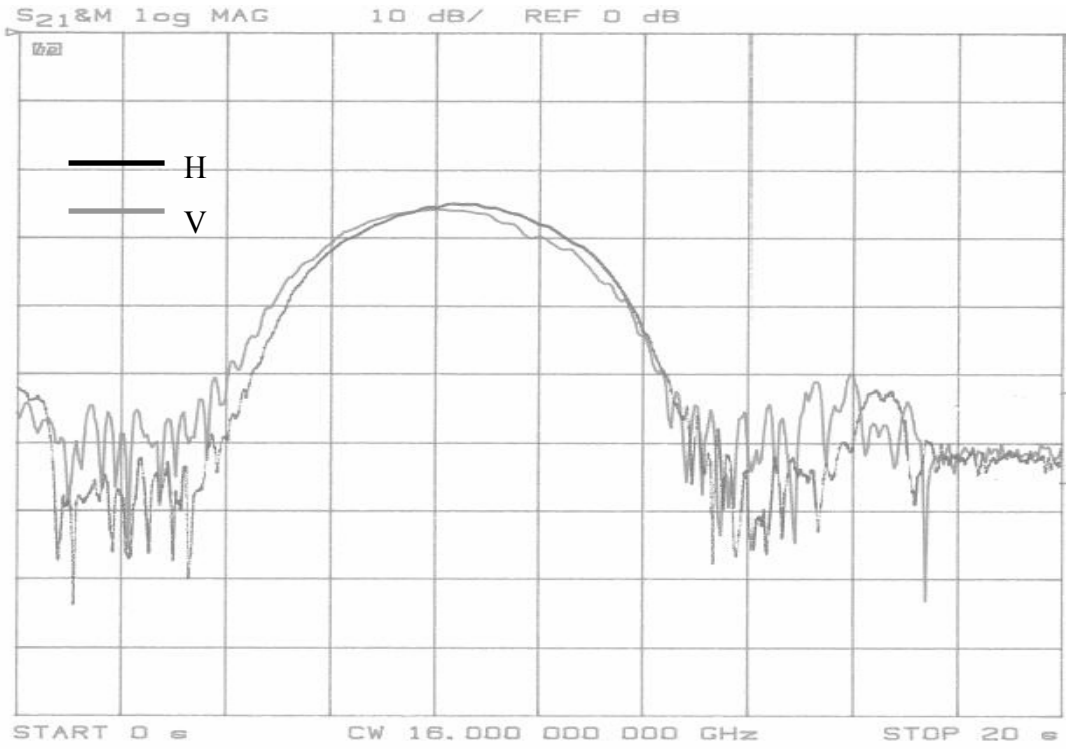
S21&M log MAG
10 dB/ REF 0 dB
H
V
START 0 s
CW 16.000 000 000 GHz
STOP 20 s

(b)

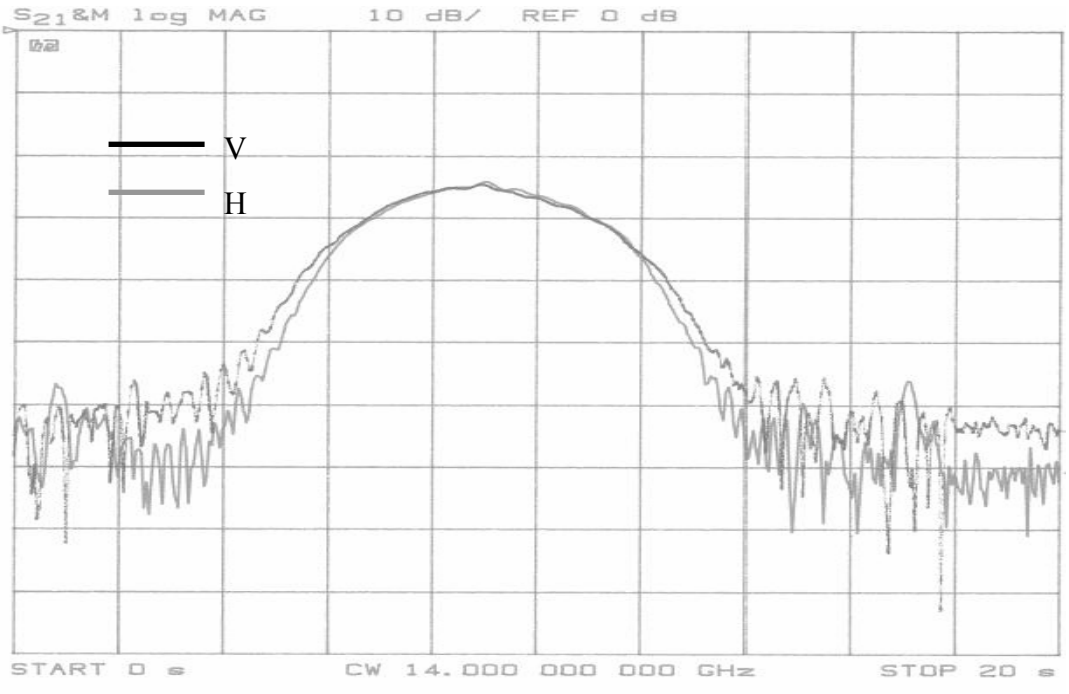
S21&M log MAG
10 dB/ REF 0 dB
V
H
START 0 s
CW 14.000 000 000 GHz
STOP 20 s

(c)

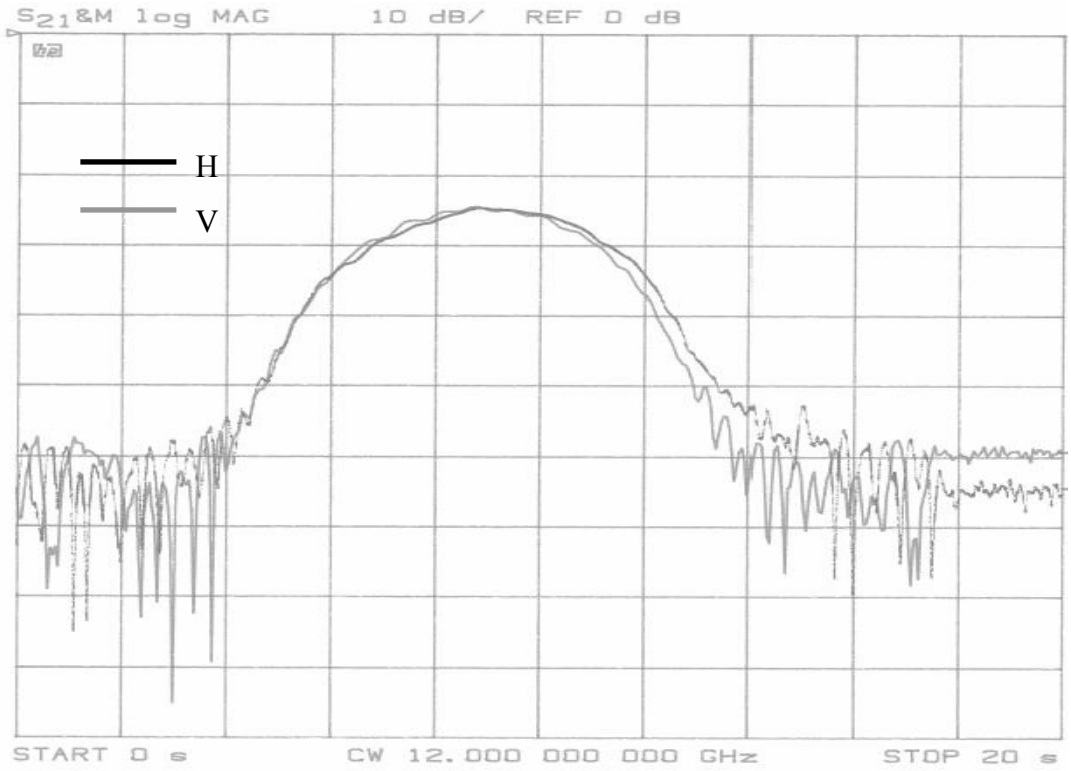
S21&M log MAG
10 dB/ REF 0 dB
H
V
START 0 s
CW 12.000 000 000 GHz
STOP 20 s

(d)

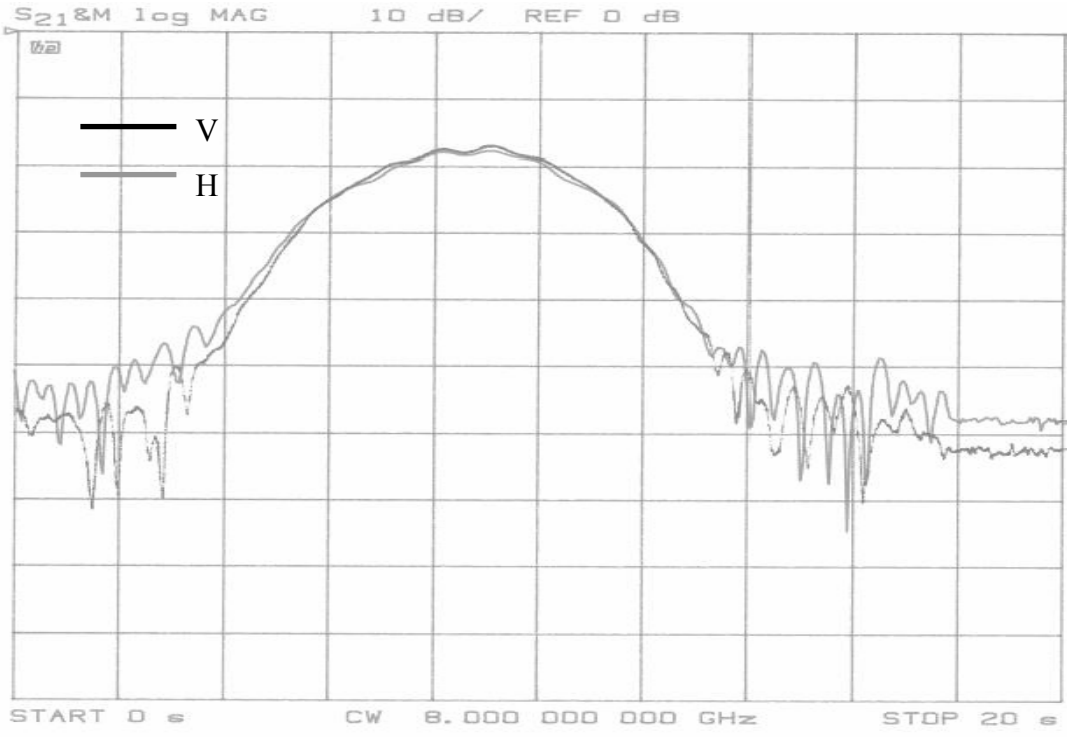
S21&M log MAG
10 dB/ REF 0 dB
V
H
START 0 s
CW 8.000 000 000 GHz
STOP 20 s

(e)

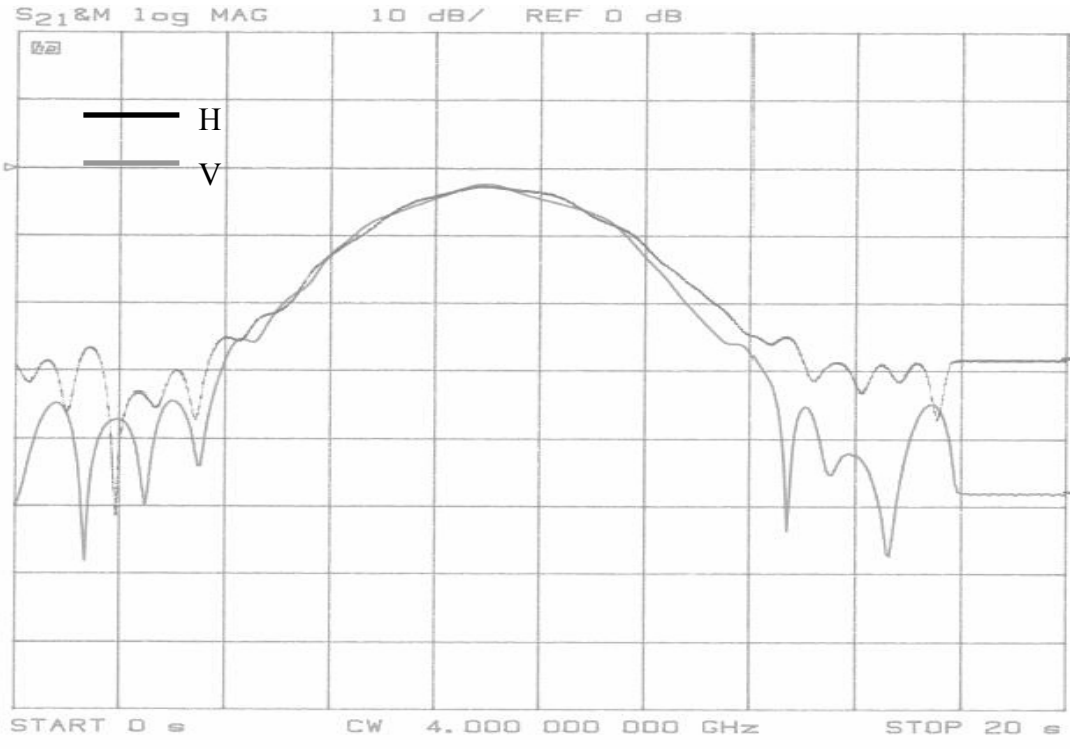
S21&M log MAG
10 dB/ REF 0 dB
H
V
START 0 s
CW 4.000 000 000 GHz
STOP 20 s

(f)

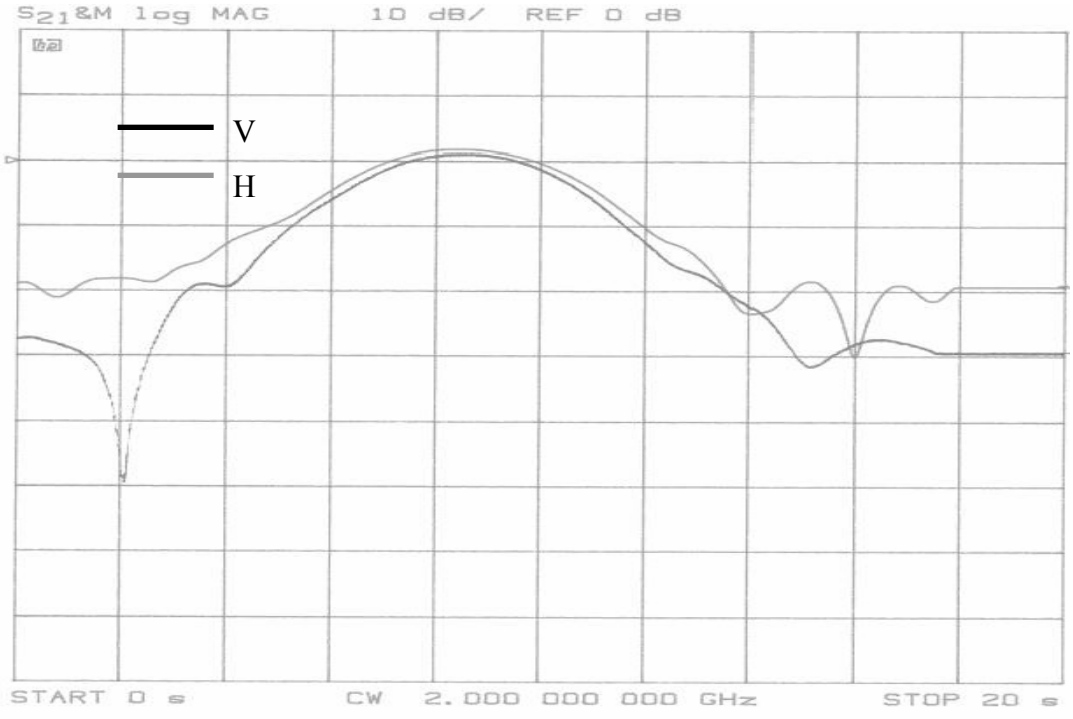
S21&M log MAG
10 dB/ REF 0 dB
V
H
START 0 s
CW 2.000 000 000 GHz
STOP 20 s

(g)

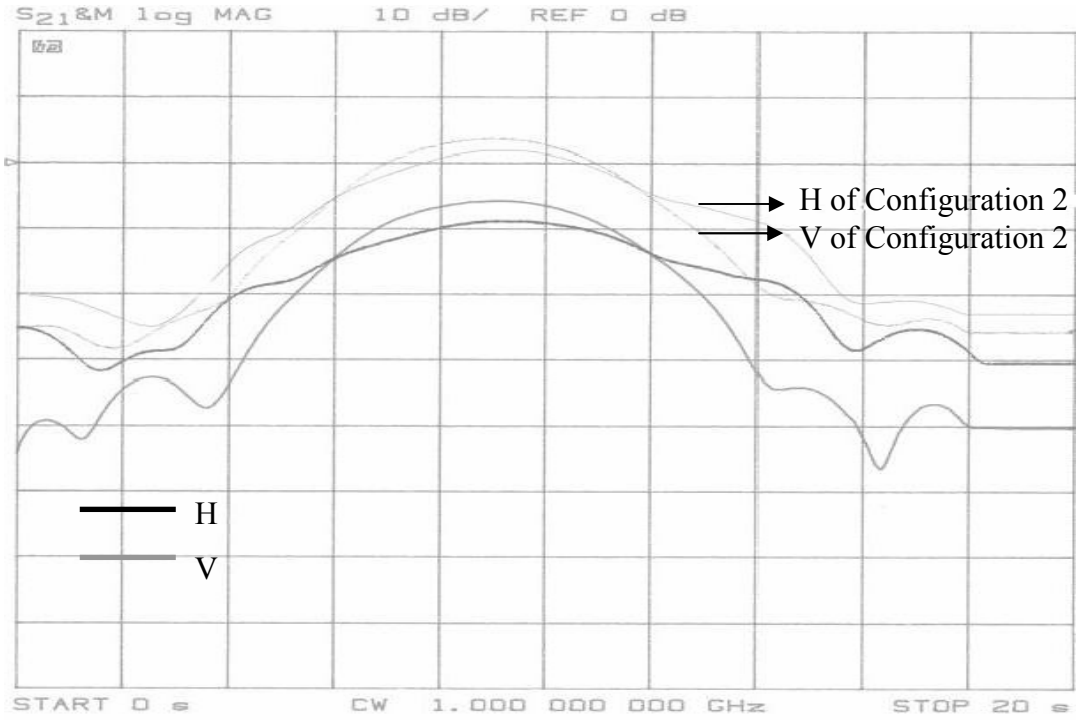

(h)

Figure 5.8 Radiation pattern of Spiral 1 at 18(a), 16(b), 14(c), 12(d), 8(e), 4(f), 2(g) and 1(h) GHz for vertical(V) and horizontal(H) transmitters (Configuration 1)

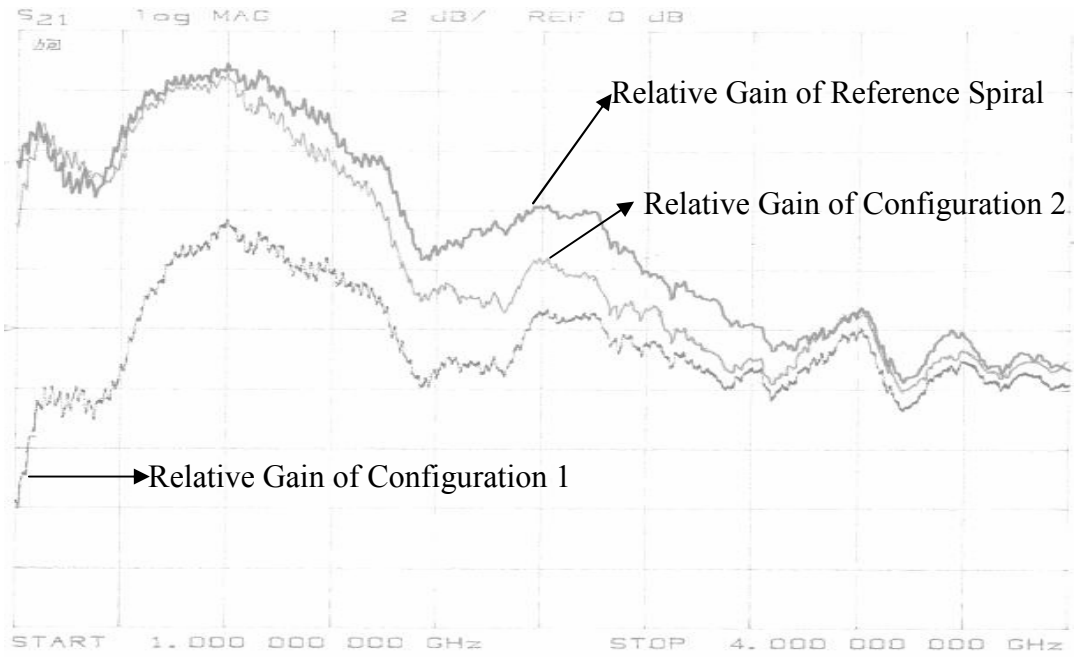

Figure 5.9 Relative gain of Spiral 1 for first and second assemblies compared to reference spiral antenna at lower frequencies

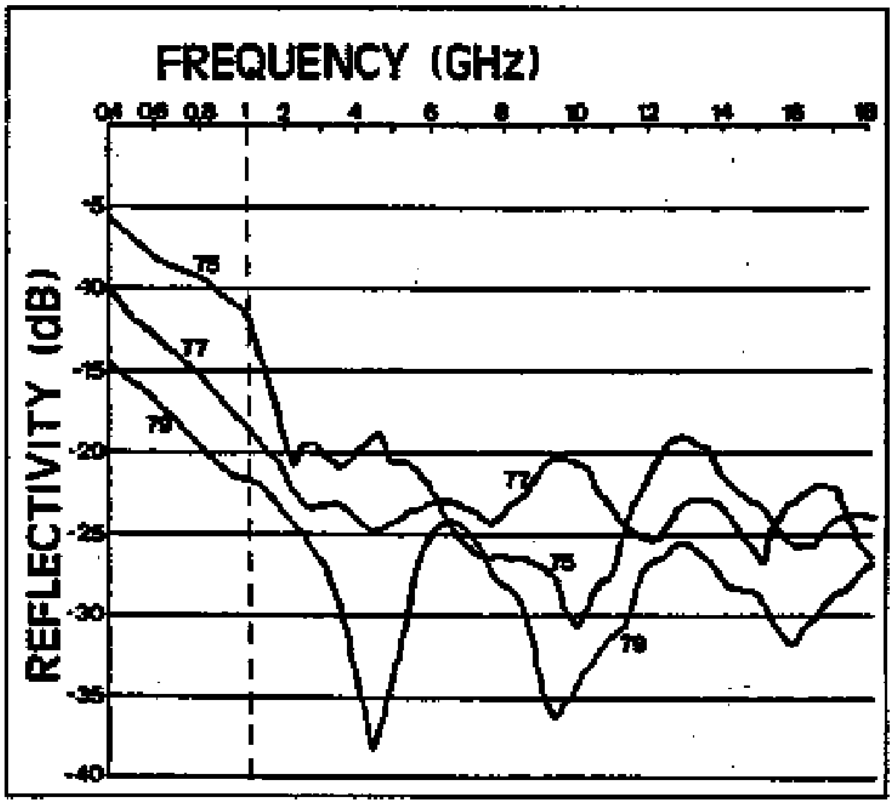

Figure 5.10 Reflectivity versus frequency characteristics of Eccosorb® AN-77 absorber [3]

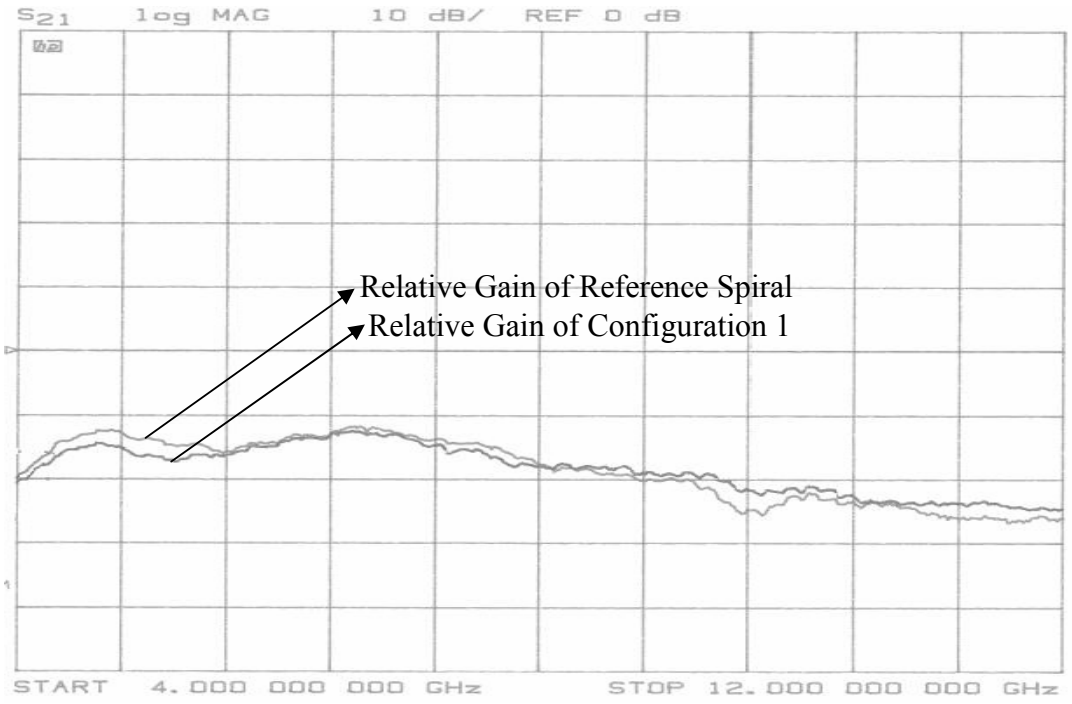

(a)

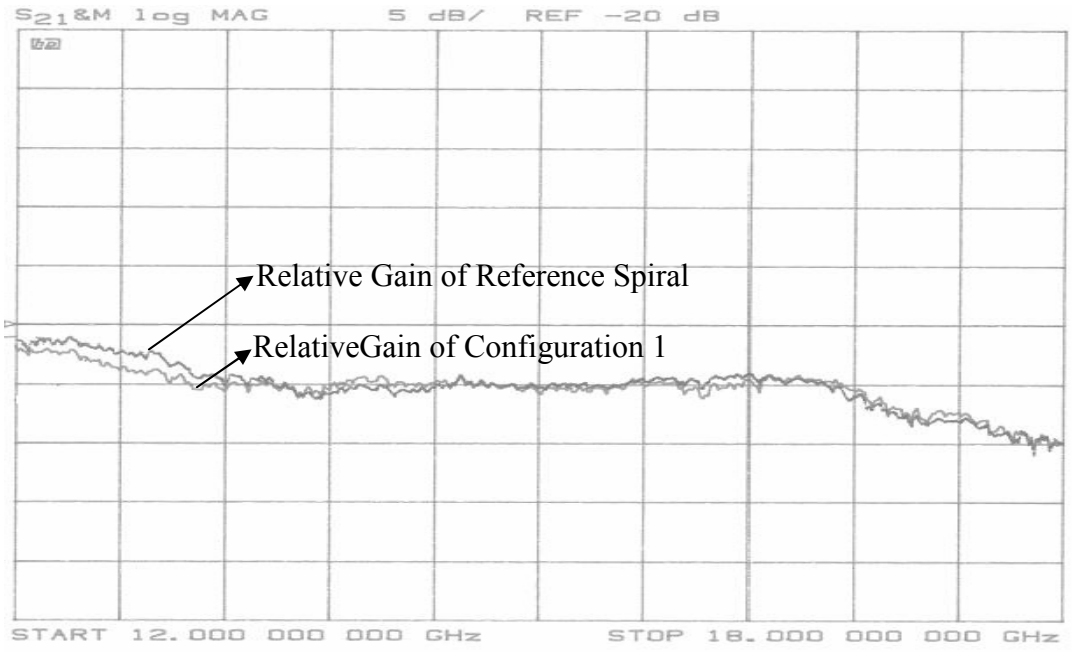

(b)

Figure 5.11 Relative gain of Spiral 1 for first assembly compared to reference spiral antenna at higher frequencies 4-12 GHz (a), 12-18 GHz (b)

Configuration 2 is given below Figure 5.12.

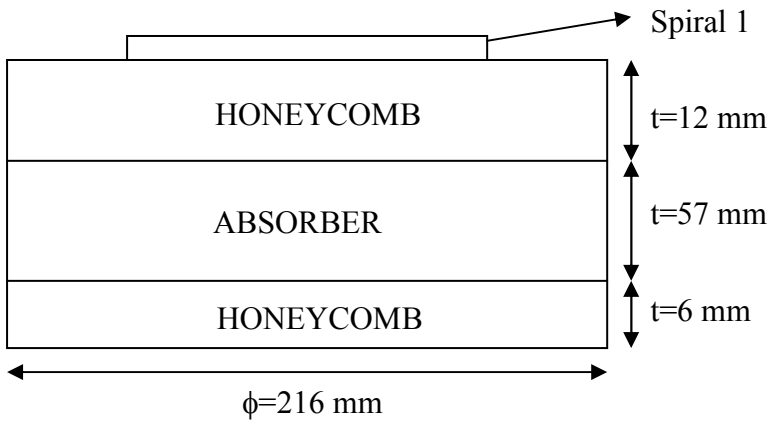

Figure 5.12 Second assembly of Spiral 1

First measurements were done for these two configurations. For the second case, the gain of the Spiral 1 is almost same as with the gain of the reference spiral. But, in this configuration, there are some radiation pattern distortions at higher frequencies especially for horizontally polarized electric

fields. At lower frequencies axial ratio value of the spiral antenna is very high. This is due to end-reflected currents radiated from the boundary of the case of the antenna. Using an absorber at the terminations of the arms will reduce this effect. Radiation pattern graphs and gain charts related with the second configuration are given below Figure 5.13 and Figure 5.14.

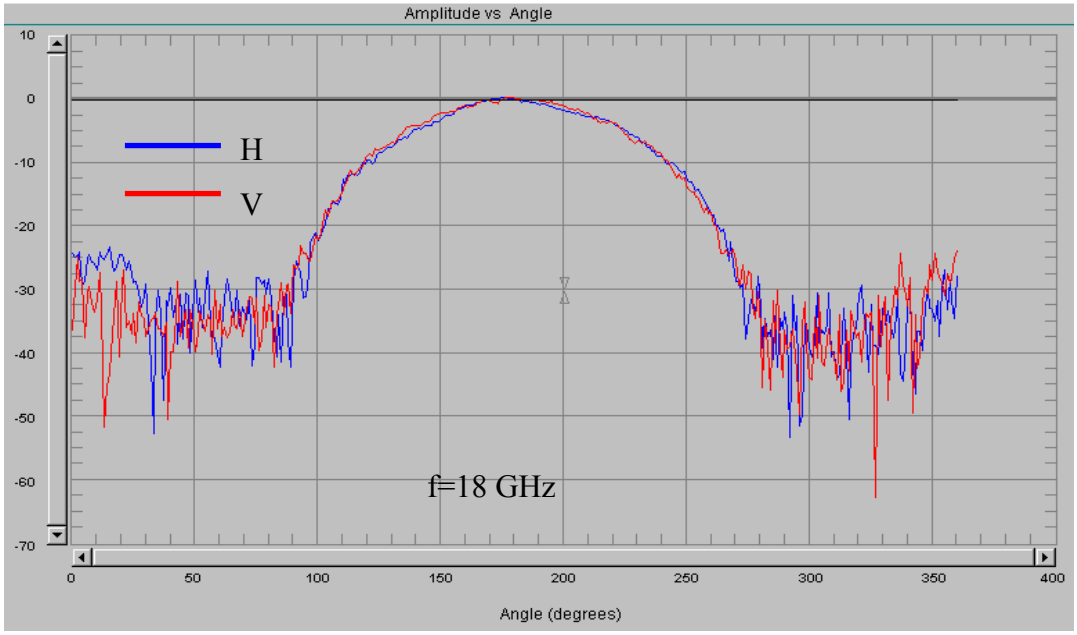

(a)

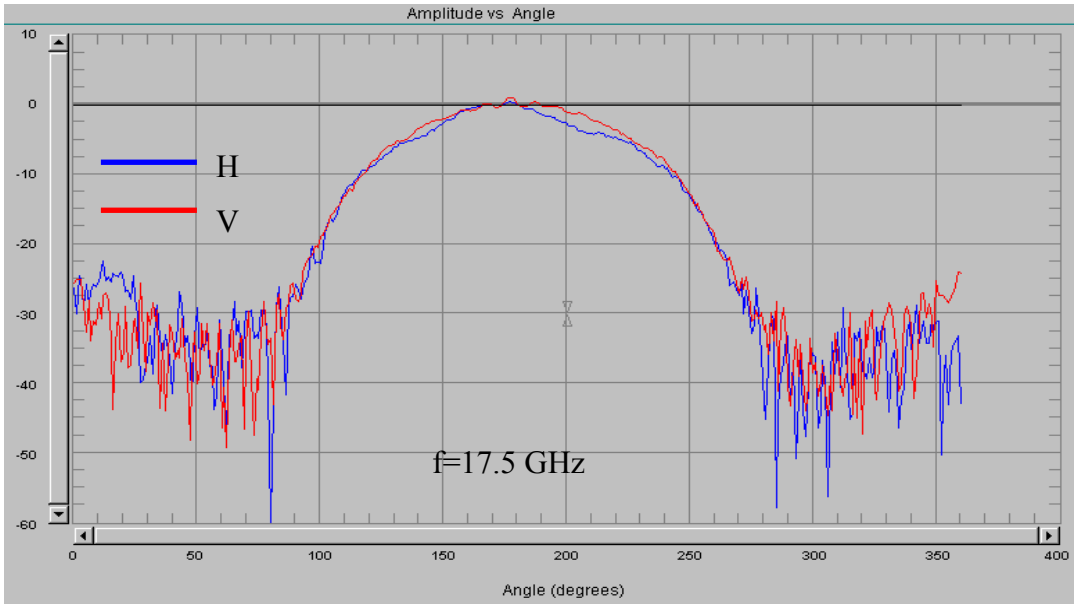

(b)

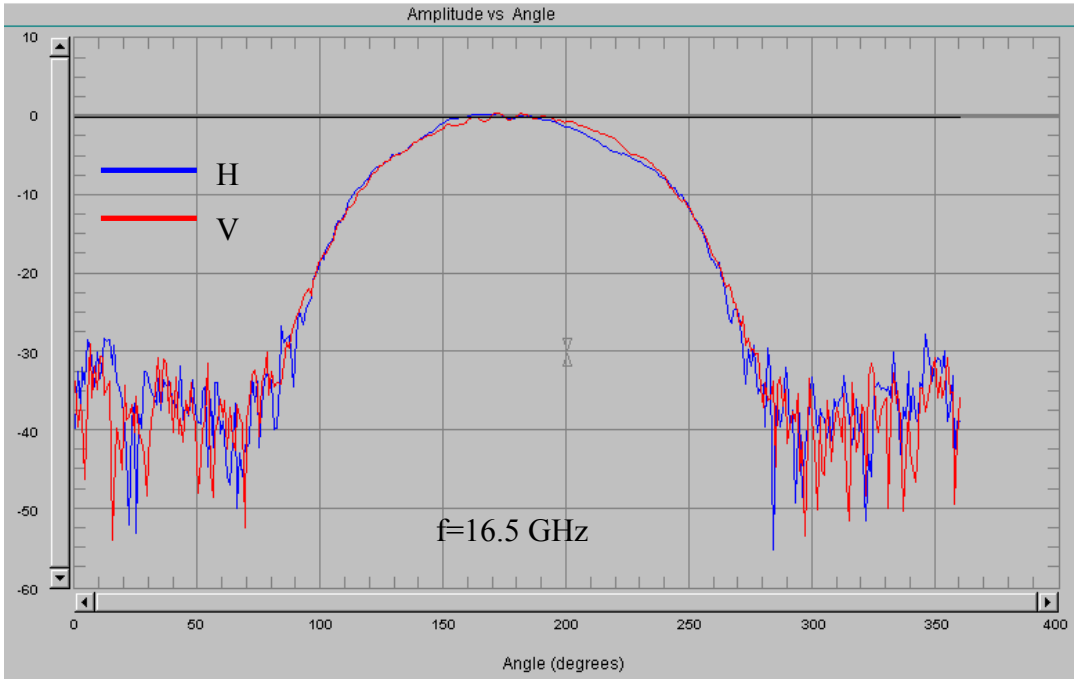
Amplitude vs Angle
10
0
-10
-20
-30
-40
-50
-60
H
V
f=16.5 GHz
0
50
100
150
200
250
300
350
400
Angle (degrees)

(c)

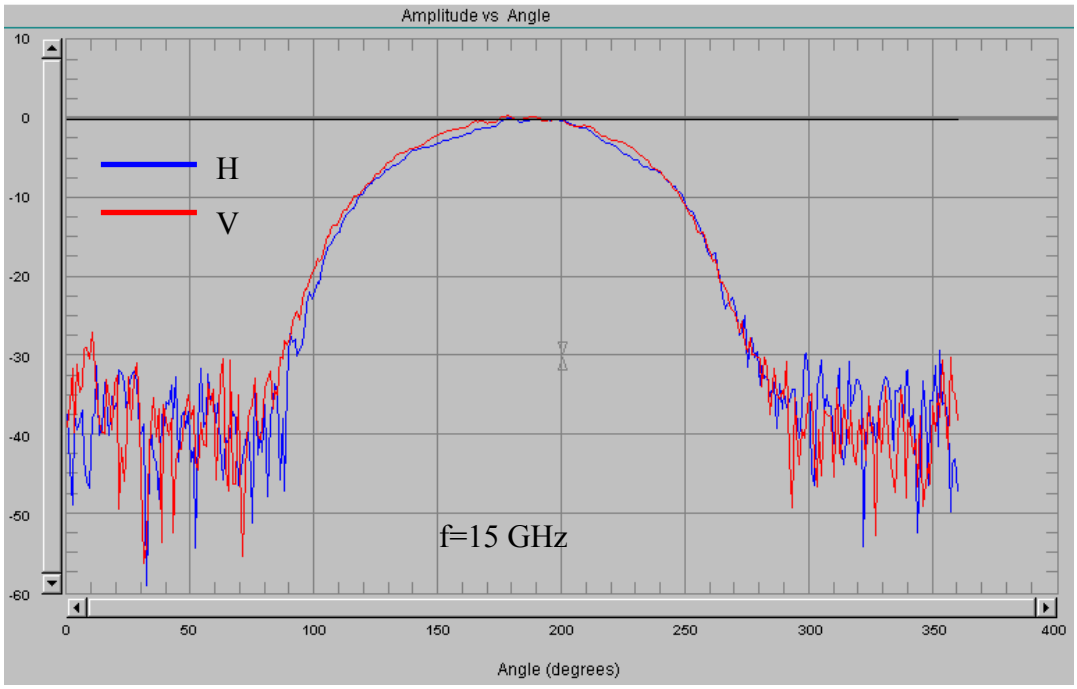
Amplitude vs Angle
10
0
-10
-20
-30
-40
-50
-60
H
V
f=15 GHz
0
50
100
150
200
250
300
350
400
Angle (degrees)

(d)

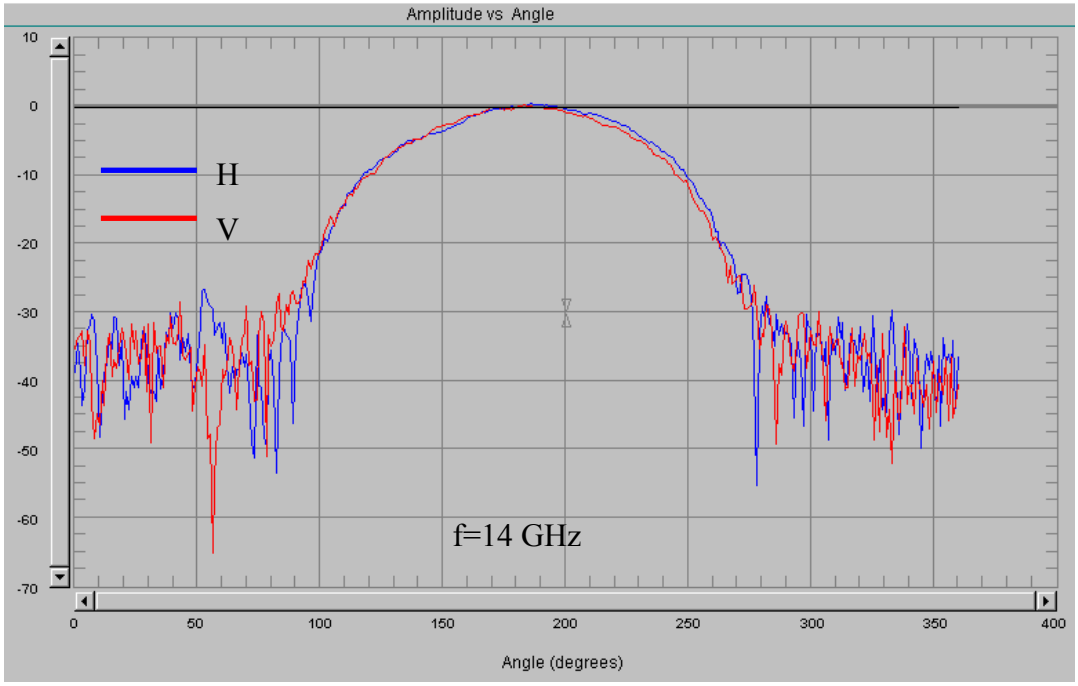
Amplitude vs Angle
10
0
-10
-20
-30
-40
-50
-60
-70
H
V
f=14 GHz
0
50
100
150
200
250
300
350
400
Angle (degrees)

(e)

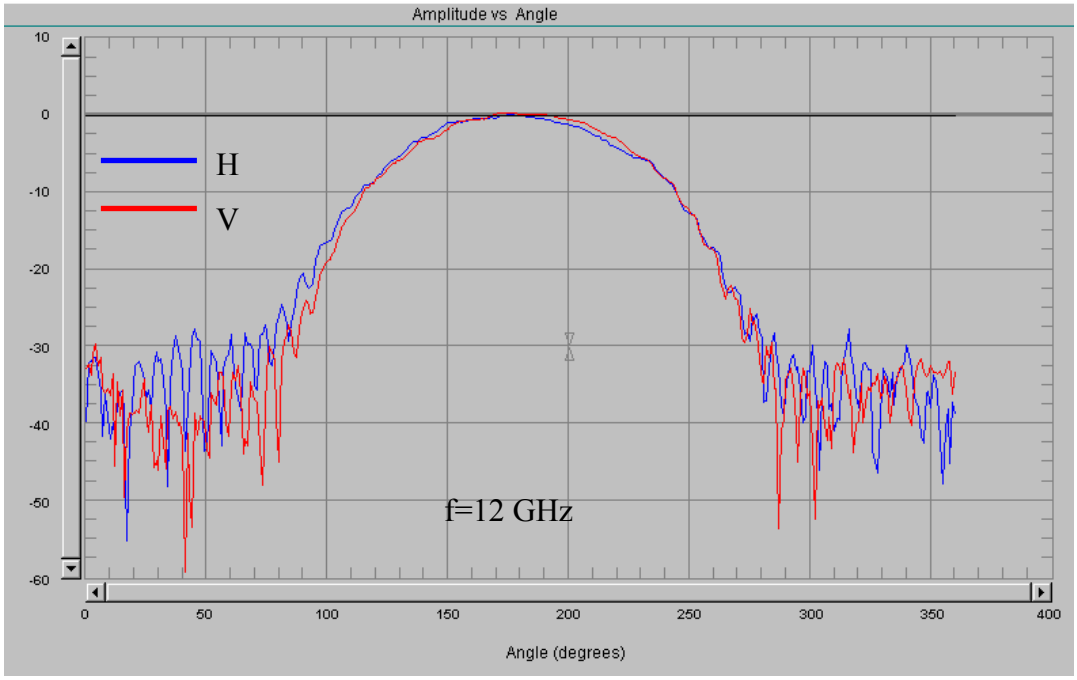
Amplitude vs Angle
10
0
-10
-20
-30
-40
-50
-60
H
V
f=12 GHz
0
50
100
150
200
250
300
350
400
Angle (degrees)

(f)

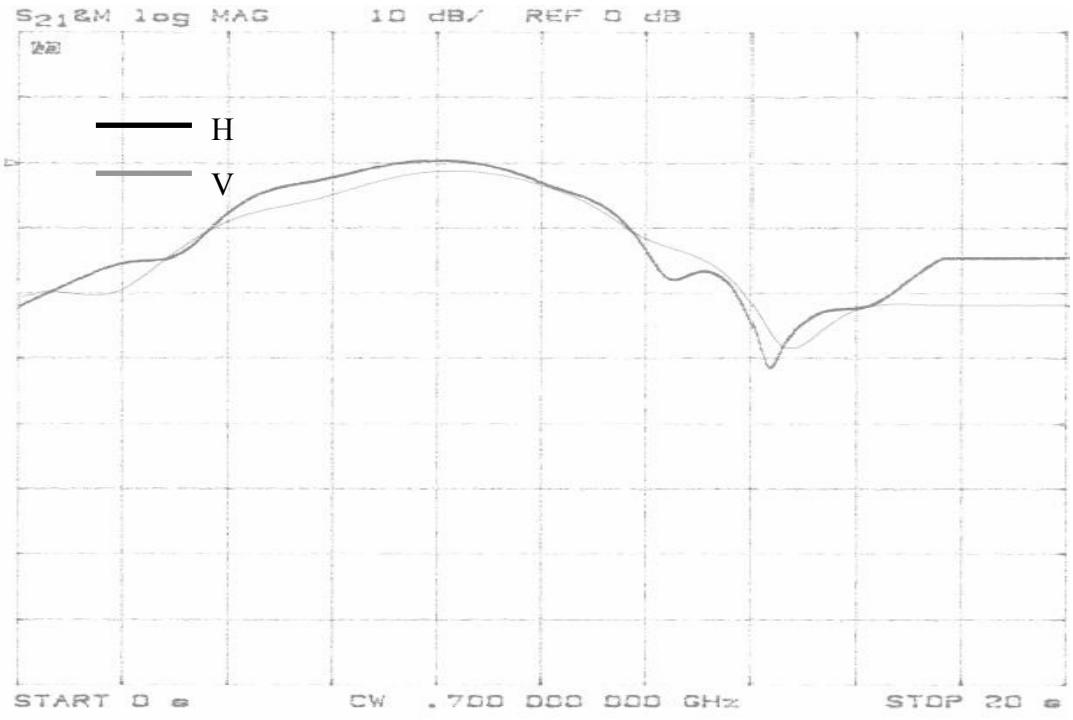

(g)

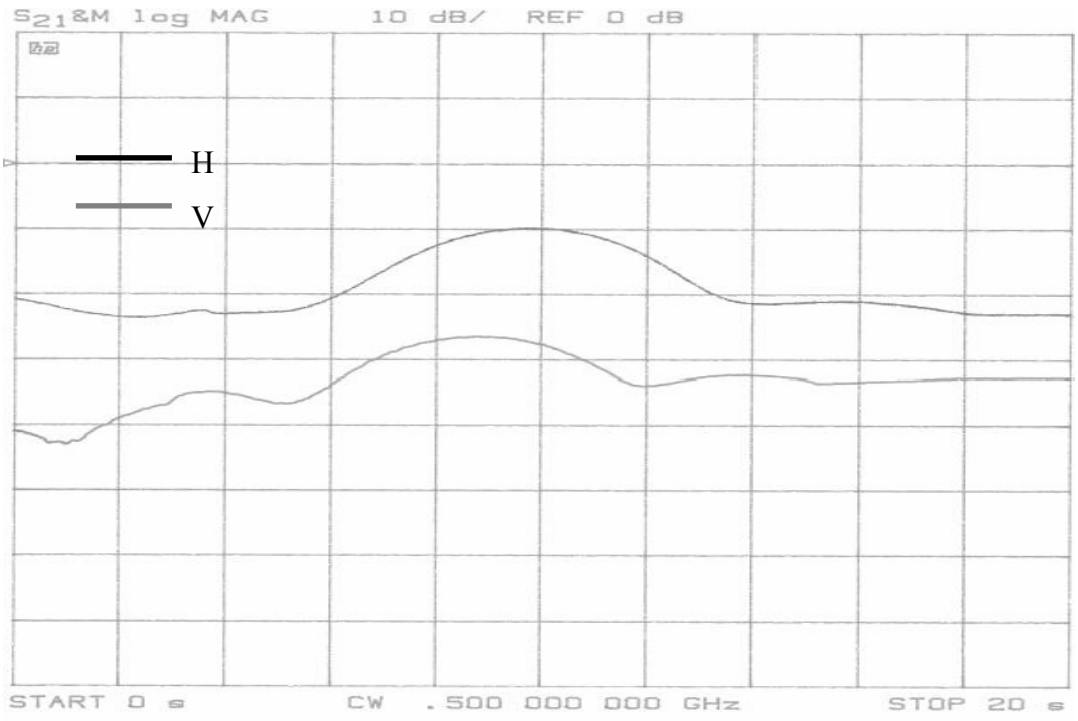

(h)

Figure 5.13 Radiation pattern of Spiral 1 at frequencies 18(a), 17.5(b), 16.5(c), 15(d), 14(e), 12(f), 0.7(g) and 0.5(h) GHz for vertical (V) and horizontal (H) transmitters (Configuration 2)

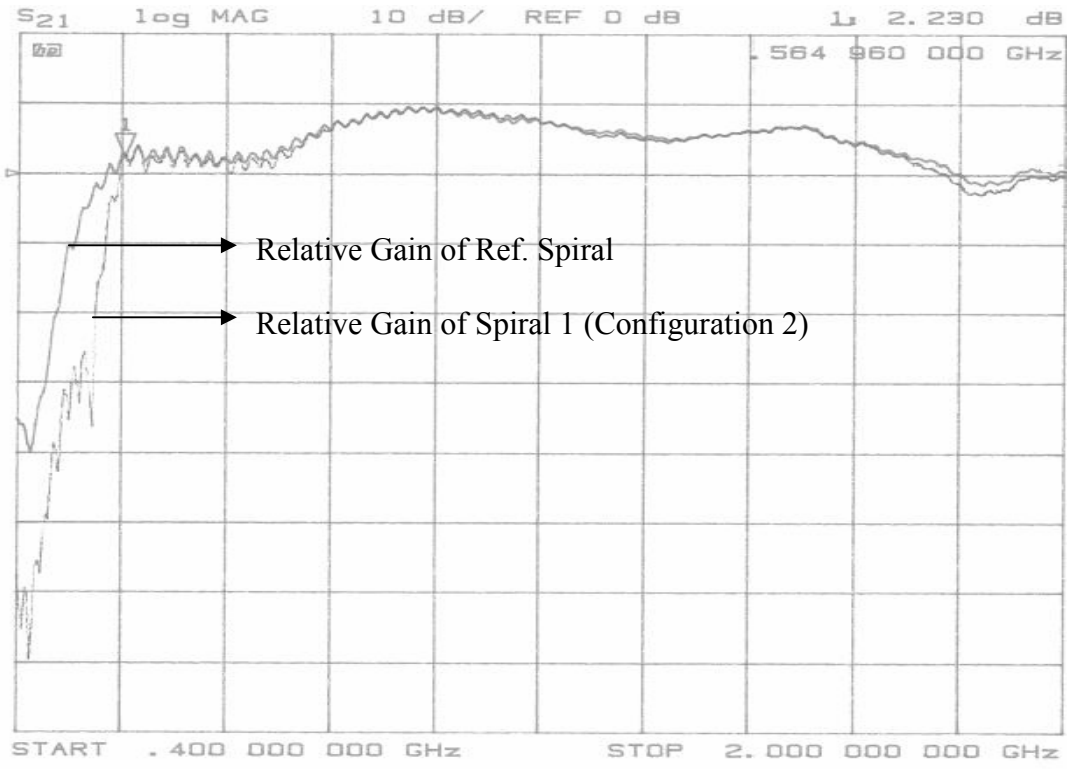

Figure 5.14 Relative gain of Spiral 1 for second assembly compared to reference spiral antenna at lower frequencies

After these first trials, I have decided to improve the lower frequency performance of the antenna because there was a gain reduction at the lower cut off frequency. So, I decided to enlarge the spiral card and I have designed two new spiral PCBs'. But there were some problems on the implementation of these two spiral PCBs' because of the detailed drawing of modulation cycles (wiggles). Therefore AutoCAD® drawings of spirals were assigned to LINTEK® Pty. Limited in order to implement these PCBs. Consequently, I have received the spirals and used them in an antenna assembly.

Secondly, boundary of the cavity backing the spiral antenna should be determined. So, three cases of the same size with spiral PCBs are designed. So every spiral was put into its own case.

Also, in order to reduce the effects of end-reflected currents Eccosorb® FGM-U-40 (thickness=1 mm) absorbing rubber ring was put on the periphery of the spiral PCB. Honeycomb replaced with Rohacell® HF 71 a foam material

whose dielectric constant is nearly 1.1 and behaves like air. Rohacell® is a good choice that it can more easily be processed compared to honeycomb.

Configuration 3 is given below Figure 5.15.

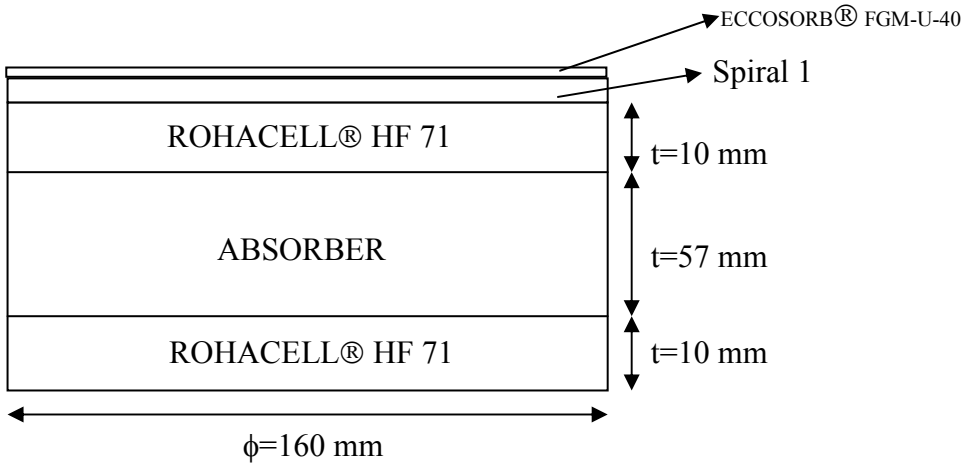

Figure 5.15 Third assembly of Spiral 1

For this configuration, distortions in the radiation pattern of the antenna increased due to the metallic case of the antenna. Especially distortions in the horizontal polarized electric fields are more deterministic than the distortions in the vertical polarized electric fields. This caused an enlargement in the E-Plane beamwidth of the antenna. Gain charts and radiation pattern graphs related with the third configuration are given below Figure 5.16 and Figure 5.17. 3 dB Beamwidth and Beamsquint values are given below Table 5.2.

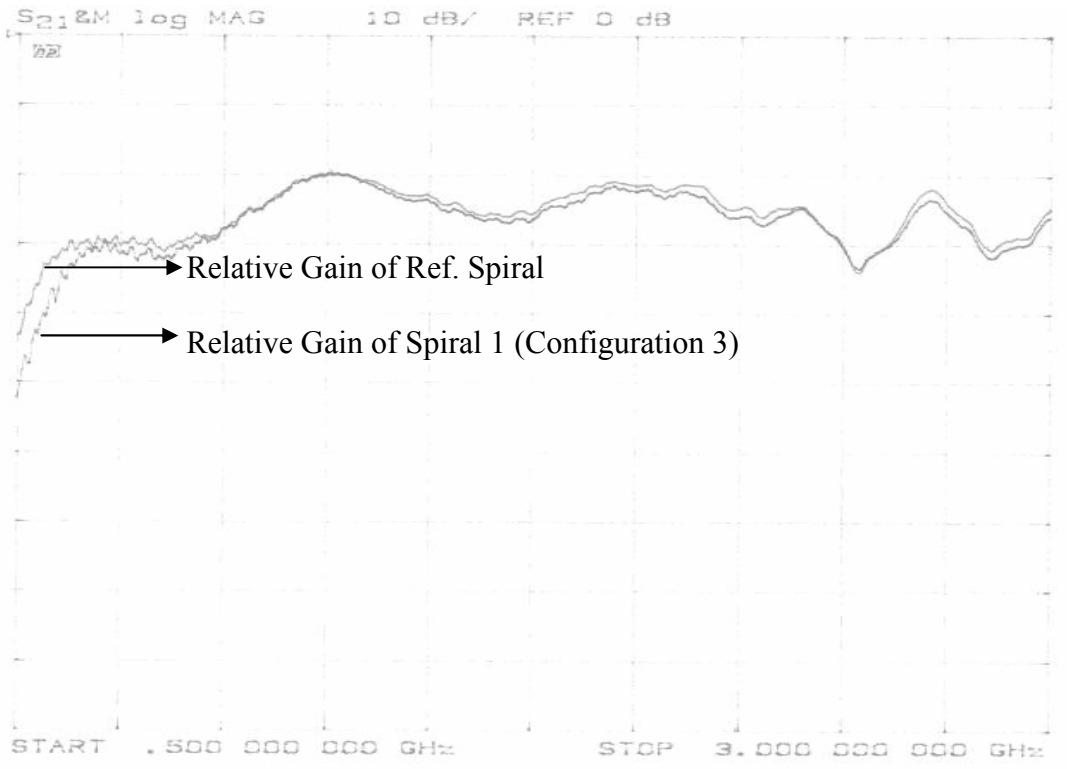

Figure 5.16 Relative gain of Spiral 1 for third assembly compared to reference spiral antenna at lower frequencies

Table 5-2 3 dB Beamwidth and Beamsquint values of Spiral 1 for Configuration 3

	freq (GHz)	3dB Beamwidth (Azimuth)	Beamsquint (degrees)	3dB Beamwidth (Elevation)	Beamsquint (degrees)
SPIRAL 1	0.5	83	1	85	15
	1	84	1	89	1
	2	66	0	68	-1
	4	82	-14	82	-13
	8	84	9	83	11
	12	69	0	69	-17
	15	76	8	60	20
	18	64	-1	46	-8

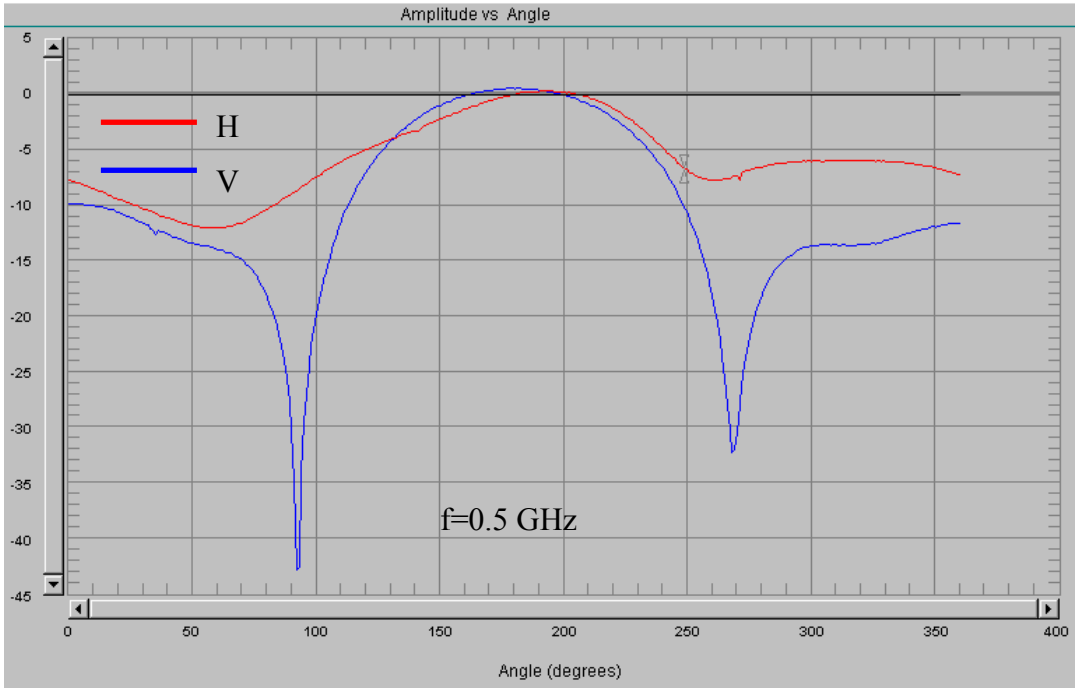
Amplitude vs Angle
H
V
f=0.5 GHz
Angle (degrees)

(a)

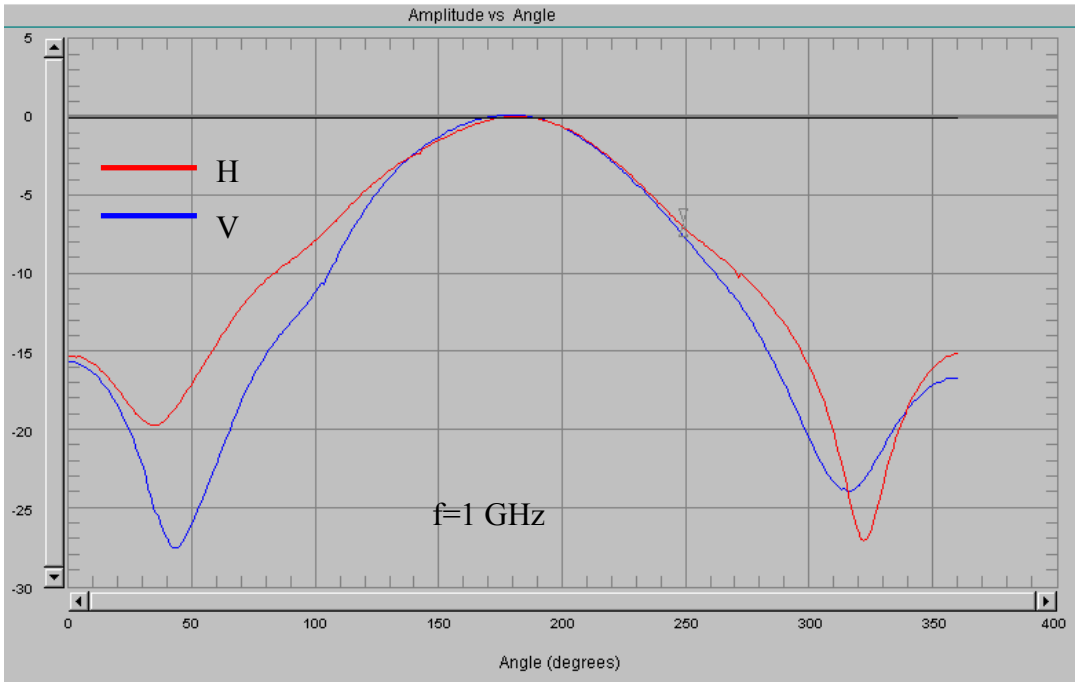
Amplitude vs Angle
H
V
f=1 GHz
Angle (degrees)

(b)

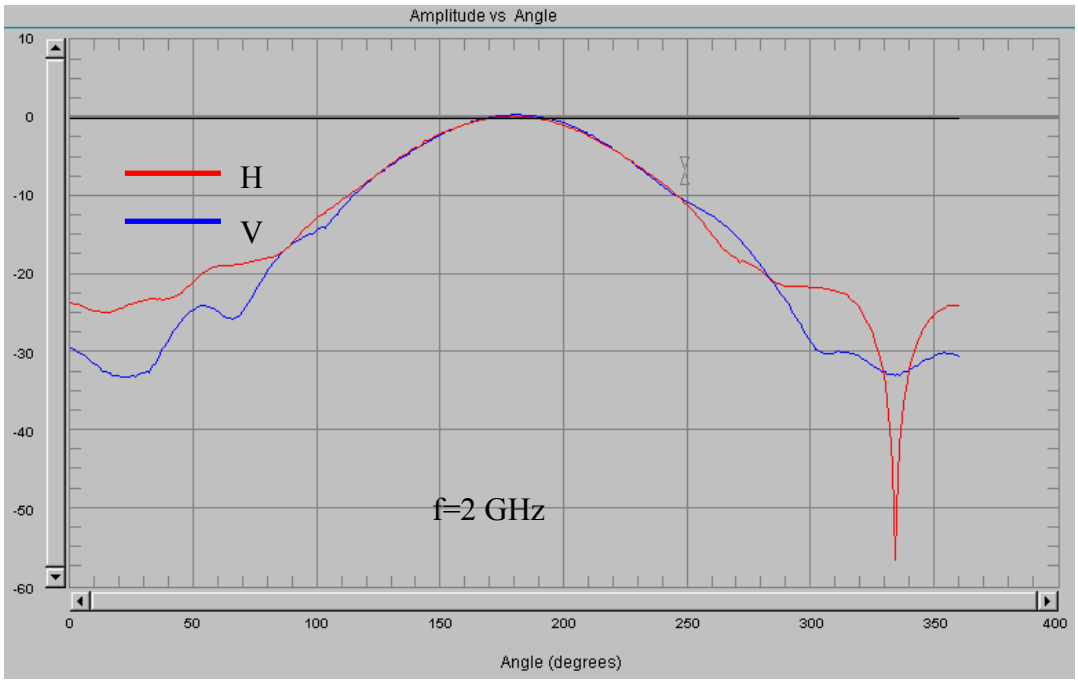
Amplitude vs Angle
10
0
-10
-20
-30
-40
-50
-60
H
V
f=2 GHz
0
50
100
150
200
250
300
350
400
Angle (degrees)

(c)

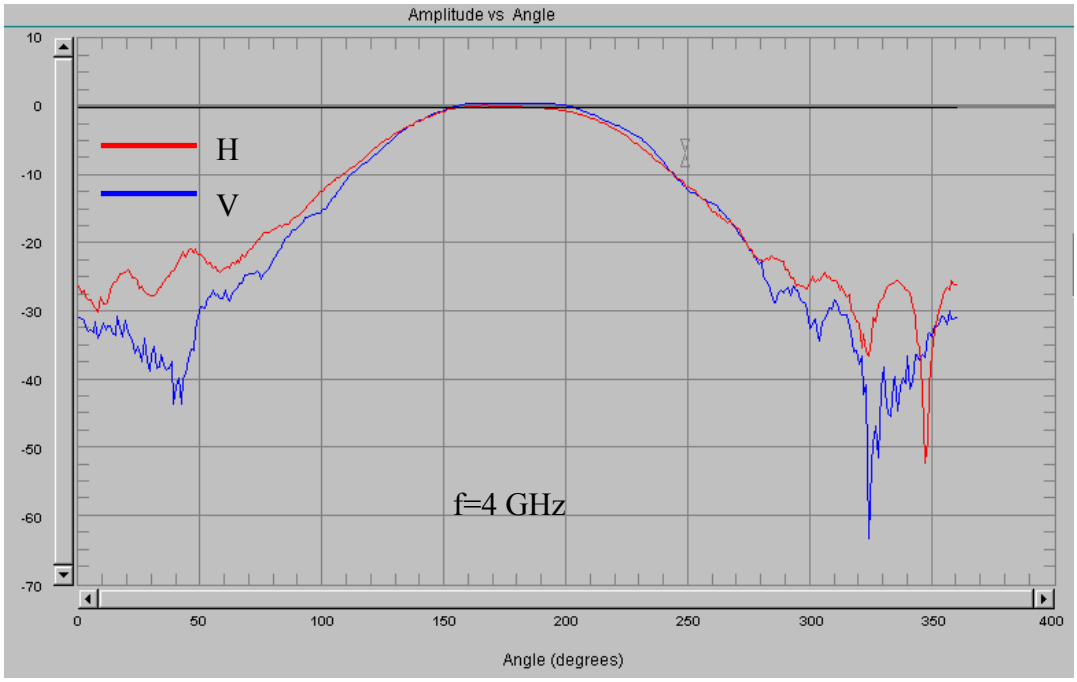
Amplitude vs Angle
10
0
-10
-20
-30
-40
-50
-60
-70
H
V
f=4 GHz
0
50
100
150
200
250
300
350
400
Angle (degrees)

(d)

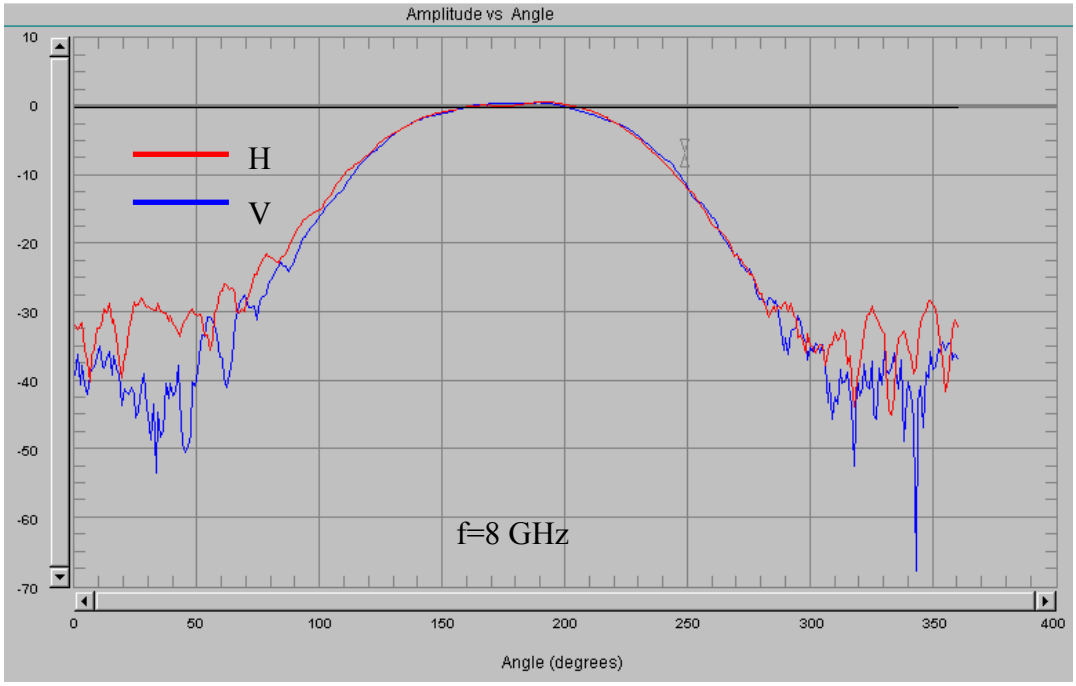
Amplitude vs Angle
H
V
f=8 GHz
Angle (degrees)

(e)

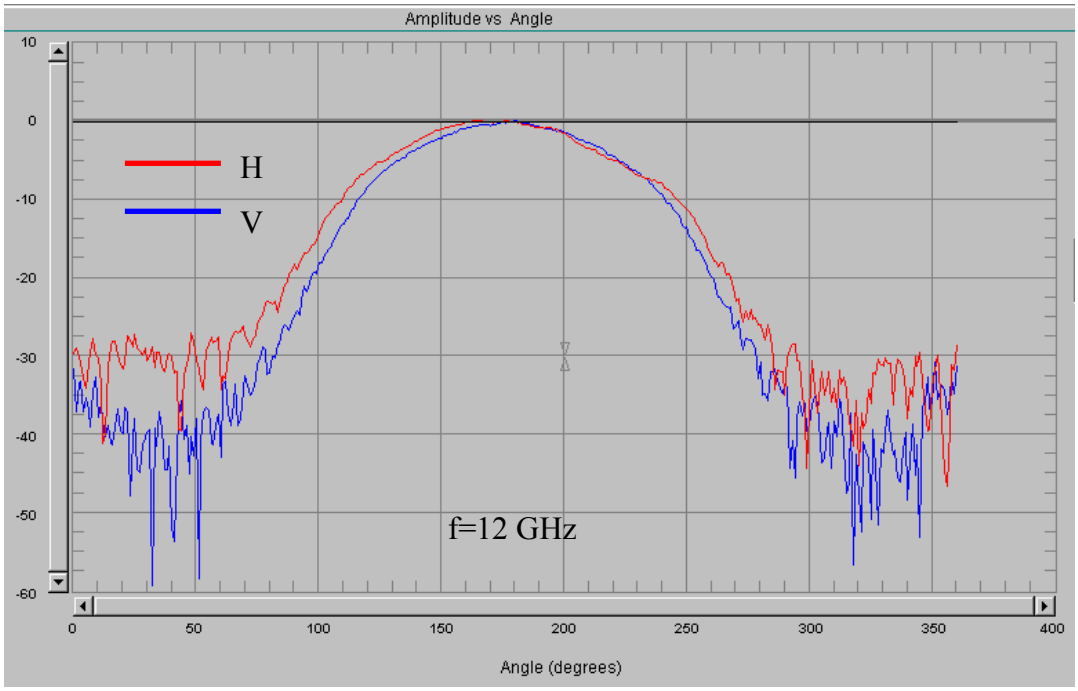
Amplitude vs Angle
H
V
f=12 GHz
Angle (degrees)

(f)

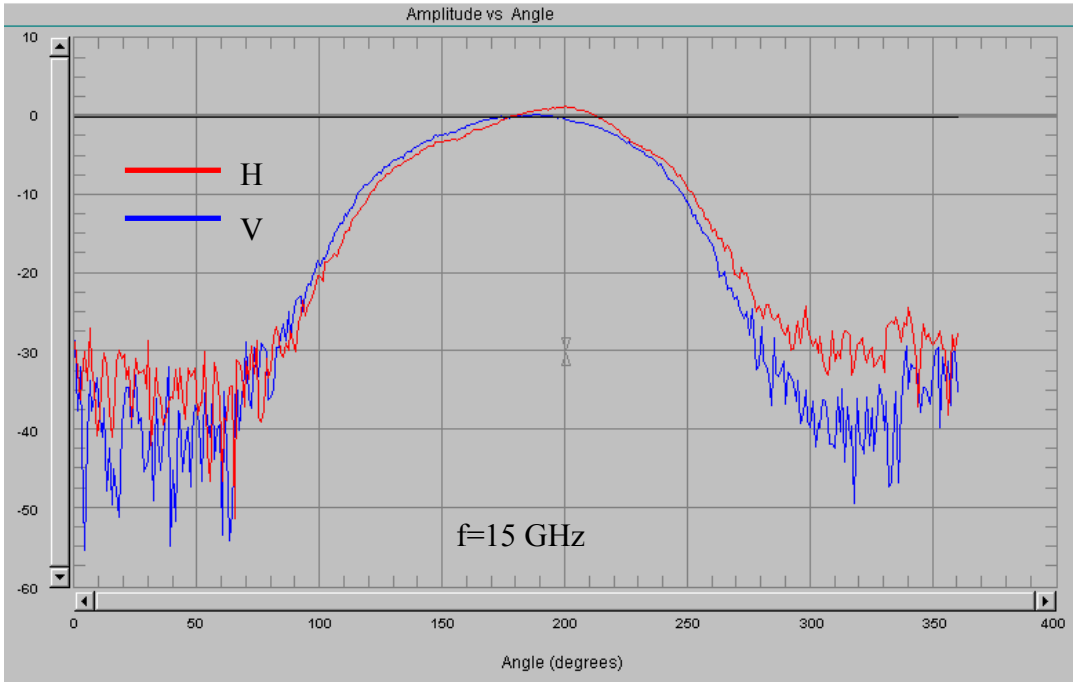

(g)

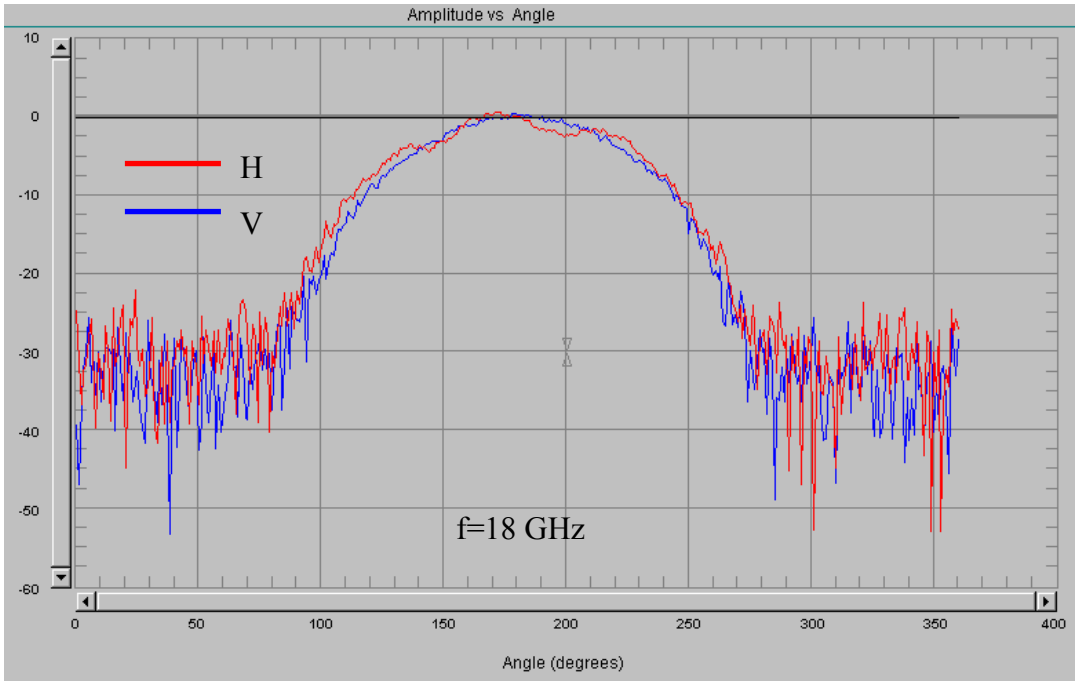

(h)

Figure 5.17 Radiation pattern of Spiral 1 at frequencies 0.5(a), 1(b), 2(c), 4(d), 8(e), 12(f), 15(g) and 18(h) GHz for vertical (V) and horizontal (H) transmitters (Configuration 3)

Fourth and fifth configurations are different applications of modulation cycles. There is a drastic increase in modulation cycles for these two configurations. So, the electrical length at lower cut of frequency is increased, but the limiting factor on the gain of the antenna is the aperture width of the spiral and the resistive loss of the antenna for longer arms. In conclusion, there was not a drastic increase in the bandwidth of the antenna as expected. The solution to this problem may be holding a larger sized PCB than the original spiral drawing. Gain charts and radiation pattern graphs related with the fourth and fifth configurations are given below Figure 5.19 and Figure 5.20 (Configuration 4); Figure 5.22 and Figure 5.23 (Configuration 5). 3 dB Beamwidth and Beamsquint values are given below Table 5.3 and Table 5.4.

Configuration 4 is given below Figure 5.18.

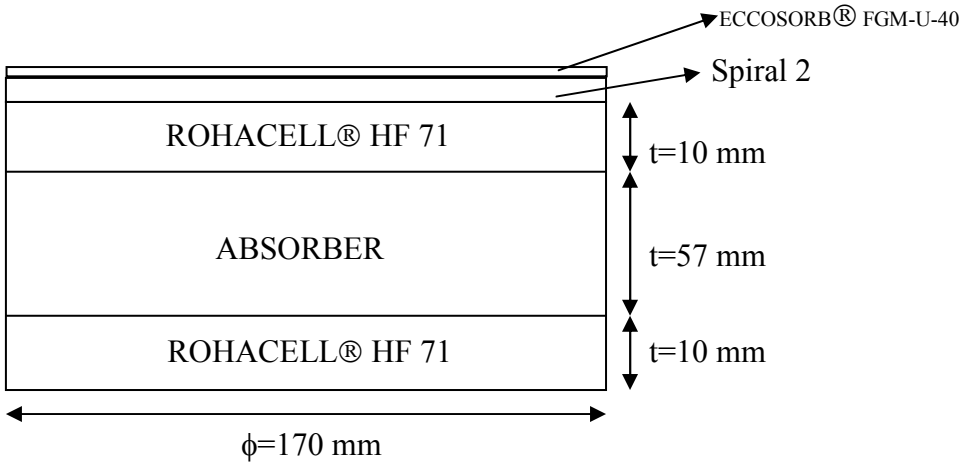

Figure 5.18 Assembly of Spiral 2

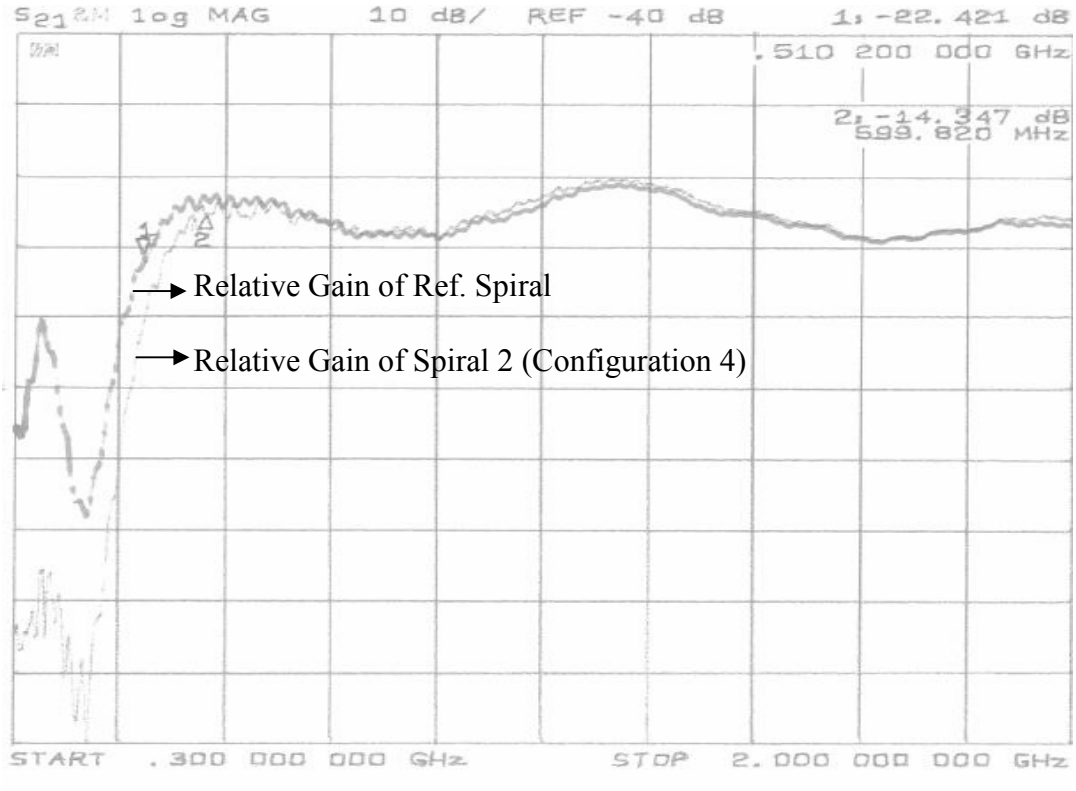

Figure 5.19 Relative gain of Spiral 2 compared to reference spiral antenna at lower frequencies (Configuration 4)

Table 5-3 3 dB Beamwidth and Beamsquint values of Spiral 2 for Configuration 4

	freq (GHz)	3dB Beamwidth (Azimuth)	Beamsquint (degrees)	3dB Beamwidth (Elevation)	Beamsquint (degrees)
SPIRAL 2	0.5	90	2	104	9
	1	79	2	101	-6
	2	65	-4	72	-6
	4	80	-4	84	-21
	8	83	2	83	-25
	12	80	-8	90	-14
	15	79	5	74	6
	18	74	13	68	13

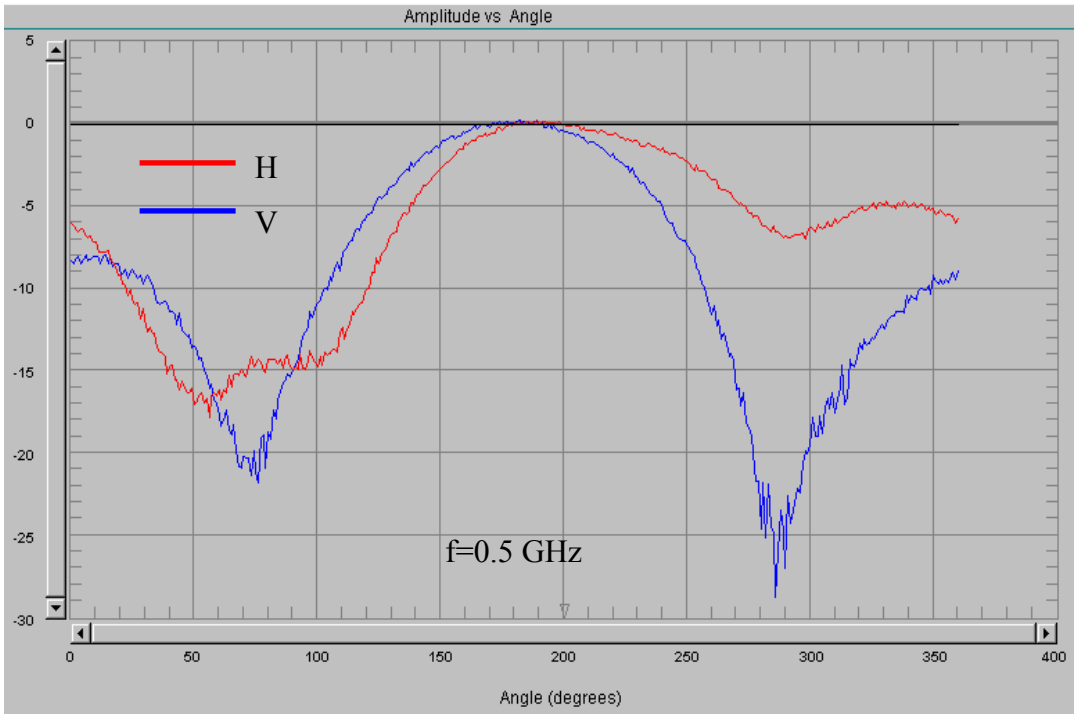
Amplitude vs Angle
H
V
f=0.5 GHz
Angle (degrees)

(a)

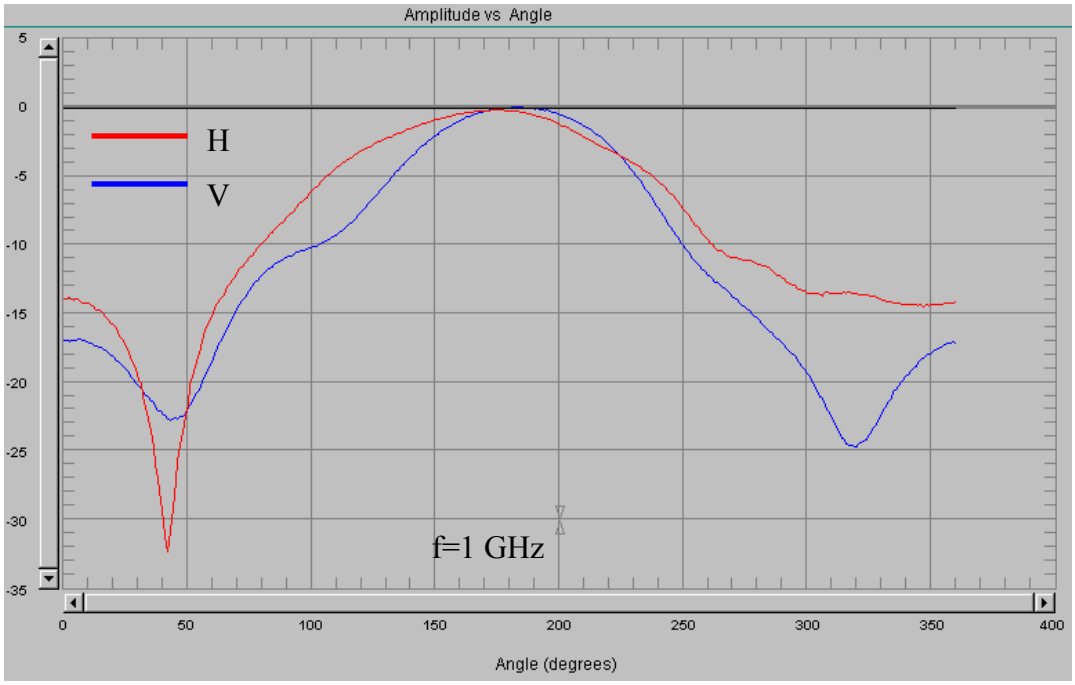
Amplitude vs Angle
H
V
f=1 GHz
Angle (degrees)

(b)

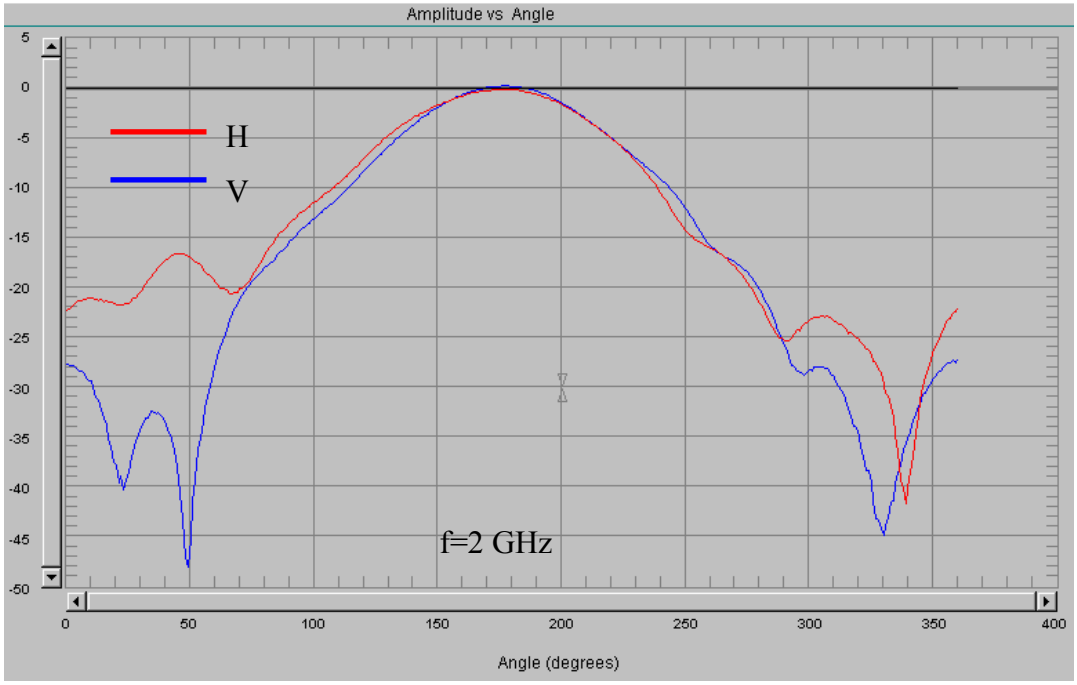
Amplitude vs Angle
H
V
f=2 GHz
Angle (degrees)

(c)

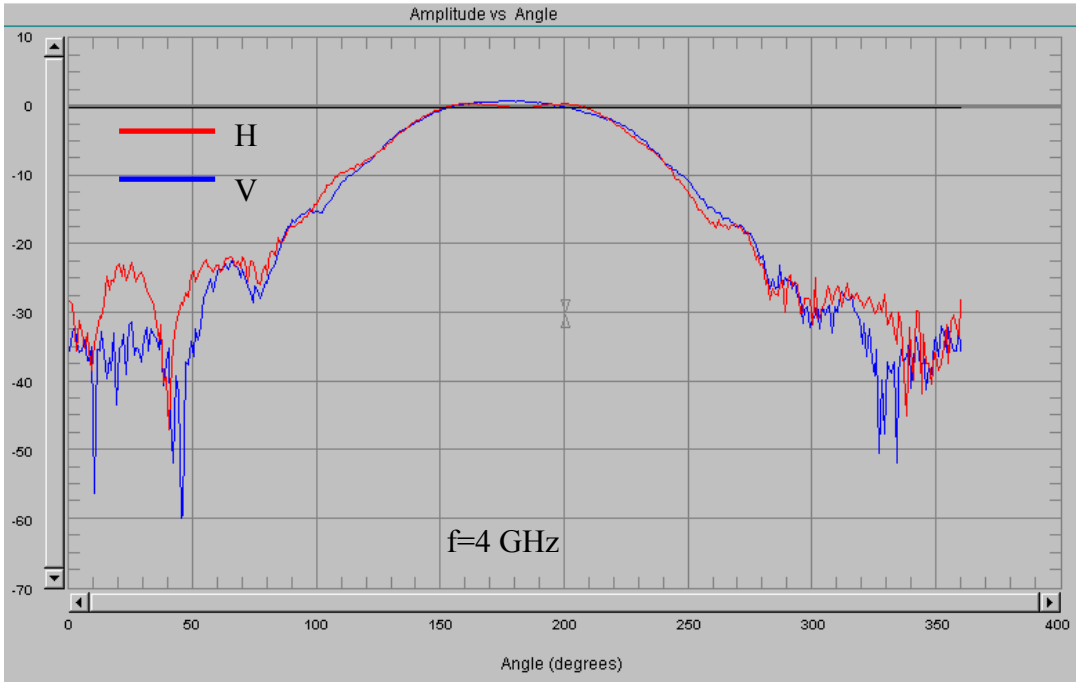
Amplitude vs Angle
H
V
f=4 GHz
Angle (degrees)

(d)

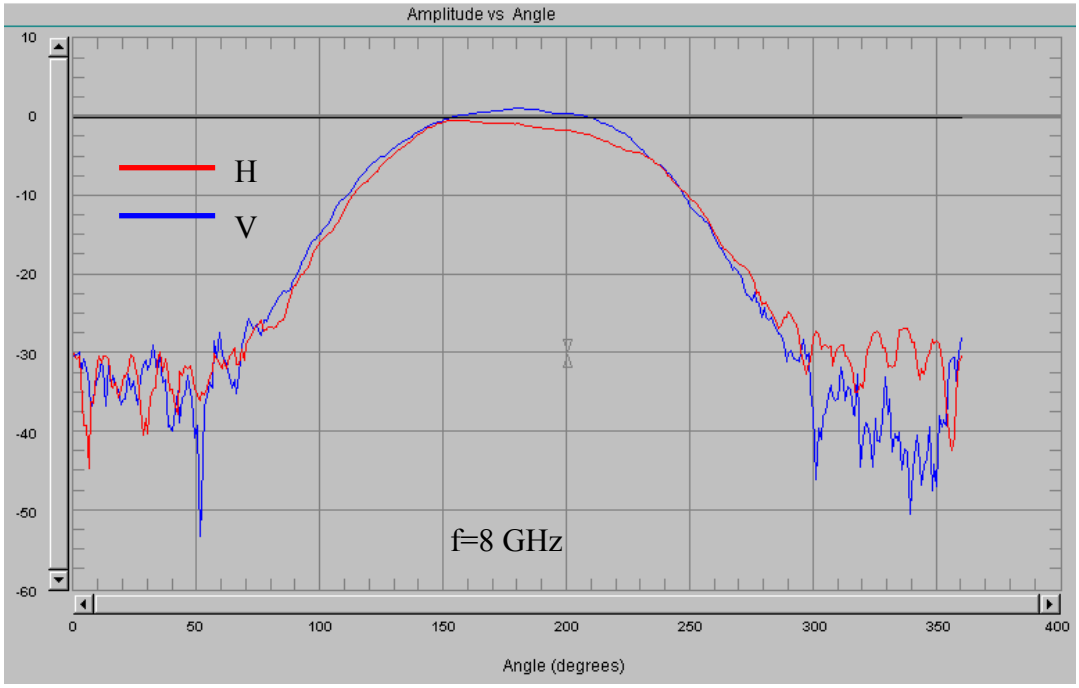
Amplitude vs Angle
10
0
-10
-20
-30
-40
-50
-60
H
V
f=8 GHz
0
50
100
150
200
250
300
350
400
Angle (degrees)

(e)

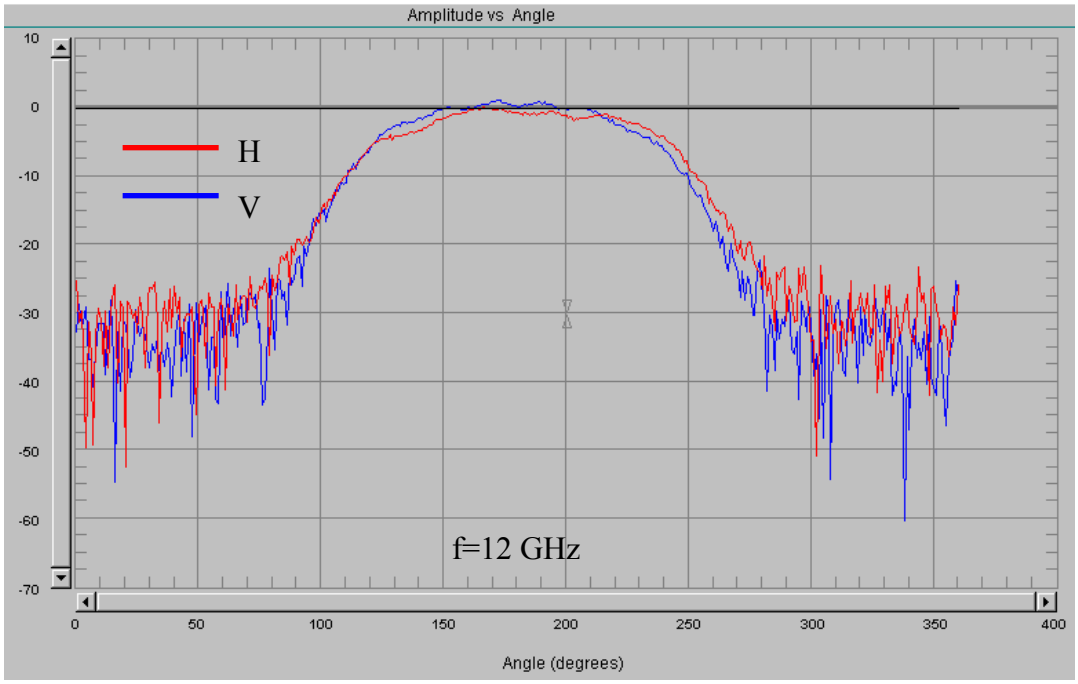
Amplitude vs Angle
10
0
-10
-20
-30
-40
-50
-60
-70
H
V
f=12 GHz
0
50
100
150
200
250
300
350
400
Angle (degrees)

(f)

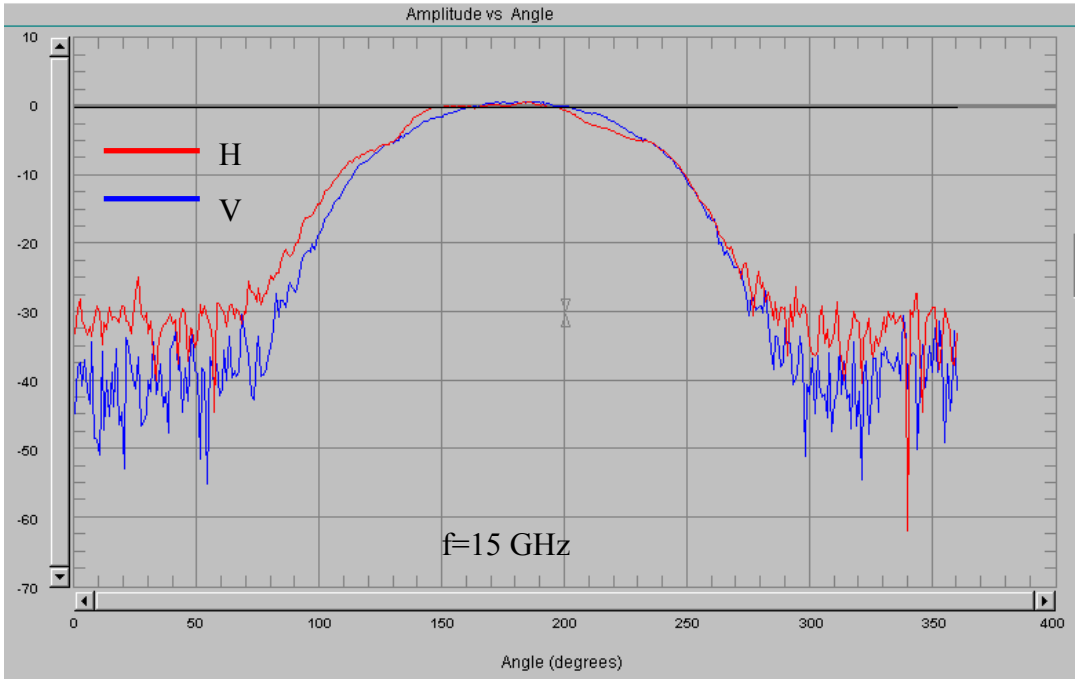

(g)

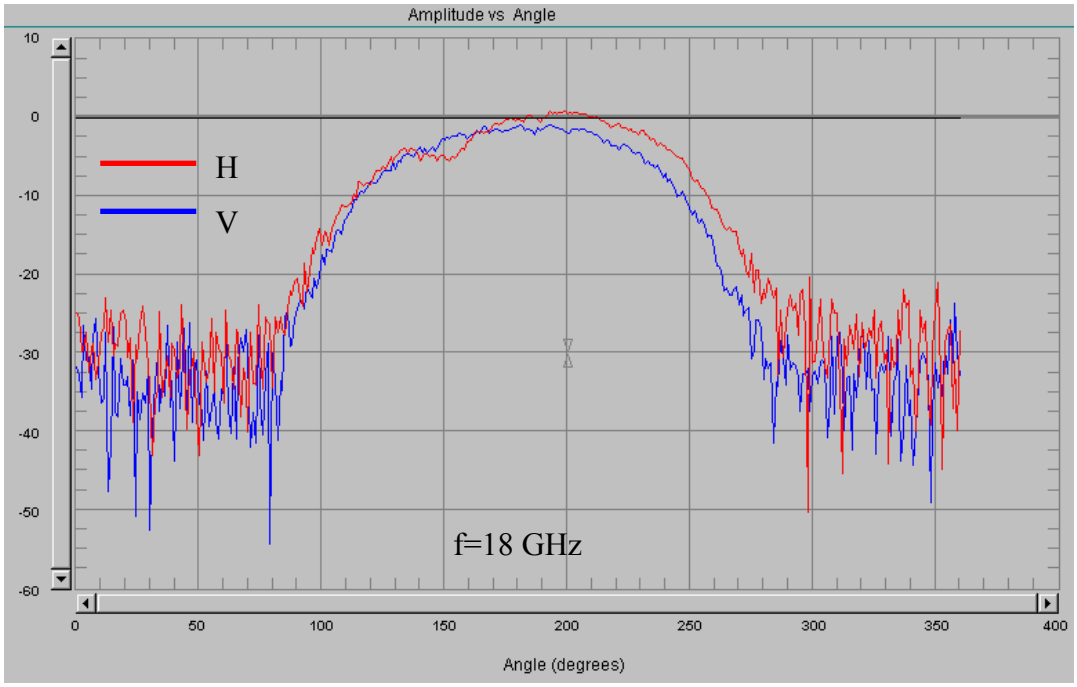

(h)

Figure 5.20 Radiation pattern of Spiral 2 at frequencies 0.5(a), 1(b), 2(c), 4(d), 8(e), 12(f), 15(g) and 18(h) GHz for vertical (V) and horizontal (H) transmitters (Configuration 4)

Configuration 5 is given below Figure 5.21.

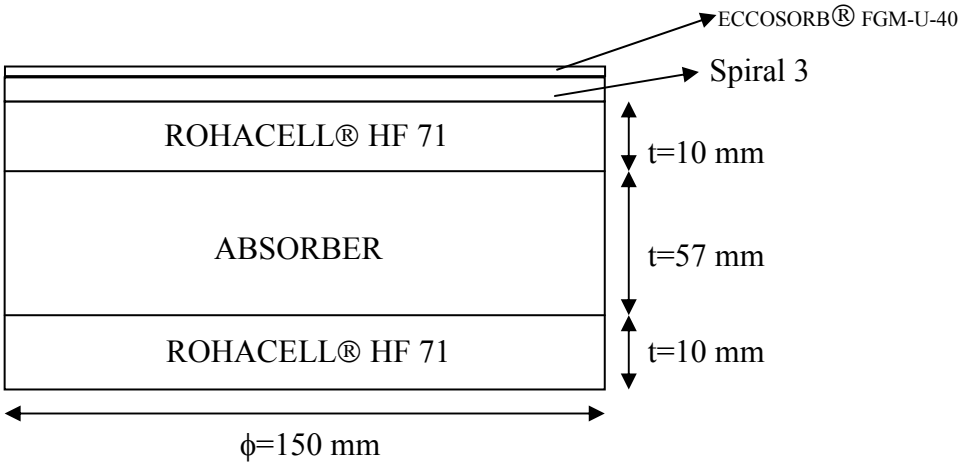

Figure 5.21 Assembly of Spiral 3

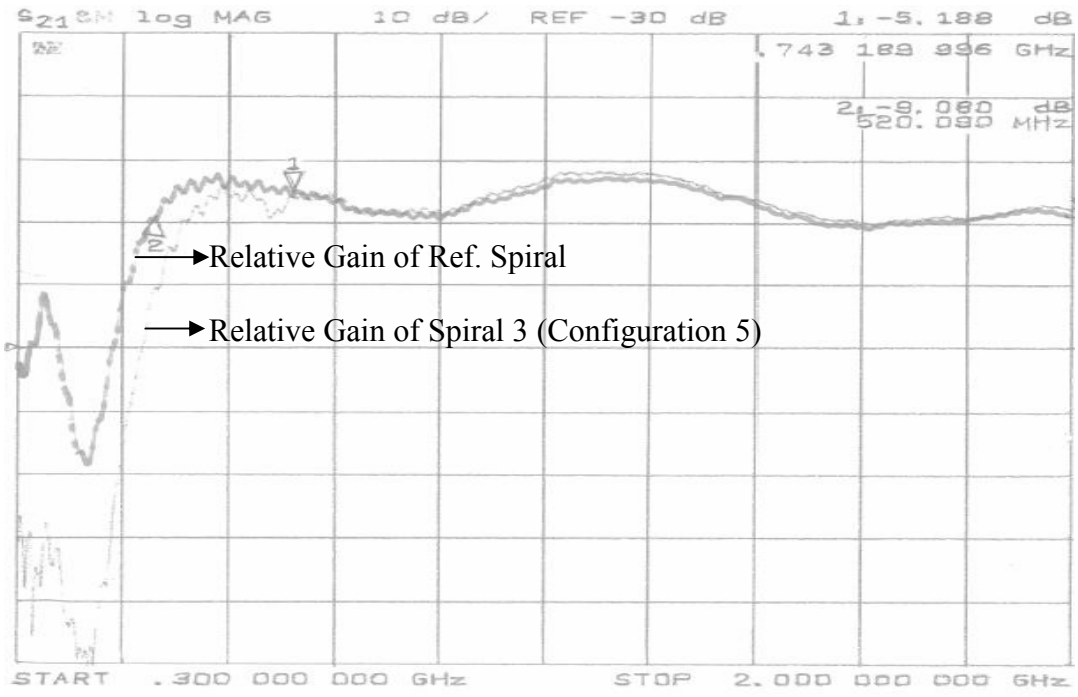

Figure 5.22 Relative gain of Spiral 3 compared to reference spiral antenna at lower frequencies (Configuration 5)

Table 5-3 3 dB Beamwidth and Beamsquint values of Spiral 3 for Configuration 5

	freq (GHz)	3dB Beamwidth (Azimuth)	Beamsquint (degrees)	3dB Beamwidth (Elevation)	Beamsquint (degrees)
SPIRAL 3	0.5	78	1	120	50
	1	80	2	115	-8
	2	66	2	76	3
	4	84	15	84	16
	8	77	6	88	1
	12	74	3	84	6
	15	82	9	85	-22
	18	79	8	46	8

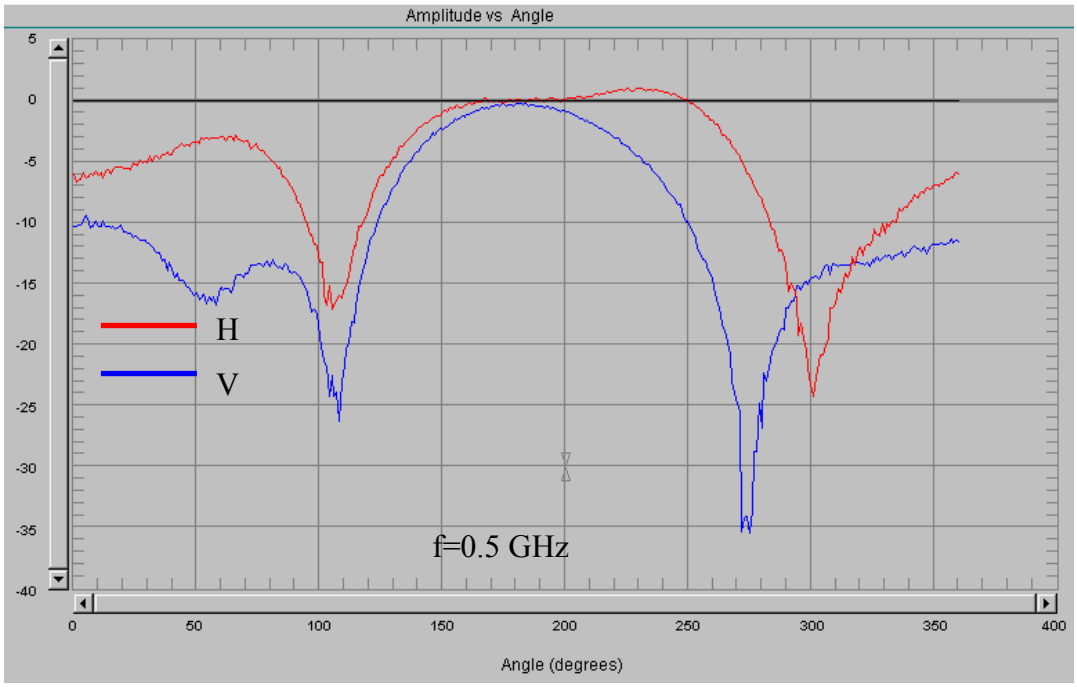
Amplitude vs Angle
5
0
-5
-10
-15
-20
-25
-30
-35
-40
H
V
f=0.5 GHz
0
50
100
150
200
250
300
350
400
Angle (degrees)

(a)

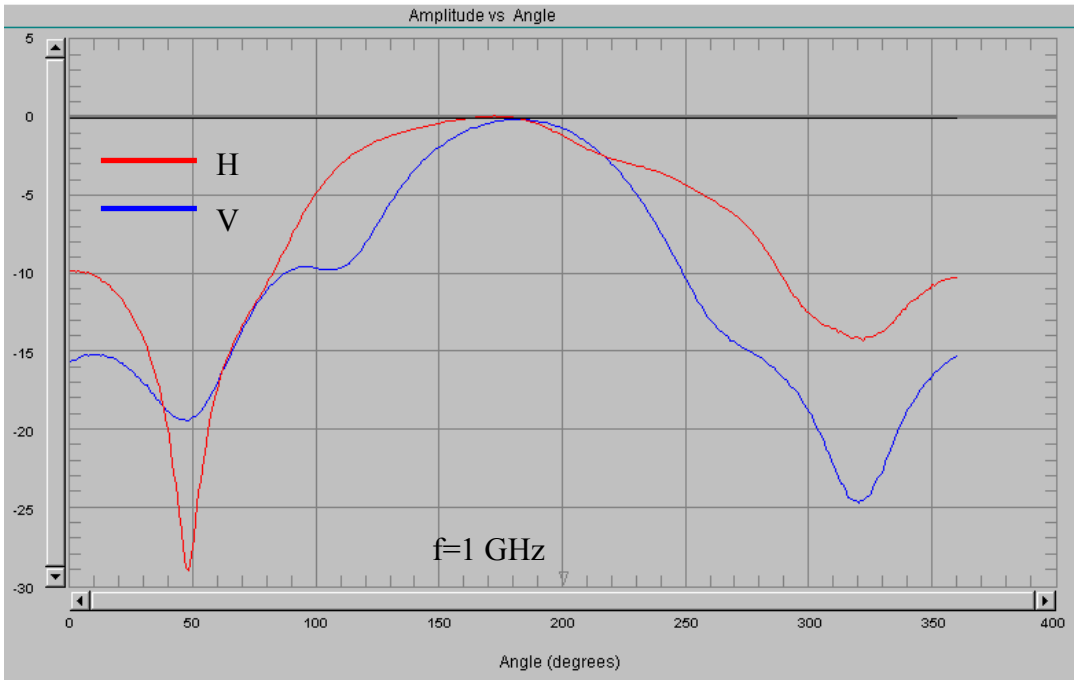
Amplitude vs Angle
5
0
-5
-10
-15
-20
-25
-30
H
V
f=1 GHz
0
50
100
150
200
250
300
350
400
Angle (degrees)

(b)

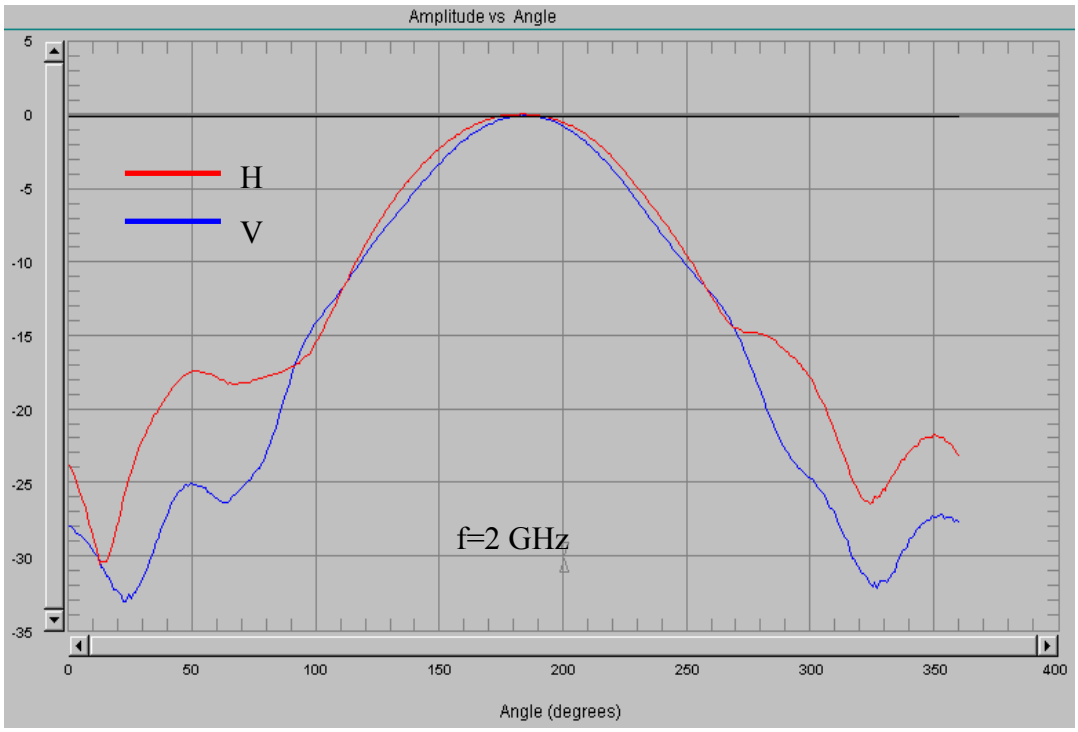
Amplitude vs Angle
5
0
-5
-10
-15
-20
-25
-30
-35
H
V
f=2 GHz
0
50
100
150
200
250
300
350
400
Angle (degrees)

(c)

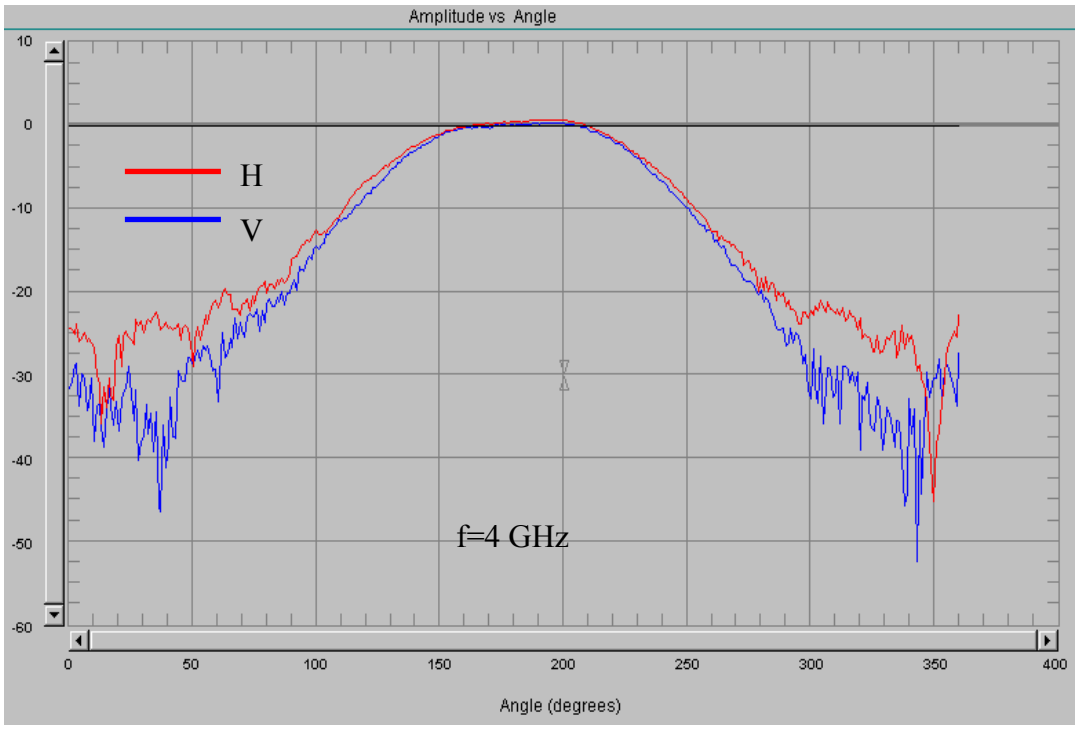
Amplitude vs Angle
10
0
-10
-20
-30
-40
-50
-60
H
V
f=4 GHz
0
50
100
150
200
250
300
350
400
Angle (degrees)

(d)

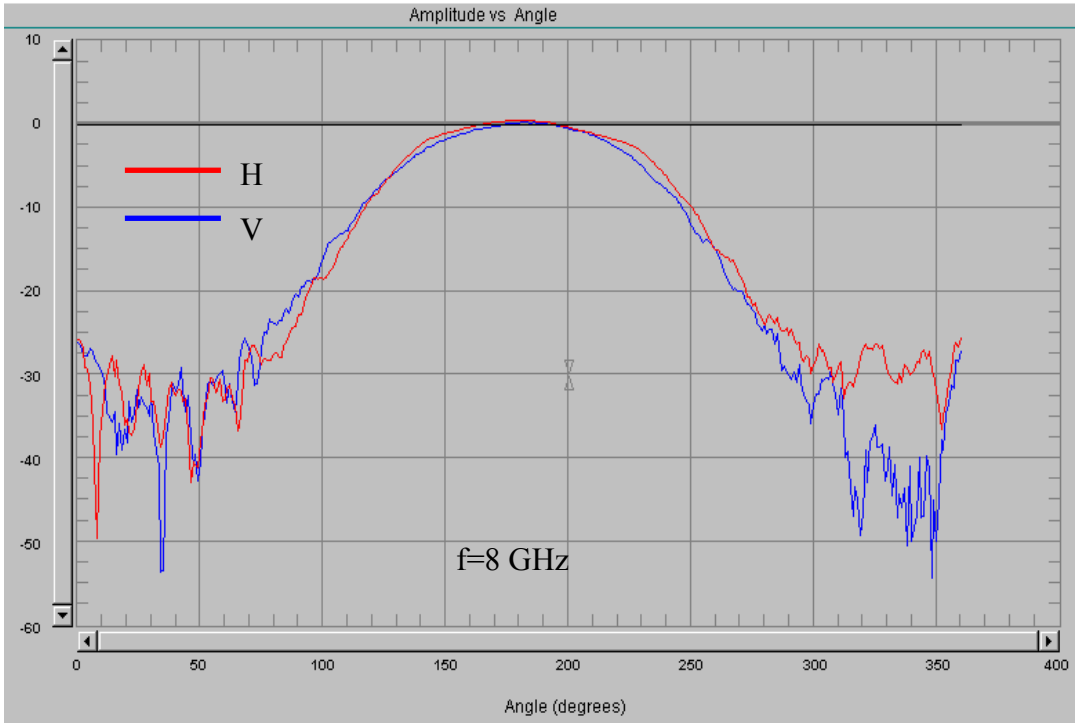
Amplitude vs Angle
H
V
f=8 GHz
Angle (degrees)

(e)

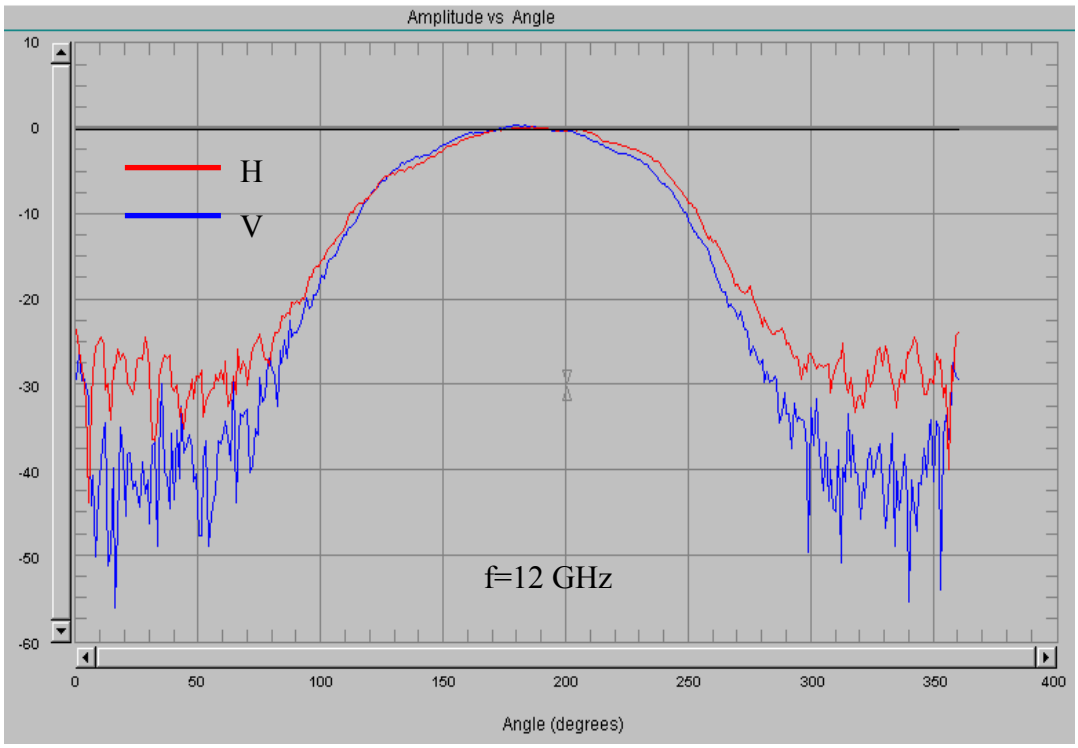
Amplitude vs Angle
H
V
f=12 GHz
Angle (degrees)

(f)

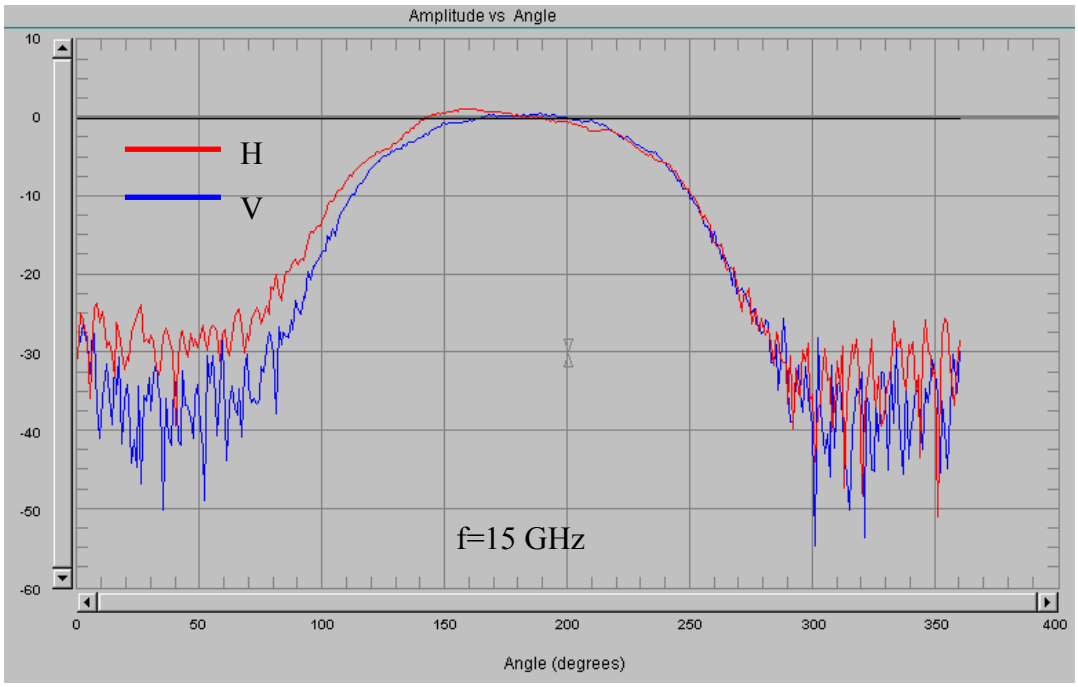

(g)

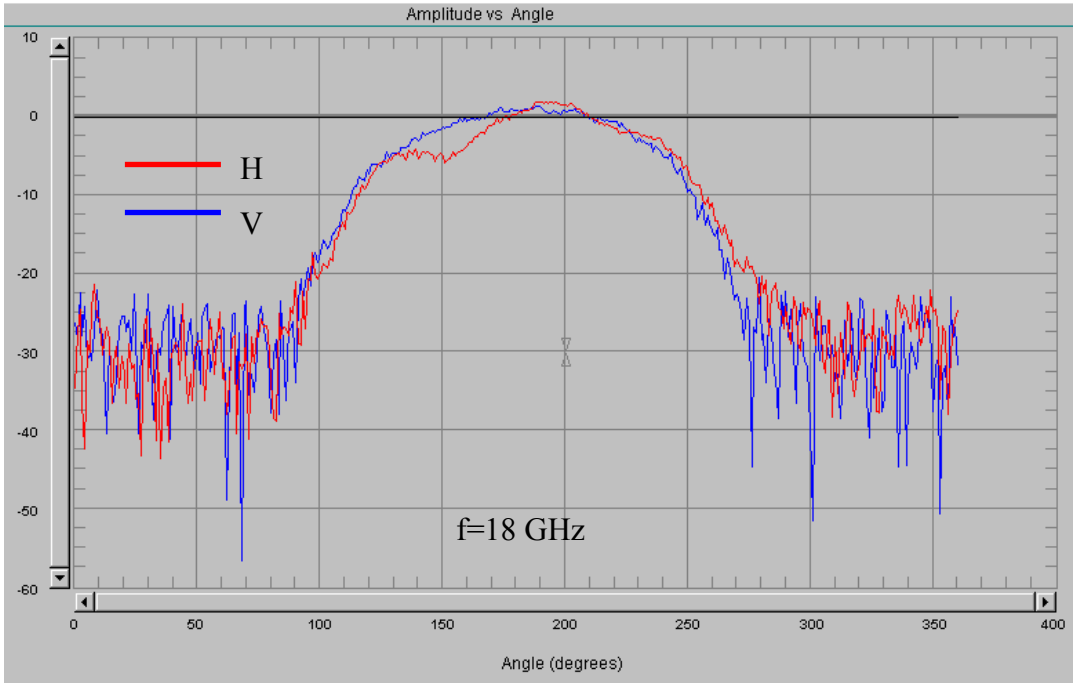

(h)

Figure 5.23 Radiation pattern of Spiral 3 at frequencies 0.5(a), 1(b), 2(c), 4(d), 8(e), 12(f), 15(g) and 18(h) GHz for vertical (V) and horizontal (H) transmitters (Configuration 5)

Absolute gain measurements were done by the method described in Chapter 4 Section 3. Related gain chart is shown in Figure 5.24. Absolute gain of the antennas found unexpectedly high. Since the gain of the antennas is measured with respect to linear polarization, antenna gain is 3 dB larger than the given values due to the circular polarization of spiral antenna. For this case, the gain of the antenna approximately becomes 6-8 dB, which is an unexpected gain value for a spiral antenna. The problem may be arisen from the given gain values of horn antenna. Gain of horn antenna should be lower than the given values.

Also as seen from the graph, gain of all spiral antennas nearly same except Spiral 1. At the beginning this was considered as a measurement error and gain of Spiral 1 is measured again but we have confronted with the same result. Consequently, antenna may be damaged or its feed solder may be broken off due to any other shock during the gain measurements.

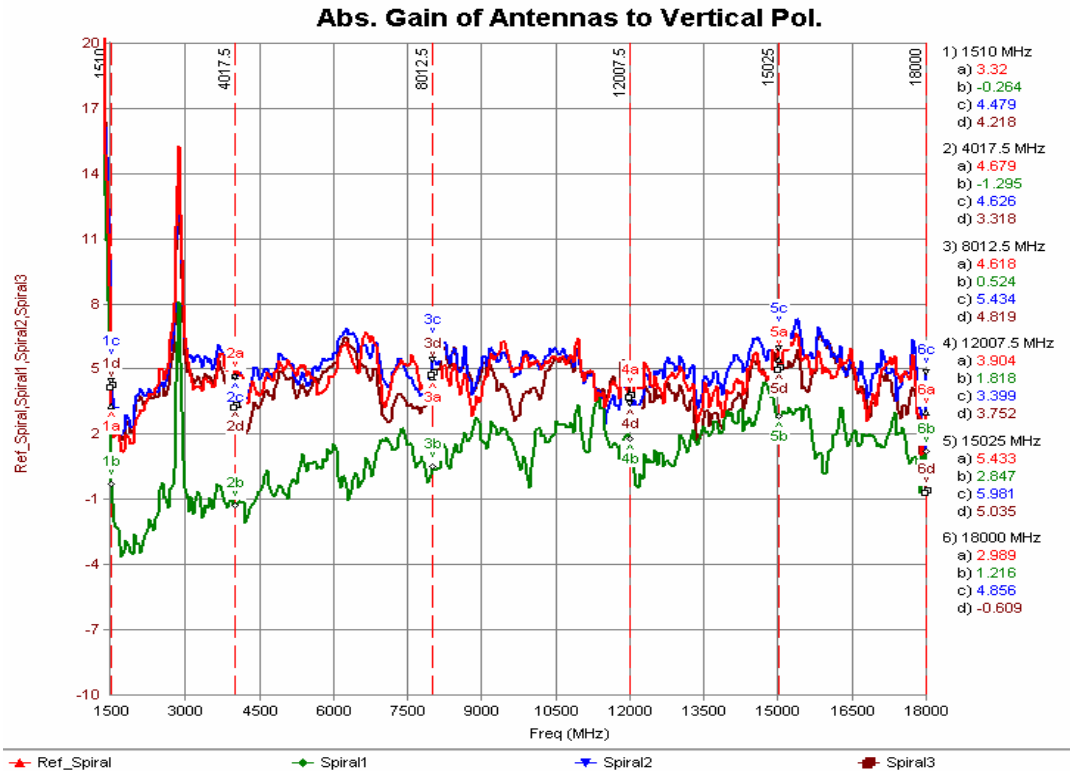

Figure 5.24 Absolute gains of spiral antennas in 1.5-18 GHz frequency range (V polarization)

5.5.3 Polarization Pattern Measurements of Spiral Antennas

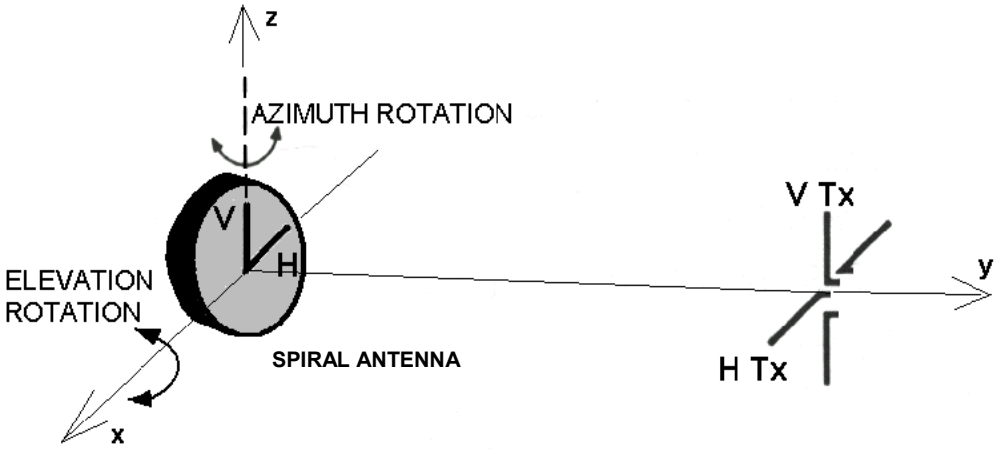

Figure 5.25 The measurement setup showing the terms [3].

Polarization measurements of spiral antennas are made as described in Chapter 4 Section 4. Since spiral antennas all resemble to each other as their radiation pattern and gain measurements are compared, only polarization pattern of Spiral 1 is measured. Polarization measurements of the other antennas were left for later work. Results of the measurements are shown below Figure 5.26. Polarization ellipticity (axial ratio) of spiral antennas is increasing near the lower cut off frequency and as the frequency getting higher, axial ratio decreases and a circularly polarized radiation pattern is obtained successfully.

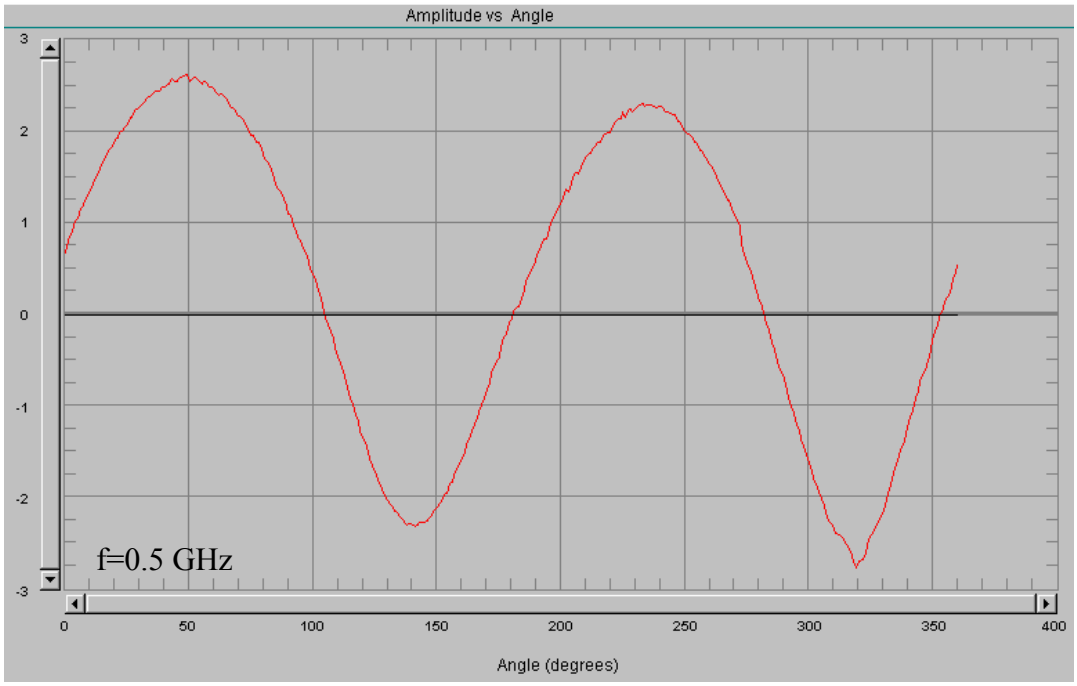
Amplitude vs Angle
3
2
1
0
-1
-2
-3
f=0.5 GHz
0
50
100
150
200
250
300
350
400
Angle (degrees)

(a)

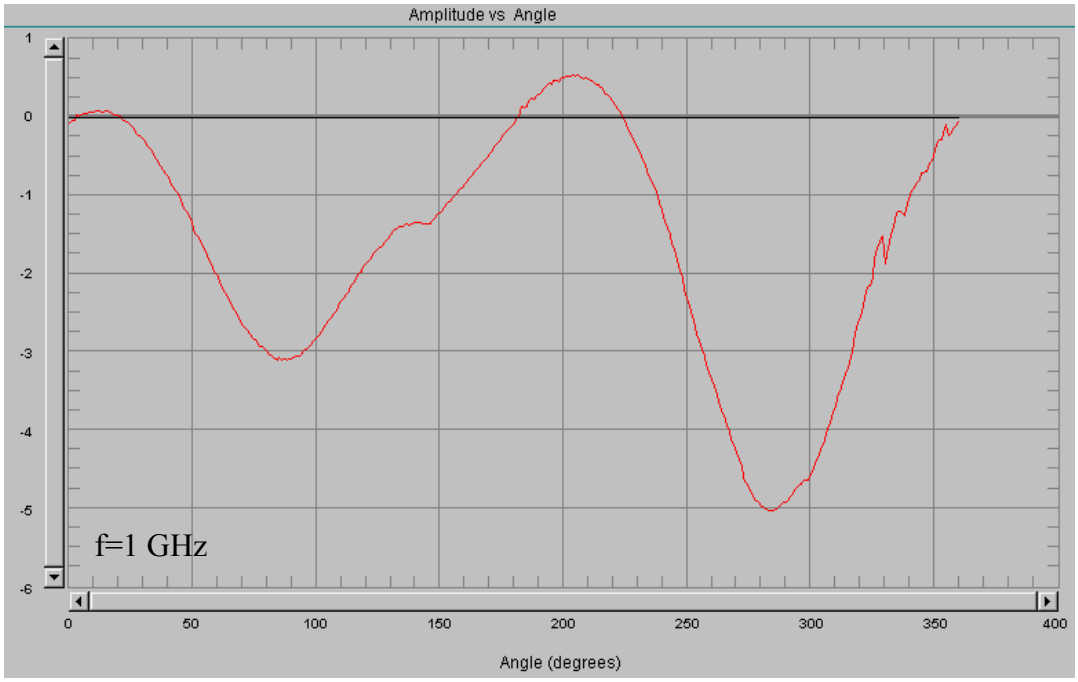
Amplitude vs Angle
1
0
-1
-2
-3
-4
-5
-6
f=1 GHz
0
50
100
150
200
250
300
350
400
Angle (degrees)

(b)

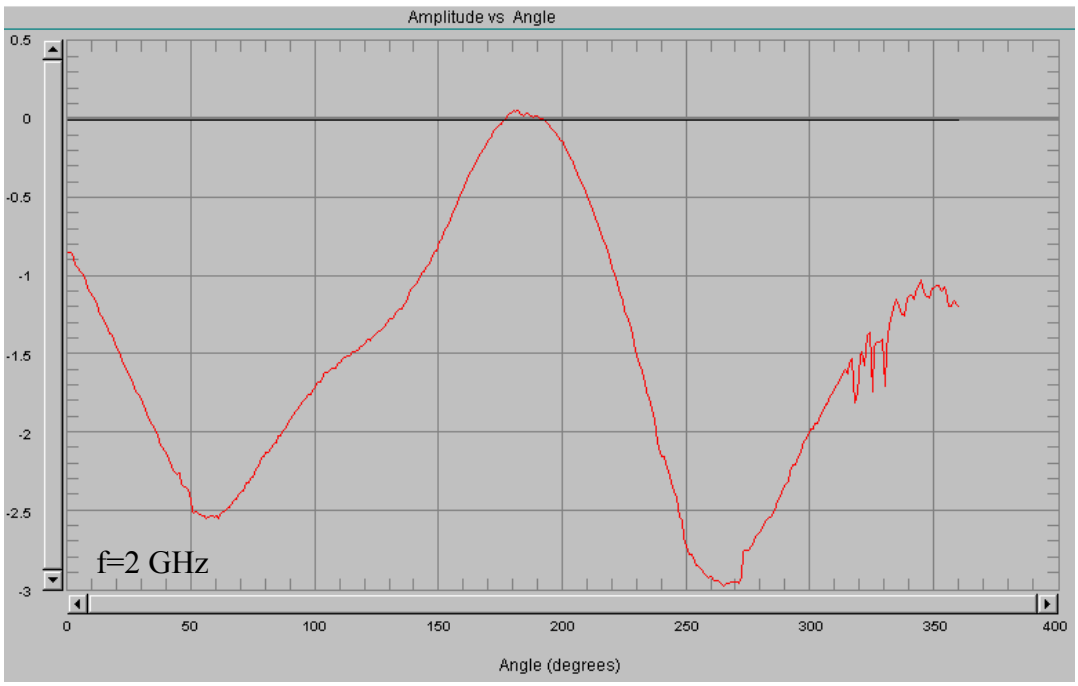
Amplitude vs Angle
0.5
0
-0.5
-1
-1.5
-2
-2.5
-3
f=2 GHz
0
50
100
150
200
250
300
350
400
Angle (degrees)

(c)

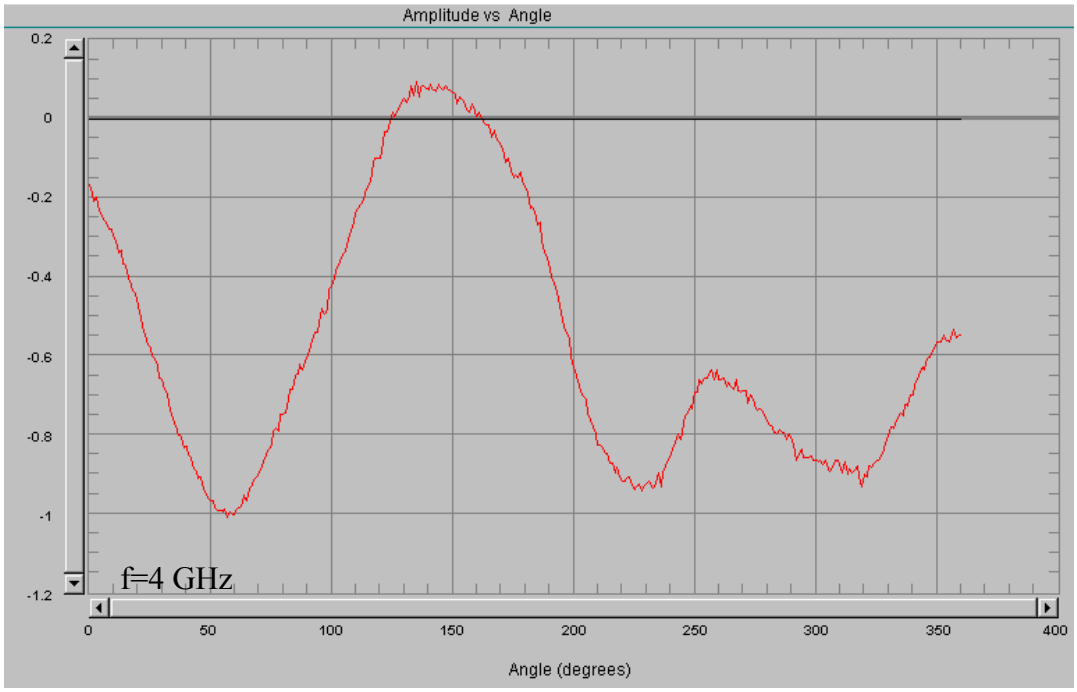
Amplitude vs Angle
0.2
0
-0.2
-0.4
-0.6
-0.8
-1
-1.2
f=4 GHz
0
50
100
150
200
250
300
350
400
Angle (degrees)

(d)


Amplitude vs Angle
0.3
0.2
0.1
0
-100m
-0.2
-0.3
-0.4
-0.5
f=8 GHz
0
50
100
150
200
250
300
350
400
Angle (degrees)

(e)

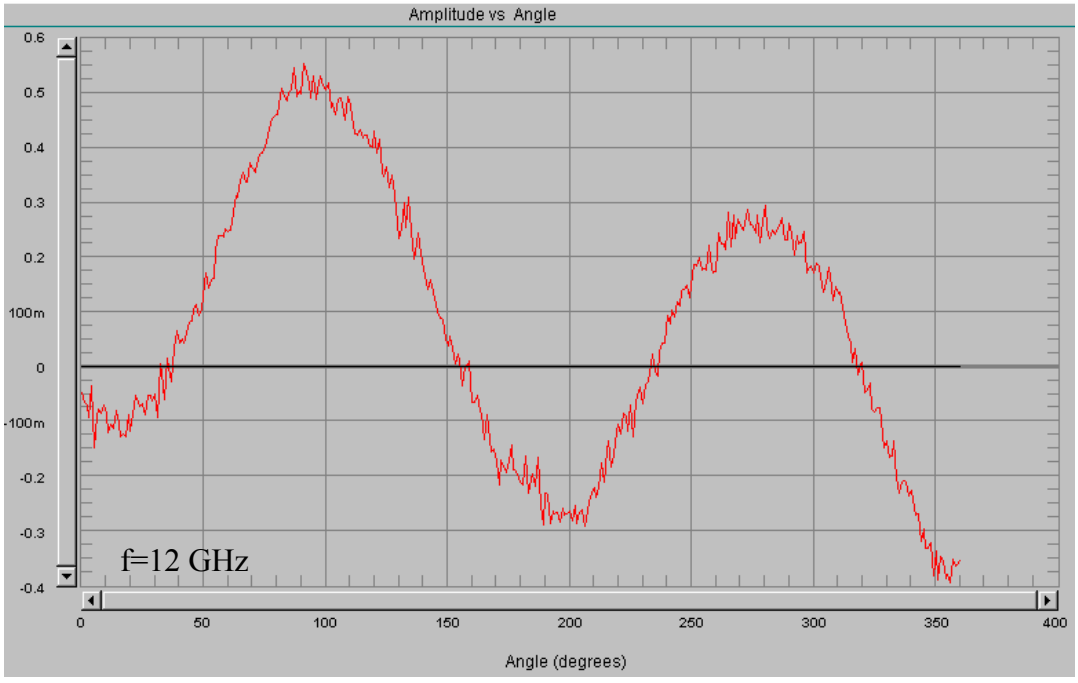
Amplitude vs Angle
0.6
0.5
0.4
0.3
0.2
100m
0
-100m
-0.2
-0.3
-0.4
f=12 GHz
0
50
100
150
200
250
300
350
400
Angle (degrees)

(f)

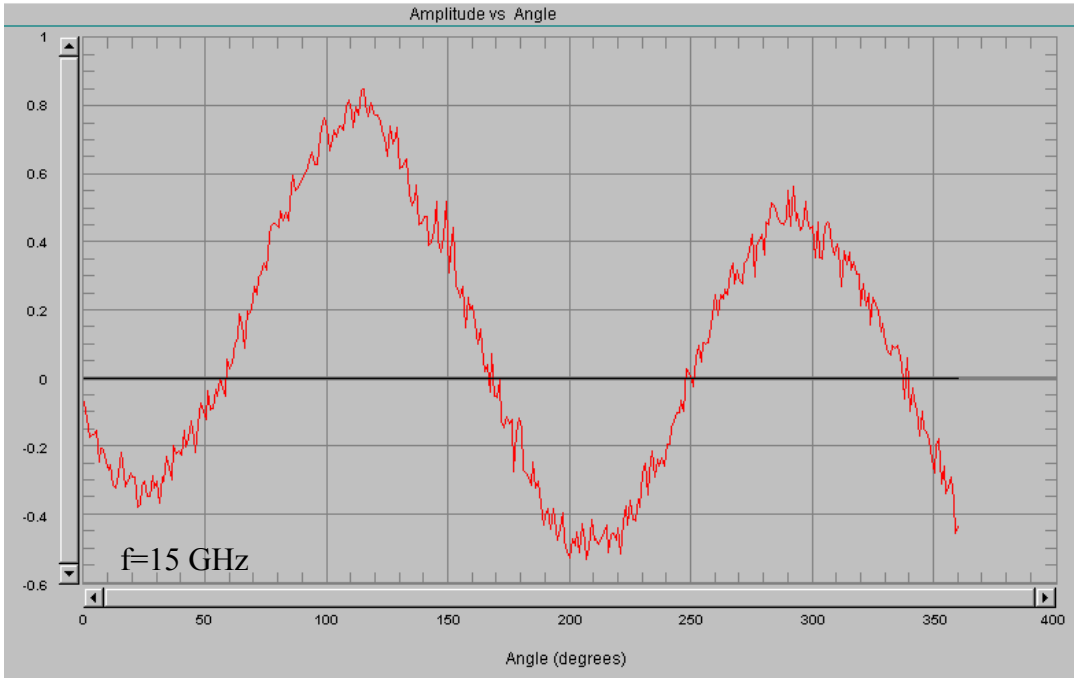

(g)

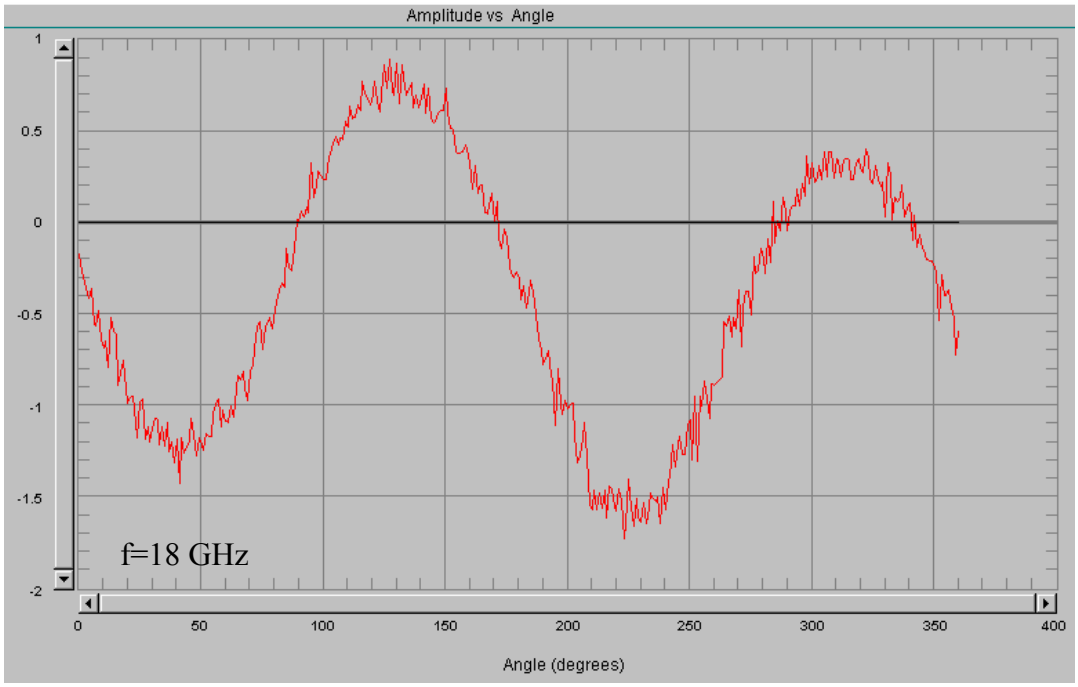

(h)

Figure 5.26 Polarization pattern of Spiral 1 at frequencies 0.5(a), 1(b), 2(c), 4(d), 8(e), 12(f), 15(g) and 18(h) GHz (Configuration 3)

CHAPTER 6

CONCLUSION

Throughout this thesis, microstrip tapered balun was investigated theoretically and experimentally in order to feed spiral antennas properly. Then, theoretical aspects of two arm planar spiral antennas were considered. Reduced size spiral antennas were designed, implemented and measured.

Predesigned microstrip tapered balun used in reference spiral antenna was examined using Ansoft® HFSS™ software. First port impedances of the balun were calculated using the formulas given in Appendix B and the dimensions of the balun structure were evaluated as 50 Ohms at unbalanced port and 120 Ohms at balanced port. Then, the balun structure was simulated using Ansoft® HFSS™ software and it was observed that balun structure has been working properly. Baluns were implemented and measurements were made using an HP® 8722 D vector network analyzer on back-to-back configuration. The results were highly successful and it seemed that they could be used for feeding sections of reduced size spiral antennas, with a return loss of smaller than 10 dB along the frequency band.

Design parameters of two arm planar spiral antennas were studied theoretically. Using the previous studies on spiral antennas made by Altunkan HIZAL and Ekrem ORAN, three reduced size spiral antennas were designed. Using the AutoLISP® program written by Ekrem ORAN, designed reduced size spiral antenna PCBs' were implemented. Spiral 1 was manufactured by ASELSAN® Inc.; Spiral 2 and Spiral 3 were manufactured by LINTEK® Pty Ltd.

Antenna measurement techniques were revised and measurement methods and set-ups were defined. Measurements were done in Anechoic Chamber of ASELSAN® Inc. and successful results were obtained.

All of the designed reduced size spiral antennas showed almost same radiation and gain characteristics with the reference spiral antenna that has a larger size. There is only a small gain reduction at the lower cut off frequency compared to the reference spiral antenna due to the aperture reduction. On the other hand, equiangular start and transition to archimedean has a positive effect on polarization ellipticity although it has a negative effect on gain due to increasing ohmic loss. But it won't be a problem for operation of the antenna since spiral antennas are usually used as receiving antennas that the gain is not the critical parameter. Since spiral antennas are generally used for direction finding purposes at receive site, radiation pattern and axial ratio are more crucial parameters than gain. Radiation pattern of spiral antennas (Spiral 1, Spiral 2 and Spiral 3) were nearly same as the measurements were examined.

Consequently, we can say that size reduction has a negligible effect on radiation pattern of the antenna. Also number of modulation cycles on spiral arms has not any effect since Spiral 1 has 16 wiggles but Spiral 2 and Spiral 3 have 100 wiggles. Axial ratios of the antennas are nearly same too. So, it can be stated that modulation of spiral arms has a negligible effect on polarization ellipticity [12,21].

Common problem related with all of the spiral antennas, can be considered as distortions in radiation patterns at higher frequencies (larger than 15 GHz), especially for horizontal polarized transmitter. First predicted reason for this configuration is the contact of spiral PCB with the antenna case. Because there is not any distortion on antenna pattern for Configuration 1 but distortions can be easily seen for other configurations. Second predicted reason is the distance between spiral PCB and the absorber. Distortions are increasing with increasing distance between two media. Last reason is the sensitivity of the feed point of the antenna. In order to obtain smooth radiation patterns, balun ribbons should be soldered carefully on pads of antenna PCB. Any gap should not exist between two substrates.

In conclusion, a general knowledge on spiral antennas, microstrip tapered baluns and antenna measurement techniques were acquired. For later work, spiral antenna may be implemented on another substrate, because dimensions are getting narrower with increasing dielectric constant of substrate as a result of wavelength reduction. But the impedance of the antenna will change for this case so new balun structures should be designed.

REFERENCES

[1] Oran, Ekrem, “Design and Construction of a Planar Spiral Antenna in the 1-18 GHz Frequency Range” A Master Thesis in Electrical and Electronics Engineering, Middle East Technical University, August 1991

[2] Hızal, Altunkan, “Design and Construction of a Cavity-Backed Spiral Antenna in the Frequency Range of 1-12 GHz” Submitted to ASELSAN® Inc., under research contract No.83-03-01-03 February 1986

[3] Kanlıoğlu, Osman, “Design and Construction of Planar and Conical Sinuous Antennas in the 1-18 GHz Frequency Range” A Master Thesis in Electrical and Electronics Engineering, Middle East Technical University, December

[4] Saygıner, Erdal, “Design and Realization of a Circular Array of Vivaldi Antennas” A Master Thesis in Electrical and Electronics Engineering, Middle East Technical University, June 1994

[5] Rumsey, V. H., “Frequency Independent Antennas”, IRE National Convention Record pt.I, PP. 114-118, 1957

[6] J. A. Kaiser, “The Archimedean Two-Wire Spiral Antenna” IRE Transactions on Antennas and Propagation, Vol.AP-8 PP.312-323, 1960

[7] Booker, G. H., “Slot Aerials and their Relation to Complementary Wire Aerials (Babinet’s Principle)”

[8] N. M. Blackman, “The Effects of Noise on Bearings Obtained by Amplitude Comparison” IEEE Trans. Aerosp. Electron. Syst. Sept. 1971, PP. 1007-1009

[9] Erzin, Serhat Salih, “Range Evaluation of the Anechoic Chamber in ASELSAN® Inc.” A Master Thesis in Electrical and Electronics Engineering, Middle East Technical University, February 1991

[10] IEEE Standard “Test Procedures for Antennas” Std.149, 1979

[11] Stutzman, Warren L., “Polarization in Electromagnetic Systems”, Artech House Inc., 1993, pp. 67-94

[12] T. E. Morgan, “Reduced Size Spiral Antenna”, Marconi Space and Defence Systems Ltd, Warren Lane, Stanmore, Middx, England

[13] Report written in ASELSAN® Inc. on spiral antenna design, January 1997

[14] Collin, R. E., “Foundations for Microwaves Engineering” Mc-Graw Hill, Inc., 1992

[15] Kobayashi, M., “A Dispersion Formula Satisfying Recent Requirements in Microstrip CAD” IEEE Trans. on Microwave Theory and Techniques, vol. MTT-36, no.8, August 1988, pp. 1246-1250

[16] Halavut, Erhan, “On The 3D Modelling Of A Circumferential Slot Antenna On A Shaped Finite Circular Conducting Cylinder And A Four Arm Difference Mode Spiral Antenna” A Master Thesis in Electrical and Electronics Engineering, Middle East Technical University, September 2001

[17] Sivan-Sussman, R., “Various modes of the Equiangular Spiral Antenna” IEEE Trans. on Antennas and Propagation, September 1963, pp. 533-539

[18] Laxpati, S.R., Mittra, R., “Boundary-value Problems Associated with Source-Excited Planar Equiangular Spiral Antennas”, Proc. IEE, 1967, Vol.114, PP. 352-359

[19] DuHamel, H. R., Chadwick, G. G., “Frequency Independent Antennas” Antenna Engineering Handbook, Second Edition, Johnson, C. R., Jasik, H., Ed. McGraw-Hill Book Company 1984

[20] Antenna Engineering Handbook, Second Edition, Johnson, C. R., Jasik, H., Ed. McGraw-Hill Book Company 1984, Ch. 14-16

[21] European Patent Application, EP 1 026 777 A2, Broad band spiral and Sinuous Antennas, 9/8/2000 Bulletin 2000/32

[22] Harold A. Wheeler, Fellow IEEE, “Transmission Line Properties of Parallel Strips Separated by a Dielectric Sheet” IEEE Trans. on Microwave Theory and Techniques, March 1965, pp. 172-185

APPENDIX A

"USER FRIENDLY AutoLISP® PROGRAM FOR PLANAR SPIRAL ANTENNA DRAWING" by EKREM ORAN

```
(Defun C:Wiggle()
        (Defun dtr (a)
                (setq a ( * ( / a 180.0 ) pi ))
        )
        (Defun rtd (a)
                (setq a (* (/ a pi) 180))
        )

        (setq fullarchi nil wiggler nil Nwiggle nil Magwiggle nil)
        (setq addwiggle 0)
        (setq fmax nil rad18 nil fmin nil rad1 nil rad1recom nil n nil winit nil balun
nil rin nil aeq nil deltaphi nil rout nil wida nil a nil rtransit nil koln nil x nil lamda0
nil lay nil ceneq nil rin2 nil aeq2 nil angeq nil ceneq nil ainceq nil rnow nil angle
nil ang nil angle1 nil angle2 nil)



        (initget 6)
        (setq fmax (getreal "Upper cutoff frequency  in GHz <18 GHz>:"))
        (cond ((null fmax) (setq fmax 18)))
        (setq rad18 (/ 3e11 (* fmax 1e9 2 pi)))
```

```
(initget 6)
(setq fmin (getreal "Lower cutoff frequency  in GHz <1 GHz>:"))
(cond ((null fmin) (setq fmin 1)))
(setq rad1 (/ 3e11 (* fmin 1e9 2 pi)))
(setq rad1recom (/ (* 3e11 1.18) (* fmin 1e9 2 pi)))

(initget 6)
(setq n (getint "Number of arms <2 arms>:"))
(cond ((null n) (setq n 2)))

(initget 6)
(setq winit (getreal "innermost width in mm <0.1mm>:"))
(cond ((null winit) (setq winit 0.1)))

(setq deltaphi pi)
(while (> deltaphi (/ pi 2))
        (initget 6)
        (setq balun (getreal "Balun dielectric in mm <0.790>:"))
        (cond ((null balun) (setq balun 0.790)))
        (setq rin (/ balun (sqrt 2)))
        (setq aeq (/ (* n (log (+ 1 (/ winit rin)))) pi))
        (setq deltaphi (/ (* 2 pi rin (- (exp (/ (* aeq pi 2) n)) 1) (sqrt (+ (/ 1
(* aeq aeq)) 1))) (/ 3e11 (* fmax 1e9))))
        (if (> deltaphi (/ pi 2)) (prin1 "Re-enter a smaller sized balun.") t)
        (if (> deltaphi (/ pi 6)) (prin1 "You will get bad performance at the
upper cutoff frequency.") t)
        (prin1 (/ (* deltaphi 180) pi))
)

(setq wida (/ winit 2))
(while (< wida winit)
```

```
                (initget 6)
                (setq wida (getreal "Archimedean arm width <0.25mm>:"))
                (cond ((null wida) (setq wida 0.25)))
                (if (< wida winit) (prin1 "Re-enter a larger value.") t)
        )
        (setq a (/ (* wida n) pi))
        (setq rtransit (/ wida (- (exp (/ (* aeq pi) n)) 1)))
;       (setq rtransit (/ a aeq))


        (initget "Y N")
        (setq fullarchi (getkword "Full archi <Y/N>"))
        (if (= fullarchi "N")
                (progn
                        (initget 6)
                        (setq koln (getreal "Maximum number of strips inside the
radiating band which are in phase <8>:"))
                        (cond ((null koln) (setq koln 8)))
                        (setq Magwiggle 0)

        (setq aeq2 (/ 1 (* 2 pi (/ koln 4) (/ koln 4))))
        (setq rin2 (/ wida (- (exp (/ (* aeq2 pi) n)) 1)))
        (if (< rin2 rtransit) (setq rin2 rtransit) t)
        (setq rout (/ rad1 3))
        (If (< rin2 (- rad1 (sqrt (* a rad1 2 pi)))) (setq rad1recom  (* rad1 (exp (* (/
koln 4) pi 2 aeq2)))) (setq rad1recom (+ rad1 (sqrt (* a rad1 2 pi)))) )
        (while (< rout (/ rad1 2))
                (initget 6)
                (setq rout (getdist "Outer Radius in mm <optimum>:"))
                (cond ((null rout) (setq rout rad1recom)))
                (if (< rout (/ rad1 2)) (prin1 "Re-enter a larger outer radius") t)
```

```
            (if (< rout rad1recom) (prin1 "You will get bad performance at the
lower cutoff frequency.") t)
            (prin1 (/ rad1recom rout))
        )
        (if (> rtransit rout) (setq rtransit rout) t)
        (if (> rin2 rout) (setq rin2 rout) t)

                                    (setq Nwiggle 1)
                                    (setq Magwiggle 0)

            )

            (progn
                (initget "Y N")
                (setq wiggler (getkword "To wiggle or not to wiggle
<Y/N>"))
                (if (= wiggler "Y")
                    (progn
                        (initget 6)
                        (setq Nwiggle (getint "Number of wiggles in
360 degrees <18>:"))
                        (cond ((null Nwiggle) (setq Nwiggle 18)))
                        (initget 6)
                        (setq Magwiggle (getreal "Magnitude of
wiggles (between 0.1 and 1) <0.5>:"))
                        (cond ((null Magwiggle) (setq Magwiggle
0.5)))
                    )
                    (progn
                        (setq Nwiggle 1)
                        (setq Magwiggle 0)
```

```
                                )
                            )

        (setq rout (/ rad1 3))
        (setq rad1recom (+ rad1 (sqrt (* a rad1 2 pi))))
        (while (< rout (/ rad1 2))
                (initget 6)
                (setq rout (getdist "Outer Radius in mm <optimum>:"))
                (cond ((null rout) (setq rout rad1recom)))
                (if (< rout (/ rad1 2)) (prin1 "Re-enter a larger outer radius") t)
                (if (< rout rad1recom) (prin1 "You will get bad performance at the
lower cutoff frequency.") t)
                (prin1 (/ rad1recom rout))
        )
        (setq rin2 rout)



                )


        )

;       Length of spiral arm from main radiating radius to outer radiating radius
;       ro*(exp(koln/4*pi*2*aeq2))
;       (1+aeq2^-2)^0.5*(lamda/2/pi())*(exp(koln/4*pi()*2*aeq2)-
1)=(koln/4+0.5)*lamda
;
        (1/aeq2)*(1/(2*pi()))*((koln/4*pi()*2*aeq2)+(koln/4*pi()*2*aeq2)^2/2)(ko
ln/4+0.5
;       (1/(2*pi()))*((koln/4*pi()*2)+(koln/4*pi()*2)^2*aeq2/2)(koln/4+0.5
;       aeq2 ( 1 / (koln/4)^2/2/pi()
```

```
	(initget 6)
	(setq lay (getint "Drawing color <2>:"))
	(cond ((null lay) (setq lay 2)) (t nil))

	(setq rout (/ rad1 3))
	(while (< rout (/ rad1 2))
		(initget 6)
		(setq rout (getdist "Outer Radius in mm <optimum>:"))
		(cond ((null rout) (setq rout rad1recom)))
		(if (< rout (/ rad1 2)) (prin1 "Re-enter a larger outer radius") t)
		(if (< rout rad1recom) (prin1 "You will get bad performance at the
lower cutoff frequency.") t)
		(prin1 (/ rad1recom rout))
	)

	(setq angeq 361)
	(while (<= (/ 360 n) angeq)
		(initget 6)
		(setq angeq (getreal "Spiral arm width angle <Self complementary
(180/n)>:"))
		(cond ((null angeq) (setq angeq (/ 180 n))))
	)
	(setq angeq (dtr angeq))

;Spiral's center is ceneq
	(setq ceneq (list 50.0 50.0))

; input the desired resolution of the spiral drawing.
	(initget 6)
	(setq ainceq (getdist "Points per rotation <180>:"))
	(cond ((null ainceq) (setq ainceq 180)) (t nil))
```

```
        (setq ainceq (/ (* 2 pi) ainceq))

; Input the 2 times copper etching value in micrometers
        (Setq pwid winit)
        (while (>= pwid winit)
                (Initget 6)
                (setq pwid (getdist "2 times etching tolerance <NONE>:"))
                (If (null pwid) (setq pwid 0.0) (setq pwid (/ pwid 2)))
        )

; initialize the screen.
        (setq cs (getvar "cmdecho"))
        (setq bs (getvar "blipmode"))
        (setvar "blipmode" 0)
        (setvar "cmdecho" 0)

; Draw circles at radii rin rtransit rin2 rout.
        (command "layer" "s" 6 "")
        (Command "circle" ceneq rin)
        (command "layer" "s" 7 "")
        (Command "circle" ceneq rtransit)
        (command "layer" "s" 8 "")
        (Command "circle" ceneq rin2)
        (command "layer" "s" 9 "")
        (Command "circle" ceneq rout)

; Draw the first arm.
        (command "layer" "s" 1 "")
        (setq angle 0.0)
        (setq rnow rin)
; Draw the initial equiangular feed.
```

```
        (command "pline" (setq tp (polar ceneq 0.0 (- rin pwid))) "width" 0.0 0.0)
        (while (< rnow rtransit)
                (setq angle (+ angle ainceq))
                (setq rnow (* rnow (exp (* aeq ainceq))))
                (setq tp (polar ceneq angle (- rnow pwid)))
                (command tp)
        )
;;      (command)
        (setq angle1 angle)
; Draw the archimedean section.
;;      (command "layer" "s" 2 "")
;;      (command "pline" (setq tp (polar ceneq angle (- rnow pwid))) "width" 0.0
0.0)
        (setq anglewig angle addwiggle (* wida magwiggle))
        (while (< (+ rnow wida addwiggle) rin2)
                (setq angle (+ angle ainceq))
                (setq rnow (+ rnow (* a ainceq)))
                (setq addwiggle (* wida magwiggle (sin(* (- angle anglewig)
Nwiggle)) rnow (/ 1 rout)))
                (setq rnowwiggle (+ rnow addwiggle))
                (setq tp (polar ceneq angle (- rnowwiggle pwid)))
                (command tp)
        )
;;      (command)
        (setq angle2 angle)
; Draw the final eqiangular section.
;;      (command "layer" "s" 3 "")
;;      (command "pline" (setq tp (polar ceneq angle (- rnow pwid))) "width" 0.0
0.0)
(if (= fullarchi "N")
        (progn
```

```
                (while (< rnow rout)
                        (setq angle (+ angle ainceq))
                        (setq rnow (* rnow (exp (* aeq2 ainceq))))
                        (setq tp (polar ceneq angle (- rnow pwid)))
                        (command tp)
                )
; Draw circular end.
                (setq ang 0.0)
                (while (< ang angeq)
                        (setq angle (- angle ainceq) ang (+ ang ainceq))
                        (setq tp (polar ceneq angle (+ rnow pwid)))
                        (command tp)
                )
        )
        (progn
                (setq rnow (+ rnow wida))
                (setq rnowwiggle (+ rnow addwiggle))
                (setq tp (polar ceneq angle (+ rnowwiggle pwid)))
                (command tp)
        )
)
; RETURN
; Return final equiangular section.
        (while (< angle2 angle)
                (setq angle (- angle ainceq))
                (setq rnow (* rnow (exp (* aeq2 (- 0 ainceq)))))
                (setq tp (polar ceneq angle (+ rnow pwid)))
                (command tp)
        )
;;      (command)
; Draw return Archimedean section.
```

```
;;      (command "layer" "s" 2 "")
;;      (command "pline" (setq tp (polar ceneq angle (+ rnow pwid))) "width" 0.0
0.0)
(print "ilkangle")
(print angle)
        (while (< angle1 angle)
                (setq angle (- angle ainceq))
                (setq rnow (+ rnow (* a (- 0 ainceq))))
                (setq addwiggle (* wida magwiggle (sin(* (- angle anglewig)
Nwiggle)) (- rnow wida) (/ 1 rout)))
                (setq rnowwiggle (+ rnow addwiggle))
                (setq tp (polar ceneq angle (+ rnowwiggle pwid)))
                (command tp)
)
;;      (command)
; Draw return equiangular feed.
;;      (command "layer" "s" 1 "")
;;      (command "pline" (setq tp (polar ceneq angle (+ rnow pwid))) "width" 0.0
0.0)
        (while (< (- 0.0 angeq) angle)
                (setq angle (- angle ainceq))
                (setq rnow (* rnow (exp (* aeq (- 0 ainceq)))))
                (setq tp (polar ceneq angle (+ rnow pwid)))
                (command tp)
        )
; Draw linear feed
        (setq tp (polar ceneq 0.0 (- rin pwid)))
        (command tp)

        (command)
```

```
; Construct array of n arm spiral
        (command "array" "all" "" "p" ceneq n "360" "y")
; Refresh the screen.
        (command "redraw")
        (setvar "blipmode" bs)
        (setvar "cmdecho" cs)

)
4
```

APPENDIX B

EFFECTIVE DIELECTRIC CONSTANT AND CHARACTERISTIC IMPEDANCE OF MICROSTRIP LINES

The characteristic impedance of a microstrip line of width w and metallization thickness t, over a dielectric substrate of dielectric constant ε_r and thickness h, at the frequency f is given below [14,15,16].

$$\varepsilon_e(f) = \varepsilon_r - \frac{\varepsilon_r - \varepsilon_e(0)}{1 + (f/f_a)^m}$$

$$\varepsilon_e(0) = \frac{\varepsilon_r + 1}{2} + \frac{\varepsilon_r - 1}{2}\left(1 + \frac{12h}{w}\right)^{-1/2} + F(\varepsilon_r, h) - 0.217(\varepsilon_r - 1)\frac{t}{\sqrt{wh}}$$

$$F(\varepsilon_r, h) = \begin{cases} 0.02(\varepsilon_r - 1)(1 - w/h)^2 & w/h \le 1 \\ 0 & w/h > 1 \end{cases}$$

$$f_a = \frac{f_b}{0.75 + (0.75 - 0.332\varepsilon_r^{-1.73})(w/h)}$$

$$f_b = \frac{299.7924562}{2\pi h\sqrt{\varepsilon_r - \varepsilon_e(0)}} \tan^{-1}\left[\varepsilon_r \sqrt{\frac{\varepsilon_e(0) - 1}{\varepsilon_r - \varepsilon_e(0)}}\right]$$

$$m = \begin{cases} m_o m_c & m_o m_c \le 2.32 \\ 2.32 & m_o m_c > 2.32 \end{cases}$$

$$m_o = 1 + \frac{1.0}{1 + \sqrt{w/h}} + \frac{0.32}{(1 + \sqrt{w/h})^3}$$

$$m_c = \begin{cases} 1 + \frac{1.4}{1 + w/h}\left[0.15 - 0.235e^{-0.45f/f_a}\right] & w/h \le 0.7 \\ 1 & w/h > 0.7 \end{cases}$$

$$Z_c = \sqrt{\frac{\mu_o \varepsilon_o}{\varepsilon_e}} \frac{1}{C_a}$$

where

$$C_a = \begin{cases} \dfrac{2\pi\varepsilon_o}{\ln\left(\dfrac{8h}{w} + \dfrac{w}{4h}\right)} & w/h \le 1 \\ \varepsilon_o \left[\dfrac{w}{h} + 1.393 + 0.667 \ln(w/h + 1.444)\right] & w/h > 1 \end{cases}$$

APPENDIX C

CHARACTERISTIC IMPEDANCE OF PARALEL STRIPS SEPARATED by A DIELECTRIC SHEET

The characteristic impedance of parallel strips with line of width W, and separation H, separated by a dielectric sheet with dielectric constant ε_r, is given as [22]:

$$Z_c = \frac{Z_o}{\sqrt{\varepsilon_r}} \frac{1}{\frac{W}{H} + \frac{1}{\pi}\ln 4 + \frac{\varepsilon_r + 1}{2\pi\varepsilon_r}\ln\frac{\pi\varepsilon_r}{2}\left(\frac{W}{H} + 0{,}94\right) + \frac{\varepsilon_r - 1}{2\pi\varepsilon_r{}^2}\ln\frac{\varepsilon_r\pi^2}{16}}$$

for

$$\frac{W}{H} > 1$$

and

$$Z_c = \frac{Z_o}{\pi\sqrt{\varepsilon_r}}\left[\ln\frac{4H}{W} + \frac{1}{8}\left(\frac{W}{H}\right)^2 - \frac{1}{2}\frac{\varepsilon_r - 1}{\varepsilon_r + 1}\left(\ln\frac{\pi}{2} + \frac{1}{\varepsilon_r}\ln\frac{4}{\pi}\right)\right]$$

for

$$\frac{W}{H} \le 1$$

APPENDIX D

RF OHMIC RESISTANCE AND CURRENT DISTRIBUTION OF A SPIRAL ANTENNA

RF ohmic resistance of a spiral arm length L is different from the DC ohmic resistance and can be calculated from

$R=L*R_s/(2w)$ ohms; $R_s=(\pi f\mu_0/\sigma)^{1/2}$ ohms

Where R_s is the surface resistance, w is the Archimedean arm width, f is the frequency and σ is the conductivity. For copper $\sigma=5.8*10^7$ mhos/m and $R_s=83.16*10^{-4}\Omega/\sqrt{}$GHz. The distance from the origin of the spiral to any point, "r_p" on the arm is given by $L(r_p)$ where

$$L(r)=\int_0^L dl=\int_0^r \sqrt{1+(rd\phi/dr)^2}\,dr=\int_0^r 1/a\sqrt{(a^2+b^2)}dr$$

$$L(r)=1/a[r/2\sqrt{(a^2+r^2)}+a^2/2\ln(r+\sqrt{a^2+r^2})\,]$$

For the conditions that $a^2<<1$ and $r_1<r<r_2$ length formula can be approximated by

$L(r)=r^2/2a+(a/2)*\ln(2r)$

However a value of L_r, which takes into account the current distribution of the Archimedean spiral arm, is needed for a more realistic case. Laxpati and Mittra [18] gave an approximate analytical formula for the current distribution in the case of the Equiangular spirals. The RF loss resistance $R_L(f)$, where f is the frequency, taking into the account the current distribution whose approximate variation given below Figure-1(appx.), can be calculated from [1,2,13]

$$R_L = \frac{1}{|I_0|^2} * \int_{L_0}^{L} \frac{|I_{(L)}|^2 * R_s}{2w} dl = R_L * L_{eff}$$

where I_0 is the feed current at $r=r_1$, I(L) is the current distribution, $L_1(f)$ is L_r at $I(L)=0.9I_0$, $L_2(f)$ is L_r at $I(L)=0.1I_0$ and R_L is the uniform loss resistance per unit length given by

$R_L=R_s/(2w)\ \Omega/m$

For a spiral radiating at around a circumference of λ in a width of 0.18λ [19], the length L_r of the radiating region can be found from

$L_r=L(0.5\lambda/\pi+0{,}09\lambda)- L(0.5\lambda/\pi-0{,}09\lambda)$

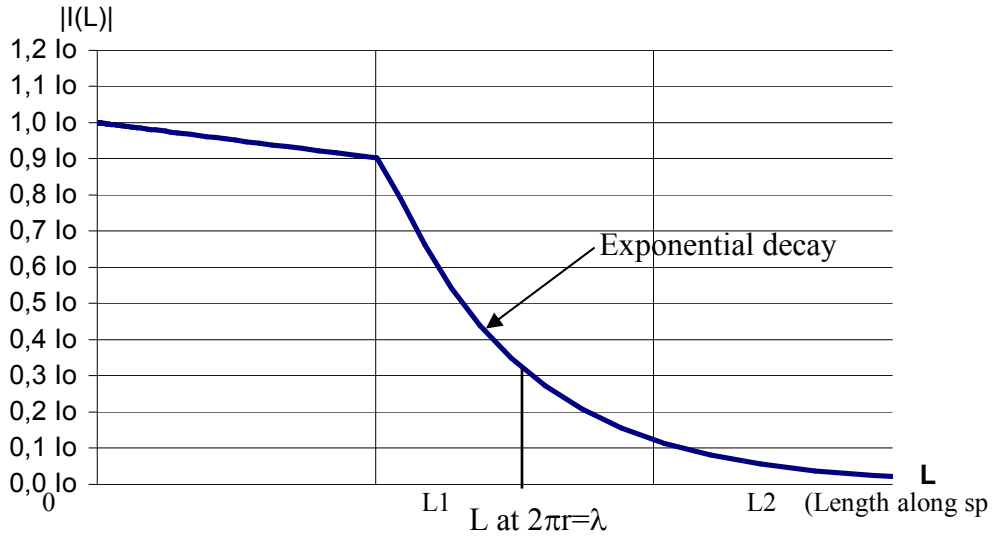

Figure-1(appx.) The approximate current distribution of an Archimedean spiral antenna: $k=2\pi/\lambda$, where λ is the effective wavelength and L is the length along the spiral arm. The main radiating region is 0.18λ in width and located at L corresponding to $2\pi r=\lambda$ circumference. $L_1(r-0.09\lambda)$ and $L_2(r+0.09\lambda)$ [1].